Molecular and physiological responses during thermal acclimation of leaf photosynthesis and respiration in rice

Rashid, Fatimah Azzahra Ahmad

2020-03

Rashid , F A A , Crisp , P A , Zhang , Y , Berkowitz , O , Pogson , B J , Day , D A , Masle , J , Dewar , R , Whelan , J , Atkin , O K & Scafaro , A P 2020 , ' Molecular and physiological responses during thermal acclimation of leaf photosynthesis and respiration in rice ' , Plant, Cell and Environment , vol. 43 , no. 3 , pp. 594-610 . https://doi.org/10.1111/pce.13706

http://hdl.handle.net/10138/323527
https://doi.org/10.1111/pce.13706

acceptedVersion

Plant, Cell & Environment

Molecular and physiological responses during thermal acclimation of leaf photosynthesis and respiration in rice

Journal:	*Plant, Cell & Environment*
Manuscript ID	PCE-19-1106.R1
Wiley - Manuscript type:	Original Article
Date Submitted by the Author:	n/a
Complete List of Authors:	Rashid, Fatimah; Australian National University, Research School of Biology; Sultan Idris education University, Department of Biology Crisp, Peter; University of Minnesota, Department of Plant and Microbial Biology Zhang, You; CSIRO Plant Industry Berkowitz, Oliver; La Trobe University, Dept. of Animal, Plant and Soil Science / ARC Centre of Excellence in Plant Energy Biology Pogson, Barry; Australian National University, Research School of Biology Day, David A.; Flinders University, College of Science & Engineering Masle, Josette; Australian National University, Research School of Biology Dewar, Roderick; Australian National University, Research School of Biology Whelan, James; La Trobe University, Dept. Animal, Plant and Soil Sciences Atkin, Owen; Australian National University, ARC Centre of Excellence in Plant Energy Biology, Division of Plant Sciences Scafaro, Andrew; Australian National University, Research School of Biology
Environment Keywords:	heat, cold
Physiology Keywords:	respiration, photosynthesis: carbon reactions
Other Keywords:	acclimation, cytochrome c oxidase (COX), rice, RNA-seq
Abstract:	To further our understanding of how sustained changes in temperature affect the carbon economy of rice (*Oryza sativa*), hydroponically-grown plants of the IR64 cultivar were developed at 30/25°C (day/night) before being shifted to 25/20°C or 40/35°C. Leaf mRNA and protein abundance, sugar and starch concentration, gas-exchange and elongation rates were measured on pre-existing leaves (PE) already developed at 30/25°C, or leaves newly-developed (ND) subsequent to temperature transfer. Following a shift in growth temperature, there was a transient adjustment in metabolic gene transcript abundance of PE leaves before homeostasis was reached within 24 h, aligning with R_{dark} (leaf dark respiratory CO_2 release) and A_n (net CO_2 assimilation) changes. With longer exposure, the central respiratory protein CYTOCHROME C OXIDASE (COX) declined in abundance at 40/35°C. In contrast to R_{dark},

	A_n was maintained across the three growth temperatures in ND leaves. Soluble sugars did not differ significantly with growth temperature, and growth was fastest with extended exposure at 40/35°C. The results highlight that acclimation of photosynthesis and respiration is asynchronous in rice, with heat-acclimated plants exhibiting a striking ability to maintain net carbon gain and growth when exposed to heat-wave temperatures, even while reducing investment in energy-conserving respiratory pathways.

Molecular and physiological responses during thermal acclimation of leaf photosynthesis and respiration in rice

Fatimah Azzahra Ahmad Rashid[1, 2], Peter A. Crisp[3], You Zhang[4], Oliver Berkowitz[5], Barry J. Pogson[1#], David A. Day[6,7], Josette Masle[8], Roderick C. Dewar[8], James Whelan[5#], Owen K. Atkin[1#], Andrew P. Scafaro[1]

[1] Australian Research Council Centre of Excellence in Plant Energy Biology, Research School of Biology, The Australian National University, Canberra, ACT, 2601, Australia

[2] Current address: Department of Biology, Faculty of Science and Mathematics, Sultan Idris education University, 35900 Tanjung Malim, Perak, Malaysia

[3] Department of Plant and Microbial Biology, University of Minnesota, Saint Paul, MN, 55108 USA

[4] CSIRO Plant Industry, GPO Box 1700, Canberra, ACT, 2601, Australia

[5] Australian Research Council Centre of Excellence in Plant Energy Biology, School of Life Science, AgriBio Building, La Trobe University, Bundoora, Victoria, 3083, Australia

[6] College of Science and Engineering, Flinders University, South Australia, 5001, Australia

[7] Department of Animal, Plant and Soil Sciences, AgriBio Building, La Trobe University, 5 Ring Road, Bundoora, VIC, 3086, Australia

[8] Research School of Biology, The Australian National University, Canberra, ACT, 2601, Australia

[#] The support of the Australian Research Council (ARC) Centre of Excellence in Plant Energy Biology (CE140100008) is acknowledged

Abstract

To further our understanding of how sustained changes in temperature affect the carbon economy of rice (*Oryza sativa*), hydroponically-grown plants of the IR64 cultivar were developed at 30/25°C (day/night) before being shifted to 25/20°C or 40/35°C. Leaf mRNA and protein abundance, sugar and starch concentrations, gas-exchange and elongation rates were measured on pre-existing leaves (PE) already developed at 30/25°C, or leaves newly-developed (ND) subsequent to temperature transfer. Following a shift in growth temperature, there was a transient adjustment in metabolic gene transcript abundance of PE leaves before homeostasis was reached within 24 h, aligning with R_{dark} (leaf dark

respiratory CO_2 release) and A_n (net CO_2 assimilation) changes. With longer exposure, the central respiratory protein CYTOCHROME C OXIDASE (COX) declined in abundance at 40/35°C. In contrast to R_{dark}, A_n was maintained across the three growth temperatures in ND leaves. Soluble sugars did not differ significantly with growth temperature, and growth was fastest with extended exposure at 40/35°C. The results highlight that acclimation of photosynthesis and respiration is asynchronous in rice, with heat-acclimated plants exhibiting a striking ability to maintain net carbon gain and growth when exposed to heat-wave temperatures, even while reducing investment in energy-conserving respiratory pathways.

Keywords: rice, thermal stress, acclimation, respiration, photosynthesis, heat, cold, CYTOCHROME C OXIDASE (COX)

Introduction

The response of net CO_2 assimilation (A_n) and leaf respiration in the dark (R_{dark}) to changes in temperature (T) is often dynamic. Acclimation – i.e. physiological changes that enable adjustments in the rate of A_n and R_{dark} at a given measuring T in response to sustained changes in growth T – occurs in many species, in natural and controlled environments (Atkin, Bruhn, Hurry, & Tjoelker, 2005; Berry & Bjorkman, 1980; Campbell et al., 2007; Reich et al., 2016; Smith & Dukes, 2017; Tjoelker, Oleksyn, & Reich, 2001). Acclimation can also lead to metabolic homeostasis, where similar rates of A_n and R_{dark} are exhibited by hot- and cold-acclimated plants, when compared at their respective growth Ts. Determining the extent to which R_{dark} and A_n acclimate to sustained changes in T is of growing interest, as global warming is resulting in plants of natural and managed ecosystems experiencing higher average growth Ts, often in conjunction with more frequent and severe heat waves (CSIRO & BOM, 2018; Hartmann et al., 2013). The impact of heat on A_n and R_{dark} of cereal crops, including rice (*Oryza sativa*), is of particular interest given the need to increase food production to meet the requirements of a growing and more affluent world population (Godfray et al., 2010). Rice contributes substantially to global food demand, particularly in Asia where it makes up more than 30% of all dietary energy intake (Seck, Diagne, Mohanty, & Wopereis, 2012). However, in recent years rice yields have declined in regions such as South-East Asia, with the declines being more strongly correlated with nightly minimum than daytime maximum *Ts* (Peng et al., 2004; Welch et al., 2010). Reduced yields and grain quality were also observed for rice in North America when exposed to warmer night T (Lanning, Siebenmorgen, Counce, Ambardekar, & Mauromoustakos, 2011). Given this, and the likely importance of A_n and R_{dark} for biomass and grain production (Posch et al., 2019; Yoshida, 1972), it is

crucial that we develop a better understanding of how changes in T affect these key metabolic processes in rice.

In rice and a range of other crops, RNA sequencing analysis has shown large scale perturbations to the transcript profile of plants exposed to colder or warmer T, with the changes occurring over a period of hours to days and across multiple functional categories, but especially in genes involved in primary metabolism (Bhardwaj et al., 2015; Hu, Sun, Zhang, Nevo, & Fu, 2014; Shen et al., 2014). The vast gene expression response to T-perturbations is likely mediated through heat shock transcription factors, which regulate changes in transcriptional networks. These are induced by heat stress and other abiotic stimuli, changing the protein complement of a cell (Morimoto, 1998; Ohama, Sato, Shinozaki, & Yamaguchi-Shinozaki, 2017). However, changes in protein abundance may not necessarily match changes in transcript abundance due to transcription and RNA turnover rates being influenced by T (Sidaway-Lee, Costa, Rand, Finkenstadt, & Penfield, 2014), and post-transcriptional regulation. In cases where heat stress results in changes in protein abundance, the greatest changes are seen in proteins associated with primary metabolism, with about 50% of all leaf protein abundance changes seeming to be in A_n and R_{dark} metabolic pathways (Scafaro & Atkin, 2016). In rice, cold-stress similarly perturbs a large proportion of energy metabolism pathways (Neilson, Mariani, & Haynes, 2011), emphasising the importance of changes in protein abundance in chloroplasts and mitochondria as part of the thermal acclimation process. There is growing evidence that plants can acclimate to T variations by stimulating energy metabolism at colder T and suppressing energy metabolism at warmer T, either through regulation of enzymatic velocities or changes in enzyme abundance (Armstrong et al., 2008; Badger, Björkman, & Armond, 1982; Campbell et al., 2007; Hikosaka, Ishikawa, Borjigidai, Muller, & Onoda, 2006; Scafaro et al., 2017; Strand et al., 1999; Yamori, Noguchi, & Terashima, 2005). Whether the same is true for rice remains unclear, both for pre-existing (PE) leaves that experience a sustained change in growth T, and in newly-developed (ND) leaves that form under a new thermal regime. In species other than rice, the extent of changes underpinning thermal acclimation (including changes in leaf structure, nitrogen partitioning and organelle abundance), is typically greater in ND than PE leaves (Armstrong et al., 2008; Gorsuch, Pandey, & Atkin, 2010; O'Leary, Asao, Millar, & Atkin, 2018; Tjoelker, Reich, & Oleksyn, 1999; Yamori et al., 2005).

Past studies on rice conducted during the vegetative (Glaubitz et al., 2014; Kurimoto, Day, Lambers, & Noguchi, 2004) and reproductive (Bahuguna, Solis, Shi, & Jagadish, 2017; Mohammed, Cothren, & Tarpley, 2013) phases of development have reported limited and variable levels of acclimation of R_{dark}. By contrast, A_n of rice shows strong thermal acclimation, with rates of net CO_2 uptake measured at the prevailing growth T being homeostatic or increasing as growth T is increased

from 15 to 37°C (Nagai & Makino, 2009; Yamori, Noguchi, Hikosaka, & Terashima, 2010). Such studies point to a possible asynchrony in rice acclimation, with a more dynamic A_n than R_{dark} response, although further work simultaneously comparing A_n and R_{dark} in rice is needed. Interestingly, a range of other crops and non-crop species show the opposite – greater R_{dark} than A_n acclimation capacity (Campbell et al., 2007; Drake et al., 2016; Way & Oren, 2010). Although such studies detail the physiological acclimation of energy metabolism in plants, including rice, less is known about the molecular and biochemical responses that underpin this phenotypic *T* acclimation.

It is with the above issues in mind that we conducted a study using the IR64 cultivar of *Oryza sativa* to address the following aims: (1) characterise the extent of thermal acclimation of R_{dark} and A_n; and, (2) link physiological acclimation to the underlying processes through analysis of leaf transcript, protein, sugar, and starch abundance, following changes in growth *T*. We hypothesized that: (1) initial exposure to very high growth *T* increases and decreases the rates of respiratory CO_2 release and net photosynthetic CO_2 uptake, respectively; (2) subsequent acclimation is associated with recovery of A_n, and reduced rates of R_{dark}; and (3) thermal acclimation of R_{dark} and A_n is associated with dynamic changes in gene expression and protein abundance in key pathways associated with energy capture and use.

Materials and methods

Plant material and temperature treatments

Rice (*Oryza sativa*) cultivar IR64 plants were grown hydroponically in a glasshouse facility at the Research School of Biology, Australian National University in Canberra between October and December 2015. Seeds were initially incubated at 40-42°C for two days before soaking in water for eight hours, placed on wet Whatman filter papers in petri dishes and kept in the dark at 30°C for five days. The germinated seedlings were then transferred to trays of vermiculite and placed in temperature-controlled glasshouses (30°C day and 25°C night) under natural sunlight and photoperiod, with photosynthetically active radiation (PAR) between 400 and 1200 µmol m^{-2} s^{-1}. When the third leaf had emerged, seedlings were transplanted from vermiculite to a hydroponic system. Individual plants were placed within PVC tubes with a 3.7 cm diameter and 13 cm height. Tubes were then suspended at the top of 20 L capacity hydroponic tanks (12 tanks in total), with each tank holding a maximum of 20 plants. Each tank was filled with hydroponic solution (Table S1) (Hubbart, Peng, Horton, Chen, & Murchie, 2007). The nutrient solution was replaced weekly. Sulphuric acid or sodium hydroxide were used to adjust the pH to 5-6, with pH monitored using a portable pH meter (Rowe Scientific Pty. Ltd.,

NSW, Australia). The hydroponic solution was aerated continuously using Infinity AP-950 air pumps (Kong's Pty. Ltd., Ingleburn, Australia).

After two weeks of hydroponic growth at 30/25°C ('warm' treatment), the most recently fully-expanded leaves were labelled as pre-existing (PE) leaves. Following labelling, four tanks were randomly chosen and shifted to an adjacent glasshouse room set to 25˚C day and 20˚C night (25/20˚C – 'cold' treatment), and four other tanks were moved to a room set at 40˚C day and 35˚C night (40/35˚C – 'hot' treatment); four tanks were retained at 30/25°C as controls. Relative humidity was not controlled. Newly-developed (ND) leaves that emerged under each thermal regime were labelled, with all measurements reported on ND leaves made 21 days after *T*-transfer.

Determination of transcript abundance

Plants were transferred to new thermal regimes three hours after sunrise. To quantify transcript abundance, the labelled pre-existing (PE) leaves were harvested during the photoperiod: two, six and 24 h after *T*-transfer. For each time-point and temperature treatment, approximately 8 cm long segments (less than 100 mg of fresh mass) were sampled half-way along the leaf blade, and immediately frozen in liquid N_2 and stored at -80°C until RNA extraction. Total RNA was extracted using the RNeasy plant mini protocol (Qiagen, Doncaster, VIC, AU) and treated with DNase I (Qiagen, Doncaster, VIC, AU) to remove any contaminating DNA.

For qPCR analysis, 1 µg of total RNA in a 10 µL volume was reverse- transcribed into cDNA using SuperScript III First-Strand cDNA Synthesis Kit (Invitrogen, Carlsbad, CA, USA), according to the manufacturer's instructions. The reverse-transcribed cDNA samples were diluted 10-fold. Transcript levels of six selected genes and one reference gene (refer to Table S2 for gene accession numbers and primer sequences) were analysed using a Light-Cycler® 480 System (Roche Holding AG, Basel, Switzerland) with SYBR Green I Dye (QIAGEN, Doncaster, Victoria, AU). cDNA samples from each biological replicate were assayed in two technical duplicates. The reaction-mix in each qPCR contained 0.4 µM of each pair of primers, 5 µL of SYBR Master Mix, and 4.6 µL of the diluted cDNA sample in a 10 µL total reaction volume. The raw fluorescence data were analysed using LinRegPCR (Ramakers, Ruijter, Deprez, & Moorman, 2003; Ruijter et al., 2009). Data were normalized to the reference gene, eukaryotic initiation factor 5c (*EIF5C*; LOC_Os11g21990.1), and were expressed as fold-changes against control conditions.

RNAseq libraries were prepared using the Illumina Stranded Total RNAseq kit with RiboZero rRNA depletion as per the manufacturer's guidelines (Illumina). Libraries were pooled and sequenced on a HiSeq1500 for 61 cycles in single end mode at the Centre for AgriBioscience, University of LaTrobe. Analysis pipelines for pre-processing and mapping of sequence data are available online on

GitHub (https://github.com/pedrocrisp/NGS-pipelines). Quality control was performed with *FastQC* v.0.11.2. Adapters were removed using *scythe* v.0.991 with flags -p 0. and reads were quality trimmed with *sickle* v.1.33 with flags -q 20 (quality threshold), and -l 20 (minimum read length after trimming). The trimmed and quality-filtered reads were aligned to the rice reference genome Os-Nipponbare-Reference-IRGSP-1.0 from the MSU Rice Genome Annotation Project Database v7 (http://rice.plantbiology.msu.edu/) using the *subjunc* aligner v1.5.0-p1 with -u and -H flags to report only reads with a single unambiguous best mapping location, -P 3 for phred+33 encoding (Liao, Smyth, & Shi, 2013b). Reads were then sorted, indexed and compressed using *samtools* v1.1-26-g29b0367 (Li et al., 2009) and strand-specific bigwig files were generated using *bedtools genomecov* v2.16.1 (Quinlan & Hall, 2010) and the UCSC utility *bedGraphToBigWig* for viewing in IGV (Robinson et al., 2011). Summary statistics for each sample are provided in Supplementary Dataset S1: Summary of transcriptomic datasets.

For standard differential gene expression testing, the number of reads mapping per IRGSP-1.0 gene loci was summarised using *featureCounts* v1.5.0-p1(Liao, Smyth, & Shi, 2013a) with flags -P and -c to discard read pairs mapping to different chromosomes and the -s flag set to 2 for strand specificity for a strand specific library, multimapping reads and multioverlapping reads were not counted. Reads were summarised to parent IRGSP-1.0 gene loci rather than individual splice variants by summarising to the genomic coordinates defined by the feature "gene" in the IRGSP-1.0.gff reference (last modified 7/2/2012 ftp://ftp.plantbiology.msu.edu/pub/data/Eukaryotic_Projects/o_sativa/annotation_dbs/pseudomolecules/version_7.0/all.dir/all.gff3). Only loci with an abundance of at least 1 CPM (approximately 5 reads) in at least 4 samples were retained. Statistical testing for relative gene expression was performed in R following the "*edgeR-limma-voom*" approach (https://www.bioconductor.org/help/workflows/RNAseq123/); using, *edgeR* v.3.4.2 (McCarthy, Chen, & Smyth, 2012; Robinson & Oshlack, 2010; Robinson & Smyth, 2007a, 2007b), and *voom* in the *limma* package 3.20.1 (Law, Chen, Shi, & Smyth, 2014; Smyth, Michaud, & Scott, 2005).

Determination of protein abundance

Samples of frozen PE leaf material six and 24 h after *T* transfer, as well as frozen ND leaf material, were ground to a fine powder using a chilled mortar and pestle, and protein was extracted in extraction buffer containing 100 mM tricine pH 8.0, 1 mM EDTA, 1 mM PMSF, 1x protease inhibitor cocktail, 2% (w/v) PVPP, 10 mM (w/v) ascorbate, 5 mM DTT, and distilled water. The sample was then solubilized in a NuPAGE LDS Sample Buffer (Invitrogen, Carlsbad, CA, USA) with 10% (v/v) DTT, then heated for 10 minutes at 95˚C, and centrifuged for 30 sec at 12,000 RPM. Thereafter, supernatant

was collected and 8 uL were loaded and separated on 4-12% NuPAGE Bis-Tris gel (Invitrogen, Carlsbad, CA, USA) using the MOPS-based buffer system. To blot, proteins from the gel were transferred to Immobilon-P Polyvinylidene fluoride (PVDF) membranes (Merck Millipore, Kilsyth, VIC, AU) using an XCell II Blot module (Invitrogen, Carlsbad, CA, USA). Membranes were then blocked for 2 h with 5% (w/v) skim-milk powder in Tris-buffered saline containing 0.1% (v/v) Tween-20 (TBST). To probe for cytochrome *c* oxidase (*COX*) subunit II, alternative oxidase (*AOX*), uncoupling protein (*UCP*) and voltage-dependent anion-selective channel protein (*VDAC1*-porin), the membranes were incubated for 2 h in primary antibody solution (5% w/v skim milk powder in TBST) containing commercially available polyclonal antibodies (Agrisera, Vännäs, Västerbotten, Sweden). All antibodies were diluted 1:5000. An antibody for ribulose-1,5-bisphosphate carboxylase/oxygenase (Rubisco) was received from Assoc. Prof. Spencer Whitney (Research School of Biology, Australian National University, Canberra, ACT, AU) and used at a dilution of 1:10 000. After washing with TBST, the membranes were incubated for 1 h in goat anti-rabbit antibody solution (5% w/v skim milk powder in TBST) at a dilution of 1:8000. Proteins were then visualized using the AttoPhos AP fluorescent substrate system (Promega, Madison, WI, USA), imaged using a Versa-Doc (Bio-Rad, Hercules, CA, USA) imaging system and quantified using Image Lab software (Bio-Rad, Hercules, CA, USA). Protein concentrations were determined by the Bradford method using Bovine Serum Albumin (BSA) as a standard.

Determination of soluble sugar and starch concentrations

Starch and soluble sugars of PE leaves transferred from 30/25°C to 25/20°C or 40/35°C for one and seven days, and ND leaves at the prevailing *T* were collected from separate, previously unsampled plants. Samples were collected at 9:30 to 10:00 am, corresponding to 3 h into the light period, frozen and stored at -80°C before freeze-drying at -105°C for two days (Virtis Benchtop™ "K", SP, Scientific, Gardiner, NY, USA), then ground to a fine powder from which a 5-10 mg aliquot was taken. Five-hundred µL of 80% (v/v) ethanol was added and vortexed for 20 sec. Thereafter, leaf tissues were incubated at 80°C while being centrifuged at 500 RPM for 20 min. Following further centrifugation at 12,000 RPM for 5 min, the resulting pellet and supernatant were separated. This procedure was repeated a two more times, and the three pellets and three supernatants were pooled. The pooled supernatants and pellets were used for determination of soluble sugars and starch concentrations, using a Fructose Assay Kit (Sigma-Aldrich, St Louis, MO, USA) and a Total Starch Assay Kit (Megazyme, Chicago, IL, USA), respectively. Following manufacturer's instructions, measurements were made in triplicate, at a wavelength of 340 nm, using a microtitre plate reader (Infinite® M1000 Pro; Tecan US,

Morrisville, NC) and standard curves were generated for soluble sugars using sucrose, glucose and fructose (Sigma-Aldrich, St Louis, MO, USA) at known concentrations.

Gas exchange measurements using Licor 6400XT 6 cm^2 cuvettes

Gas-exchange was measured on fully-expanded pre-existing (PE) leaves just prior to- and one, two, three, five and seven days after *T* transfer, as well as on fully-expanded newly-developed (ND) leaves 21 days after transfer, using two matched LI-6400 instruments equipped with 6 cm^2 cuvettes and a 6400-02B red-blue light source (Li-Cor, Lincoln, NE, USA). At each time point, light-saturated net CO_2 assimilation rates (A_n) and then dark respiration rates (R_{dark}) were measured during the light period (between 10 am and 2 pm) in the glasshouses, at the prevailing day-time *T* of each treatment as well as at a common temperature of 30°C for ND leaves. In call cases, A_n was measured first, with the following settings: 1000 µmol m^{-2} s^{-1} photosynthetic photon flux density (PPFD), relative humidity of 60–70%, 400 ppm reference CO_2, and a flow rate of 500 µmol s^{-1}. Photosynthesis was measured when CO_2 concentrations in the sample IRGA had stabilized, typically within 10 minutes of exposure to 1000 µmol m^{-2} s^{-1} PPFD. Thereafter, R_{dark} was measured as above but with the flow rate slowed to 300 µmol s^{-1} and turning off the light source for at least 30 minutes of darkness before taking measurements.

Gas exchange measurements using using Walz chambers

High resolution temperature response curves of R_{dark} and light-saturated A_n were made on intact ND leaves using two matched LI-6400XT portable gas exchange systems (Li-Cor, Lincoln, NE, USA) each connected to a 14 x 10 cm well-mixed, temperature-controlled Walz Gas-Exchange Chamber 3010-GWK1 (Heinz Walz GmbH, Effeltrich, Germany). For each temperature-response curve, leaf *T* was measured with a small-gauge wire copper constantan thermocouple pressed against the lower surface of the leaf and attached to a LI-6400 external thermocouple adaptor (LI6400-13, Li-Cor Inc., Lincoln, NE, USA) that enabled leaf temperature to be recorded by the LI-6400XT. As leaves were heated, net CO_2 exchange was recorded at 30 s intervals using the LI-6400XT portable gas exchange systems fitted with an empty and closed 6 cm^2 chamber that was plumbed into the airstream exiting the Walz leaf chamber (Fig. S1). A_n was measured as described for the 6 cm^2 cuvette but using a Walz LED-Panel RGBW-L084 light source (Heinz Walz GmbH, Effeltrich, Germany). A_n was monitored as leaves were heated at 1°C min^{-1} from 20 to 45°C. A water trap was used to remove water vapour, as transpiration from whole intact leaves was incompatible with Licor instrumentation. Therefore, stomatal conductance (g_s) and associated water parameters were not recorded. For R_{dark}, on separate leaves to those used for measuring A_n, the flow rate was reduced to 300 µmol s^{-1}, the light source was

turned off, and the chamber was covered with a black cloth, before increasing the leaf temperature in steps of 1°C min^{-1}, from 20 to 60°C. In parallel to quantifying the temperature-response of R_{dark}, we measured minimal chlorophyll *a* fluorescence (F_o) in the presence of a low-intensity far-red light pulse (necessary to maintain PSII in the oxidized state) every 30 sec using a Mini-PAM portable chlorophyll fluorometer (Heinz Walz, Effeltrich, Germany) fitted above the glass surface of the leaf chamber. The temperature at which F_o increased was used as an indication of heat-induced damage to photosystem II, which we hereafter refer to as T_{crit}, calculated using the template of O'Sullivan *et al.* (2013). At the cessation of measurements, leaves were photographed and analysed for leaf area using ImageJ software (Abramoff, Magelhaes, & Ram, 2004). Leaves were stored in paper bags, oven-dried at 70°C for two days and weighed to obtain the dry mass. Quadratic equations were fit to A_n temperature curves and the x- and y-axis values corresponding to the vertex taken as the *T*-optimum (T_{opt}) and A_n-optimum (A_{opt}) of net assimilation, respectively. For the R_{dark} temperature curves, the x- and y-axis values corresponding to the maximum recorded R_{dark} were taken as the *T* at which R_{dark} reached a maximum (T_{max}) and the maximum R_{dark} value recorded (R_{max}), respectively.

Leaf elongation rates

The leaf elongation rates (LER) of four leaves from separate plants from each temperature regime were measured at five separate time-points over a 24 h period. Measurements were made using a ruler, starting from the ligule of the second youngest leaf to its tip.

Statistical analysis

For all *T*-treatments and collection times, four separate leaves from four separate previously unsampled plants, one plant from each of the four hydroponic tanks (pot replicates) were sampled. One-way Analysis of Variance (ANOVA) was performed on R_{dark} and A_n gas-exchange experiments comparing temperature treatments. Two-way ANOVA was performed on LMA and protein, starch, and sugar concentrations comparing time of sampling and temperature treatments. Gas-exchange and leaf biochemical statistical analysis was performed using GraphPad Prism (v 7) software. Statistical analysis of transcript abundance was performed using *R* statistical software (v 3.6.1) and packages as mentioned above.

Data availability

RNA-seq data is available under the GEO identifier GSE136045.

Results

Molecular and biochemical responses of leaves to T

Quantitative PCR was performed on specific genes of interest to elucidate the genetic response of pre-existing (PE) leaves exposed to a change in *T* (Fig. 1). Apart from a sharp rise 6 h into the 40/35°C *T*-transfer, there was a general reduction in transcript abundance of *cytochrome c oxidase* (*cox*), a gene encoding the central respiratory electron transport chain. This reduction occurred in leaves transferred to 25/20°C and 40/35°C, over the seven days post-transfer period, . Two genes encoding respiratory proteins that potentially reduce the production of ATP – *alternative oxidase* (*aox*) and *uncoupling protein* (*ucp*) – both showed an initial increase in expression within the first 24 h of transfer to the hotter 40/35°C, followed by a decline to 30/25°C levels by 48 h. The photosynthetic electron transport gene *ferredoxin NADP reductase* (*fnr*), and the Calvin/Benson cycle gene *phosphoribulokinase* (*prk*) generally showed an increase in expression in the first 48 h at 40/35°C before being supressed for up to 5 days post-transfer. *Sucrose phosphate synthase* (*sps*), involved in the synthesis of sucrose from its precursors, also initially spiked in the first 24 h following transfer to 40/35°C, before being transiently suppressed. Both *sps* and the respiratory and photosynthetic genes – apart from *aox* – followed a similar expression profile when heat-treated, suggesting that assimilate production/consumption and sucrose synthesis were coordinated in response to heat perturbations. In general, the greatest perturbation to gene expression occurred within the first 24 h after transfer.

Based on the qPCR results, we conducted RNA-seq at two, six and 24 h after transfer of PE leaves to new *T*. Following data quality control and filtering, transcript abundance of 19,308 rice genes were retained for differential expression testing. Around 20 M reads were obtained per sample, which were aligned to the Os-Nipponbare-Reference-IRGSP-1.0 rice reference genome (Data Set S1). Principal component analysis showed a substantial treatment effect on gene expression for the heat-exposed leaves (40/35°C) during the first six hours after *T*-transfer compared to the other two 30/25°C and 25/20°C growth regimes (Fig. 2). Globally, there was little gene expression variation between the cold (25/20°C) and the warm (30/25°C) control conditions. After 24 h of growth at new *T*-regimes, limited variation in gene expression was observed between all of the three *Ts* (Table S3).

To assess changes in the expression of individual genes to the hot or cold treatments, differentially expressed genes were identified at each time point by comparison to the warm control expression levels (Data Set S2). There were very few genes differentially expressed under the cold conditions, only six genes in total (Table S3). By contrast, under hot conditions, there were 1,818 and 1,465 genes differentially expressed after two and six hours, respectively. After 24 hours, there were no differentially expressed genes under the hot conditions compared to the control plants. There was

a significant overlap between the genes differentially expressed after two and six hours of heat treatment, (Fig. 3a, b). In total, 30% of the genes upregulated after six hours were already upregulated by two hours, and 38% of genes downregulated after six hours were already downregulated by two hours. Many of the remaining genes that were significantly different in transcript abundance only after six hours were already trending in the same direction at the two-hour time point, but the difference compared to the controls did not pass the significance threshold (Fig. 3 c). Overall, these results show that there are significant short-term changes in transcript abundance in rice plants exposed to heat stress. The expression profiles of samples exposed for two and six hours show consistent changes; however, some of the changes peak at two hours and others peak at six hours and most changes dissipate within 24 hours.

In total, the heat treatment led to the up- and down-regulation of 1,337 and 1,446 genes, respectively. To investigate the extent to which these genes have a photosynthetic or respiratory function, we first examined expression of genes involved in photosynthesis, glycolysis, TCA and mitochondrial electron transport using MapMan pathway annotations (Fig. S2-4) (Thimm et al., 2004). This qualitative analysis revealed that the expression of only a small number of photosynthetic/respiratory genes were affected. To extract a list of high-confidence differentially expressed respiration-related genes, we manually curated a list of rice loci with homology to Arabidopsis respiration genes (Data Set S3). Using this list, we found that eight genes were differentially expressed at high temperature, with two genes downregulated more than 2-fold: *aox* and ATP-dependent *phosphofructokinase* (Table 1). The seemingly conflicting result of an initial increase in *aox* from the qPCR results, but a decline in *aox* during the same period from the RNA-seq results, can be explained by our qPCR primers targeting the *aox1a* isoform while the RNA-seq identified a decline in the *aox1c* isoform (Data Set S3).

It is interesting that in addition to the increase in *aox* and *ucp* gene expression, the expression of an external NAD(P)H dehydrogenase also increased, while that of Complex II decreased significantly (Table 1). Together these changes suggest that an increase in non-phosphorylating electron transport occurred in response to exposure to higher *T*, at the expense of electron transport coupled to ATP synthesis, at least in the short term. The increase in external NAD(P)H dehydrogenase gene expression may also indicate an increased need for mitochondrial oxidation of excess reductant produced in the chloroplast at higher *T*.

Given the relatively small effect of the heat treatment on the expression of respiration- or photosynthesis-related genes, we next performed Gene Ontology enrichment analysis. This revealed a notable enrichment for genes involved in primary metabolism (eg GO:0044238) and response to abiotic stimuli (eg GO:0050896), as well as in many biosynthetic pathways (Fig 4).

Protein abundance (expressed on a leaf area basis) of key mitochondrial electron transport components – CYTOCHROME C OXIDASE (COX) subunit II, ALTERNATIVE OXIDASE (AOX) and UNCOUPLING PROTEIN (UCP) – were determined by Western blots in PE leaves 6 h and one-day after *T*-transfer, and in newly developed (ND) leaves that formed under each prevailing growth *T* (Fig. 5, Fig. S4). The cold (20/25°C) and heat (40/35°C) treatments did not affect the total protein concentration of leaves, at any time after *T*-transfer (Table S4). As was the case for gene expression, there was a significant decline in COX subunit II protein abundance after 24 h. COX subunit II also declined in abundance in ND leaves when grown at 40/35°C compared to 25/20°C (Fig. 5a). We assume the changes observed in COX subunit II reflect changes in abundance of the entire complex. The abundance of AOX and UCP protein did not vary in response to growth *T* or duration of exposure to heat for either PE or ND leaves, despite the initial spike in *aox* and *ucp* gene expression after transfer to 40/35°C (Fig. 1). Interestingly two bands of AOX that varied relative to one another with temperature treatment were evident in the Western blot (Fig. S5). This is consistent with the fluctuations in expression of different *aox* genes noted above. Patterns of protein abundance were similar when the analysis was standardised to dry mass or porin abundance (Fig. S6). Porin is a voltage-dependent channel protein located at the outer membrane of mitochondria and is widely used as a proxy for mitochondrial surface area due to its stability under a wide range of environmental conditions (Noguchi, Taylor, Millar, Lambers, & Day, 2005; Shane et al., 2004). Thus, the matching results using leaf area, dry mass or porin abundance indicate that the decline in COX abundance with increased *T* was not a result of changes in Leaf Mass to Area ratio (LMA) or reduced mitochondria per unit area of leaf. There was a trend for the abundance of Rubisco to decline with the amount of time a leaf developed under 40/35°C (Fig. 5d), although there were no statistically significant *T* or developmental stage effect.

LMA and starch, glucose, fructose and sucrose concentrations were measured in PE leaves one and seven days after *T*-transfer, and in ND leaves at the prevailing temperature (Table 2). LMA did not change significantly in response to *T*, for either transferred PE leaves or ND leaves, similar to previous observations in rice over a similar *T* range (Nagai & Makino, 2009). However, ND leaves did exhibit significantly greater LMA than PE transferred leaves, suggesting an effect of leaf rank on LMA. Transferred PE and subsequently formed ND leaves exhibited consistently lower starch concentrations with increasing *T* and significantly lower starch with extended duration of development at the prevailing *T*. Unlike the dynamic responses of leaf starch concentrations to *T* change, concentrations of soluble sugars were remarkably stable across both PE and ND leaves, in terms of both *T*-regime and exposure time. Negative correlations between R_{dark} and soluble sugars were

observed among leaves within each individual *T* treatment but not among the three *T* treatments (Table S5).

CO_2 flux in responses to T

How molecular changes altered the physiological performance of rice carbon metabolism at differing growth *T* was investigated through gas-exchange measurements. Rates of A_n and R_{dark} are here presented on a dry mass (DM) basis, noting that the patterns are similar when expressed on a leaf area basis (Fig S7), reflecting the fact that growth *T* had no significant effect on LMA (Table 2). A significant change in both A_n and R_{dark} (using mid-sections of leaves placed in Licor 6400 3 x 2 cm chambers) occurred within the first 24 h of transfer to a 40/35°C *T*-regime for PE leaves, with A_n falling and R_{dark} increasing when measured at the prevailing growth *T* (Fig. 6). This was followed by stabilisation at the new rate over the subsequent six days. By contrast, A_n and R_{dark} remained relatively constant at both 30/25°C and 25/20°C over a seven-day period monitoring period. Interestingly, rates of R_{dark} for the 30/25°C treated plants decreased from day 3 to 7, compared to the first three days, resulting in slightly lower rates of R_{dark} than for the 25/20°C treated plants by day 7. This possibly reflects temperature-dependent differences in leaf senescence rates. As it could not be controlled, relative humidity in the 40/35°C glasshouse room (Fig. S8) was substantially lower than the other two rooms, leading to reduced humidity during gas-exchange measurements (Fig. 6c). As a consequence, the vapour pressure deficit between the leaf and surrounding air (VPD_{Leaf}) increased over the first seven days in PE leaves transferred to 40/35°C, resulting in a dramatic difference by day seven (Fig. 6d). The higher VPD_{Leaf} coincided with lower g_s in 40/35°C treated leaves at days three, five and seven, and lower intercellular to ambient CO_2 concentration ratios (C_i/C_a) at days five and seven (Fig. 6e, f). However, for the first two days post transfer both VPD_{Leaf} and g_s were similar between the three growth *T*s, Therefore, the decline in A_n and changes in transcript abundance within one day of transfer to 40/35°C were not attributable to water relations. Over the longer-term, water relations may have contributed to a slight reduction in C_i/C_a, but not enough to influence A_n, with A_n being stable from one to seven days after transfer irrespective of changes in g_s and C_i/C_a (Fig. 6b). The changes in g_s were not substantive enough to change leaf *T*, which was stable over the seven days, with both air *T* and leaf *T* deviating by less than 2°C from the set room *T* (Fig. S8).

Short-term temperature response curves of entire ND leaves that formed at each prevailing growth *T* regime were quantified over a 20 to 60°C range using the Walz large leaf chamber (Fig. 7; refer to Figure S9 for area-based rates and Table S6 for quadratic equations fit to curves). Over most of the range of measuring *T*s, leaves developed at 25/20°C exhibited higher rates of R_{dark} than those

developed under the other two *T*-regimes. Rates were lowest in leaves developed at 40/35°C (Fig. 7a). When normalised to rates at 30°C, differences in R_{dark} were less pronounced (Fig. 7b), indicating that while R_{dark} at a given measuring *T* was affected by growth *T*, the general shape of the R_{dark}-*T* curves remained largely similar across the three treatments. These observations are consistent with a Type II (changes in baseline) rather than Type I (changes in Q_{10}, the increase in R_{dark} with a 10°C increase in *T*) respiratory acclimation response (Atkin & Tjoelker, 2003). Importantly, while respiratory thermal acclimation occurred, it was not sufficient to result in R_{dark} being homeostatic across the three growth *T* treatments. As a result, R_{dark} measured at the growth *T* was significantly greater in the leaves developed under hot conditions than under the other two treatments (Table 3). Growth *T* also had a significant effect on the measuring *T* at which R_{dark} and A_n reached their maximum rates, with leaves developed under high *T* exhibiting higher *T*-maxima than control 30/25°C leaves (Table 3). When measured at the prevailing growth *T* of each treatment, mass-based rates of light-saturated A_n were stable (i.e. homeostatic), further supporting the occurrence of strong thermal acclimation of A_n in ND leaves (Fig. 7), contrary to PE leaves (Fig. 6). The temperature at which PSII lost functionality (T_{crit}) tended to increase with growth *T* (being 3.8°C higher in the hot-grown plants compared to those grown at 25/20°C), although the differences were not statistically significant at $p<0.05$ (Table 3). The high degree of thermal acclimation exhibited by photosynthesis resulted in the ratio of R_{dark} to A_n being lowest in the hot-grown plants, particularly at high measuring *T* (Fig. 8a); at a measuring *T* of 40°C, hot-acclimated plants exhibited R_{dark}/A_n ratios that were 50% lower than those measured for their cold-grown counterparts. Further evidence that rice acclimated to heat is seen in the fact that leaf elongation rates – taken over the day and night period – were faster for the 40/35°C grown plants at all times (Fig. 8b). Interestingly, A_n of PE leaves ranged from 1.2 to 1.8 μmol g^{-1} DM s^{-1} (Fig. 6), substantially faster than the 0.6 μmol g^{-1} DM s^{-1} in ND leaves (Fig. 7). The former were obtained from measurements on mid-leaf sections placed in a 6 cm^2 chamber, while the latter were obtained from whole leaves placed in a 14 x 10 cm Walz chamber. The lower A_n rates in the latter might reflect a lower proportion of mesophyll cells per unit of area or DM across whole blades compared to the mid-blade section.

Discussion

Our study investigated the response of photosynthetic and respiratory metabolism to short- and long-term changes in growth *T* – the highest of which is indicative of heat-wave *T*s – to explore: (1) the extent of thermal acclimation of photosynthesis and respiration; and, (2) what underlying changes in gene expression and protein abundance occur during the acclimation process. The results demonstrate

that the process of acclimation begins with abrupt changes in gene expression in PE leaves within the first 24 h of heat exposure, followed by a return to homeostatic gene expression (Fig. 1). Importantly, the abundance of the key energy-conserving respiratory protein, COX, declines in abundance when pre-existing leaves are heat-treated for 24 hours, with this phenotype being maintained in newly-developed leaves formed at 40/35°C (Fig. 5). This decline in COX was linked to a slight decline in overall rates of R_{dark} (Fig. 7). The results support the hypothesis that acclimation of photosynthesis and dark respiration are asynchronous in rice, but contrary to observations in non-crop species (Campbell et al., 2007), light-saturated A_n acclimated to a greater extent than R_{dark} (Fig. 7; Table 3). This ability to maintain photosynthetic carbon gain at 40°C is likely to be of crucial importance in helping rice maintain growth during heat-wave conditions.

Acclimation to changes in T are rapid and involve a multitude of genes

There was a substantial change in the gene expression profile of rice leaves shifted from 30°C to 40°C within the first 24 h of transfer (Figs. 1, 2, 3, and 4). As might be expected, the largest number of gene expression perturbations were in primary and cellular metabolic processes (Fig. 4). This extensive metabolic response aligns with the instability in R_{dark} and A_n fluxes over the initial 24 h post *T*-transfer (Fig. 6), which would have contributed to a metabolic imbalance through changes in assimilate supply and demand. Interestingly, the most responsive genes to the initial exposure to heat among upregulated genes were genes involved in biosynthetic processes (Fig. 4) suggesting a stimulation of growth. This is supported by the longer-term increase in leaf elongation rates observed in the 40/35°C grown plants.

When analysed in more detail, we observed that heat induced genes linked to energy dissipation (*aox* and *ucp*) over the first 24 h of 40°C heat exposure (Fig. 1, Table 1). AOX and UCP are involved in the diversion of electrons for formation of proton gradients and subsequent ATP synthesis (Krauss, Zhang, & Lowell, 2005; Vanlerberghe, 2013). Past work has shown that overexpressing *aox* in young rice seedlings imparts a benefit on growth under a *T* of 37°C for eight days, which was attributed to a reduction of excessive proton motive force and reactive oxygen species (Murakami & Toriyama, 2008). Given that AOX and UCP both divert electrons away from ATP synthesis under conditions of high reductant supply, the rapid upregulation of these genes following the initial changes in growth *T* – with rapid stimulation of R_{dark} and presumably greater reduction of ubiquinone pools (UQ) – indicates that there may have been a temporary imbalance between NAD(P)H supply and demand for ATP. The initial increases in *aox* and *ucp* gene expression (Fig. 1) did not translate into increased total AOX and UCP protein abundance (Fig. 5). However, qPCR results indicate upregulation of the *aox1a* isoform, responsive to abiotic stress in Arabidopsis mitochondria (Clifton, Millar, & Whelan, 2006; Shapiguzov

et al., 2019), while over the same period RNA-seq analysis indicated a significant decline in a separate *aox1c* isoform. It is possible that the AOX1C isoform is less tolerant of high temperatures and therefore is partially replaced by the AOX1a isoform. In this context it is interesting that in Arabidopsis AOX1a is the major stress-inducible isoform. Since AOX operates as a non-covalently linked dimer (Siedow & Umbach, 2000), the change in the relative expressions of *aox1a* and *1c* isoforms may also indicate a change in the conformation of the AOX dimer, with a different mix of homo- and hetero-dimers in response to heat. This suggests that AOX may have shifted to a more heat-tolerant conformation at 40/35°C, at least when the initial shock was imposed. This is an illustration that enzyme isoforms can be an important part of abiotic stress responses that can be easily overlooked when only considering total protein abundance.

The limited gene induction when leaves were transferred from 30 to 25°C (Fig. 3c) suggests that a shift to this colder growth *T* did not significantly perturb metabolic processes in rice leaves, consistent with the limited PE leaf response of R_{dark} or A_n when exposed to the cold (Fig. 6). However, cold-responsive transcriptional regulators and associated changes in metabolism expected from cold exposure (Zhu, Dong, & Zhu, 2007) must have been triggered by the colder *T*s. Regulatory adjustments did indeed occur in ND rather than PE leaves, with R_{dark} at a given *T* being higher in the cold-grown ND leaves (Fig. 7), and homeostasis of A_n being reached in ND leaves when measured at the prevailing growth *T* (Table 3, Fig. 7).

The most evident longer-term acclimation response is reduced COX abundance

The clearest biochemical response to increasing growth *T*, both in PE and ND leaves, was a decline in the abundance of COX (Fig. 5). A decline in COX has been reported for rice roots when grown at 25°C relative to 15°C (Kurimoto, Millar, Lambers, Day, & Noguchi, 2004). Conversely, COX content increased in *Arabidopsis thaliana* leaves grown at 5°C relative to 21°C (Armstrong et al., 2008). In all these cases, COX protein content and rates of respiration at a common measuring *T* (including in our study; Fig. 5 and Fig. 7) decreased when plants grew at hotter *T*, suggesting that thermal acclimation results in changes not only in overall rates of respiration but also in the capacity to produce ATP. The acclimation response was rapid as COX declined in abundance by 24 h after 40°C *T* transfer in PE leaves (Fig. 5).

The decline in COX abundance with hotter growth *T* is intriguing. If COX activity became rate-limiting, it is likely that more ROS would be produced as the UQ pool would quickly become over-reduced. However, other reports suggest that the UQ redox state is relatively stable, including during changes in *T*, despite higher R_{dark} (Covey-Crump et al., 2007; Wagner & Wagner, 1995). If we

assume that UQ redox poise was also stable during the greater R_{dark} at the hottest growth T in our experiments, there are two possible explanations. (1) The absolute flux of electrons through COX actually increased despite the decrease in protein abundance. This could be due to COX capacity being far greater than the capacity of the overall mETC. But since increasing Ts stimulates the relative activity of enzymes (Copeland, 2000), it is possible that the smaller amount of COX protein had higher activity. In other words, the plants could make do with less COX at hotter T. (2) Alternatively, activation of AOX at the higher T may have occurred to supplement COX activity thereby preventing overload of the UQ pool. Measuring T-dependent *in vivo* ^{18}O fluxes through COX and AOX, as well as leaf ATP content is required to determine terminal oxidase activity and ATP synthesis. Understanding what, if any, biological benefit arises from synthesising less COX at warmer growth T is another important consideration. Alternatively, a reduction in COX might be a consequence of heat directly interfering with its synthesis. In support of this, a recent report shows that COX abundance and capacity in Arabidopsis is significantly reduced by knocking out a HSP70 isoform, suggesting that heat in some way interacts with COX formation (Wei et al., 2019).

Acclimation of R_{dark} and A_n is asynchronous in rice

The R_{dark}/A_n ratio increased with short-term increases in measuring T (Fig. 8), reflecting the fact that R_{dark} is more temperature dependent than is A_n. R_{dark}/A_n ratios were similar in 25 and 30°C grown leaves, when measured at the prevailing growth T of each treatment (i.e. R_{dark}/A_n was homeostatic). Thus, the acclimation process led to the balance between carbon gain and release being maintained across this moderate range of growth Ts (Fig. 8). Acclimation was not, however, sufficient to maintain homeostasis of R_{dark}/A_n in 40°C grown plants (Fig. 8). Similar results of R_{dark}/A_n ratios in leaves and whole plants remaining relatively stable over moderate but not extremely high T have been reported (Atkin, Scheurwater, & Pons, 2006, 2007; Campbell et al., 2007; Drake et al., 2016; Loveys et al., 2003). Different to past studies, our findings in rice show that homeostasis of R_{dark}/A_n is largely the result of maintenance of A_n more than through a marked reduction in rates of R_{dark}. Our results categorically show A_n acclimates to a greater extent than R_{dark} in rice, supporting previous studies of rice that collectively point to greater A_n than R_{dark} acclimation capacity (Bahuguna et al., 2017; Glaubitz et al., 2014; Kurimoto, Millar, et al., 2004; Mohammed et al., 2013; Nagai & Makino, 2009; Yamori et al., 2010), and field studies that infer limited rice R_{dark} acclimation capacity (Peng et al., 2004; Welch et al., 2010). However, for many plant functional types, including temperate grasses, the opposite occurs; R_{dark} acclimates to a greater extent than A_n (Campbell et al., 2007; Ow, Griffin, Whitehead, Walcroft, & Turnbull, 2008; Way & Oren, 2010; Way & Sage, 2008; Yamori et al., 2005). In this context, it should be noted that the previous studies are of species from temperate rather than

tropical habitats, raising the question of whether, beyond rice, tropical grasses generally have asynchronous acclimation favouring A_n. The homeostasis of A_n and superior LER of hot-grown ND rice leaves was more remarkable when viewed alongside evidence that prolonged exposure to drier air was closing stomata and presenting slight reductions in CO_2 availability, at least in PE leaves (Fig. 6). There is evidence that stomata close following a *T*-dependent increase in VPD_{Leaf}, with the mechanism yet uncharacterised but likely involving guard cell sensing of water potential below the epidermis (Peak & Mott, 2010; Shope, Peak, & Mott, 2008). It seems that declining VPD_{Leaf} triggers stomatal closure in rice, even with unlimited root water supply.

As noted earlier, in recent years, rice yields have declined in response to increased daily mean *T*s, with the decline being more strongly correlated with increasing night rather than day *T*s (Peng et al., 2004; Welch et al., 2010). Our finding that A_n is homeostatic across growth *T*, whereas R_n is not (Table 3) – underpinned by greater acclimation of photosynthesis than respiration – suggests that one reason why yields are declining with increasing night temperatures is because high temperatures stimulate respiratory CO_2 release. This would have a negative effect on daily net carbon gain, and thus the ability to accumulate biomass in the lead up to anthesis.

Potential implications of rice leaf acclimation and starch concentration on crop yield

We found that soluble sugar concentrations of rice leaves were remarkably stable, irrespective of growth *T* or developmental time at each growth *T* (Table 2). Maintaining soluble sugar homeostasis is an important physiological requirement for many plant species, achieved through balancing CO_2 uptake and release in source leaves with sugar export to sink tissues (Rolland, Moore, & Sheen, 2002). Homeostasis of sucrose concentrations in rice leaves has been observed even when carbon demand by sink tissues is limited [e.g. reduced partitioning of sugars to grain (Wang et al., 2008)]. In our study, homeostasis of soluble sugar concentrations occurred even at 40°C, where rates of R_{dark} where significantly higher than in plants at the cooler growth *Ts*. Associated with the maintenance of sugar concentrations was a *T*-dependent decline in starch concentration, both in PE and ND leaves (Table 2). For PE leaves exposed to 40°C, assimilate supply declined, particularly for 40°C transferred leaves, due to a marked increase in R_{dark} and a decline in A_n (Fig. 6). Starch content also significantly declined with developmental duration under high *T*, contrary to soluble sugar concentrations (Table 2). It seems likely, therefore, that the reason soluble sugars did not significantly decline at warmer *T* for PE leaves – even though assimilate supply fell – was a greater draw-down in the starch pool to maintain soluble sugar concentrations (i.e. a reliance on stored assimilate). Other studies [e.g. on the temperate tree *Populus tremula* (Hüve et al., 2012)] have highlighted the importance of starch degradation in

maintaining soluble sugar concentrations, particularly under conditions that stimulate CO_2 release by respiration. Interestingly, in our study, ND leaves exhibited reduced starch concentrations while also maintaining assimilate supply; one explanation for this might be that the decline in starch and maintenance of sugars of ND leaves was linked to the increased leaf elongation rates we observed for 40°C ND leaves (Fig. 8b), with increased growth (i.e. sink demand) necessitating a greater supply of sugars mediated by the starch pool (Stitt & Zeeman, 2012).

The decline in starch concentrations for PE and ND leaves at 40°C (Table 2) has interesting implications for rice development and yield. Starch is stored in the stems in the late vegetative stage of rice, and accounts for a large proportion of the carbon accumulated in seeds, a process that is detrimentally affected by heat stress (Blum, Sinmena, Mayer, Golan, & Shpiler, 1994; Impa et al., 2018; Morita & Nakano, 2011; Yang & Zhang, 2005). Other studies using the IR64 cultivar exposed to hot night temperatures have shown an increase in R_{dark} and associated cost to vegetative growth and starch content of panicles, ultimately reducing yield (Bahuguna et al., 2017; Glaubitz et al., 2014). The reduced storage of starch in leaves with increasing T that we observed at the vegetative stage – assuming it did not reflect diversion of starch to stems – would suggest reduced potential for the storage of starch in stems and a penalty to yield of rice growing in warmer environments. This would be particularly true for rice plants exposed to transient extreme T – such as during heat waves – as we postulate the reduction in starch for PE leaves was due to a reduction in assimilate acquisition due to stimulated R_{dark} and supressed A_n. However, ND leaves did show reduced starch concentration, not as a result of reduced assimilate acquisition, but most likely associated with an increase in growth rates (Table 2; Fig. 8). Thus, it is likely that rice will experience different limitations on yield depending on the duration of thermal changes, with shorter-term exposure to rising T – over a period in which tissue cannot develop anew – likely leading to a greater suppression of yield than leaves developed under the prevailing growth T. Rice may even experience increased yield with sustained mild warming of both night and particularly day T. However, yield potential is dependent on whether heat-dependent changes in growth at the vegetative stage of rice positively contributes to yield, which may be true (Glaubitz et al., 2014; Scafaro et al., 2018), and not simply accelerate development and shorten the time to flowering.

Conclusions

Overall, the results we present here demonstrate that both leaf respiration and photosynthesis can acclimate in rice but the extent of acclimation is asynchronous and dependent on the timeframe of T exposure. Warmer growth T of 40°C relative to 25°C will have a greater impact on rice CO_2 flux,

metabolic pathways, starch concentration and ultimately growth. Consequently, rice growing in a warmer climate with more extreme heating events will likely experience *T*-dependent alterations in growth and yield. The duration and intensity of *T* changes, together with complex interactions between assimilate acquisition, storage and utilisation will determine if this warmer environment will be beneficial or detrimental to rice productivity over the coming decades. We suggest that enhancing the acclimation capacity of R_{dark} for rice at warmer growth *T* – potentially through COX, AOX and UCP regulation – could be a key target for improving rice productivity in a warmer world.

Acknowledgements

We thank Assoc. Prof Spencer Whitney for providing Rubisco antibody. The support of the Australian Research Council (ARC) Centre of Excellence in Plant Energy Biology (CE140100008) to OA, BP and JM is acknowledged. The authors have no conflict of interest to declare.

References

Abramoff, M. D., Magelhaes, P. J., & Ram, S. J. (2004). Image Processing with ImageJ. *Biophotonics International, 11*(7), 36-42.

Armstrong, A. F., Badger, M. R., Day, D. A., Barthet, M. M., Smith, P. M. C., Millar, A. H., . . . Atkin, O. K. (2008). Dynamic changes in the mitochondrial electron transport chain underpinning cold acclimation of leaf respiration. *Plant, Cell & Environment, 31*(8), 1156-1169.

Atkin, O. K., Bruhn, D., Hurry, V. M., & Tjoelker, M. G. (2005). Evans Review No. 2: The hot and the cold: unravelling the variable response of plant respiration to temperature. *Functional Plant Biology, 32*(2), 87-105.

Atkin, O. K., Scheurwater, I., & Pons, T. L. (2006). High thermal acclimation potential of both photosynthesis and respiration in two lowland *Plantago* species in contrast to an alpine congeneric. *Global Change Biology, 12*(3), 500-515.

Atkin, O. K., Scheurwater, I., & Pons, T. L. (2007). Respiration as a percentage of daily photosynthesis in whole plants is homeostatic at moderate, but not high, growth temperatures. *New Phytologist, 174*(2), 367-380.

Atkin, O. K., & Tjoelker, M. G. (2003). Thermal acclimation and the dynamic response of plant respiration to temperature. *Trends in Plant Science, 8*(7), 343-351.

Badger, M. R., Björkman, O., & Armond, P. A. (1982). An analysis of photosynthetic response and adaptation to temperature in higher plants: temperature acclimation in the desert evergreen *Nerium oleander* L*. *Plant, Cell & Environment, 5*(1), 85-99.

Bahuguna, R. N., Solis, C. A., Shi, W., & Jagadish, K. S. V. (2017). Post-flowering night respiration and altered sink activity account for high night temperature-induced grain yield and quality loss in rice (Oryza sativa L.). *Physiologia Plantarum, 159*(1), 59-73.

Berry, J., & Bjorkman, O. (1980). Photosynthetic response and adaptation to temperature in higher plants. *Annual Review of Plant Physiology, 31*(1), 491-543.

Bhardwaj, A. R., Joshi, G., Kukreja, B., Malik, V., Arora, P., Pandey, R., . . . Agarwal, M. (2015). Global insights into high temperature and drought stress regulated genes by RNA-Seq in economically important oilseed crop Brassica juncea. *BMC Plant Biology, 15*(1), 9.

Blum, A., Sinmena, B., Mayer, J., Golan, G., & Shpiler, L. (1994). Stem reserve mobilisation supports wheat-grain filling under heat stress. *Functional Plant Biology, 21*(6), 771-781.

Campbell, C., Atkinson, L., Zaragoza-Castells, J., Lundmark, M., Atkin, O., & Hurry, V. (2007). Acclimation of photosynthesis and respiration is asynchronous in response to changes in temperature regardless of plant functional group. *New Phytologist, 176*(2), 375-389.

Clifton, R., Millar, A. H., & Whelan, J. (2006). Alternative oxidases in Arabidopsis: A comparative analysis of differential expression in the gene family provides new insights into function of non-phosphorylating bypasses. *Biochimica et Biophysica Acta (BBA) - Bioenergetics, 1757*(7), 730-741.

Copeland, R. A. (2000). *Enzymes: A Practical Introduction to Structure, Mechanism, and Data Analysis* (Second Edition ed.). New York, NY: JOHN WILEY & SONS.

Covey-Crump, E. M., Bykova, N. V., Affourtit, C., Hoefnagel, M. H. N., Gardeström, P., & Atkin, O. K. (2007). Temperature-dependent changes in respiration rates and redox poise of the ubiquinone pool in protoplasts and isolated mitochondria of potato leaves. *Physiologia Plantarum, 129*(1), 175-184.

CSIRO, & BOM. (2018). *State of the Climate 2018*. Retrieved from Canberra, Australia: https://www.csiro.au/en/Research/OandA/Areas/Assessing-our-climate/State-of-the-Climate-2018

Drake, J. E., Tjoelker, M. G., Aspinwall, M. J., Reich, P. B., Barton, C. V. M., Medlyn, B. E., & Duursma, R. A. (2016). Does physiological acclimation to climate warming stabilize the ratio of canopy respiration to photosynthesis? *New Phytologist, 211*(3), 850-863.

Glaubitz, U., Li, X., Köhl, K. I., van Dongen, J. T., Hincha, D. K., & Zuther, E. (2014). Differential physiological responses of different rice (*Oryza sativa*) cultivars to elevated night temperature during vegetative growth. *Functional Plant Biology, 41*(4), 437-448.

Godfray, H. C. J., Beddington, J. R., Crute, I. R., Haddad, L., Lawrence, D., Muir, J. F., . . . Toulmin, C. (2010). Food security: the challenge of feeding 9 billion people. *Science, 327*(5967), 812-818.

Gorsuch, P. A., Pandey, S., & Atkin, O. K. (2010). Temporal heterogeneity of cold acclimation phenotypes in Arabidopsis leaves. *Plant, Cell & Environment, 33*(2), 244-258.

Hartmann, D. L., A.M.G. Klein Tank, M. Rusticucci, L.V. Alexander, S. Brönnimann, Y. Charabi, . . . Zhai, P. M. (2013). *Observations: Atmosphere and Surface. In: Climate Change 2013: The Physical Science Basis. Contribution of Working Group I to the Fifth Assessment Report of the Intergovernmental Panel on Climate Change*. Retrieved from Cambridge, United Kingdom and New York, NY, USA:

Hikosaka, K., Ishikawa, K., Borjigidai, A., Muller, O., & Onoda, Y. (2006). Temperature acclimation of photosynthesis: mechanisms involved in the changes in temperature dependence of photosynthetic rate. *Journal of Experimental Botany, 57*(2), 291-302.

Hu, T., Sun, X., Zhang, X., Nevo, E., & Fu, J. (2014). An RNA sequencing transcriptome analysis of the high-temperature stressed tall fescue reveals novel insights into plant thermotolerance. *BMC Genomics, 15*(1), 1147.

Hubbart, S., Peng, S., Horton, P., Chen, Y., & Murchie, E. H. (2007). Trends in leaf photosynthesis in historical rice varieties developed in the Philippines since 1966. *Journal of Experimental Botany, 58*(12), 3429-3438.

Hüve, K., Bichele, I., Ivanova, H., Keerberg, O., Pärnik, T., Rasulov, B., . . . Niinemets, Ü. (2012). Temperature responses of dark respiration in relation to leaf sugar concentration. *Physiologia Plantarum, 144*(4), 320-334.

Impa, S. M., Sunoj, V. S. J., Krassovskaya, I., Bheemanahalli, R., Obata, T., & Jagadish, S. V. K. (2018). Carbon balance and source-sink metabolic changes in winter wheat exposed to high night-time temperature. *Plant, Cell & Environment, 0*(ja).

Krauss, S., Zhang, C.-Y., & Lowell, B. B. (2005). The mitochondrial uncoupling-protein homologues. *Nature Reviews Molecular Cell Biology, 6*, 248.

Kurimoto, K., Day, D. A., Lambers, H., & Noguchi, K. (2004). Effect of respiratory homeostasis on plant growth in cultivars of wheat and rice. *Plant, Cell & Environment, 27*(7), 853-862.

Kurimoto, K., Millar, A. H., Lambers, H., Day, D. A., & Noguchi, K. (2004). Maintenance of growth rate at low temperature in rice and wheat cultivars with a high degree of respiratory homeostasis is associated with a high efficiency of respiratory ATP production. *Plant and Cell Physiology, 45*(8), 1015-1022.

Lanning, S. B., Siebenmorgen, T. J., Counce, P. A., Ambardekar, A. A., & Mauromoustakos, A. (2011). Extreme nighttime air temperatures in 2010 impact rice chalkiness and milling quality. *Field Crops Research, 124*(1), 132-136.

Law, C. W., Chen, Y., Shi, W., & Smyth, G. K. (2014). voom: precision weights unlock linear model analysis tools for RNA-seq read counts. *Genome Biology, 15*(2), R29.

Li, H., Handsaker, B., Wysoker, A., Fennell, T., Ruan, J., Homer, N., . . . Genome Project Data Processing, S. (2009). The Sequence Alignment/Map format and SAMtools. *Bioinformatics, 25*(16), 2078-2079.

Liao, Y., Smyth, G. K., & Shi, W. (2013a). featureCounts: an efficient general purpose program for assigning sequence reads to genomic features. *Bioinformatics, 30*(7), 923-930.

Liao, Y., Smyth, G. K., & Shi, W. (2013b). The Subread aligner: fast, accurate and scalable read mapping by seed-and-vote. *Nucleic Acids Research, 41*(10), e108-e108.

Loveys, B. R., Atkinson, L. J., Sherlock, D. J., Roberts, R. L., Fitter, A. H., & Atkin, O. K. (2003). Thermal acclimation of leaf and root respiration: an investigation comparing inherently fast- and slow-growing plant species. *Global Change Biology, 9*(6), 895-910.

McCarthy, D. J., Chen, Y., & Smyth, G. K. (2012). Differential expression analysis of multifactor RNA-Seq experiments with respect to biological variation. *Nucleic Acids Research, 40*(10), 4288-4297.

Mohammed, R., Cothren, J. T., & Tarpley, L. (2013). High night temperature and abscisic acid affect rice productivity through altered photosynthesis, respiration and spikelet fertility. *Crop Science, 53*(6), 2603-2612.

Morimoto, R. I. (1998). Regulation of the heat shock transcriptional response: cross talk between a family of heat shock factors, molecular chaperones, and negative regulators. *Genes & Development, 12*(24), 3788-3796.

Morita, S., & Nakano, H. (2011). Nonstructural carbohydrate content in the stem at full heading contributes to high performance of ripening in heat-tolerant rice cultivar Nikomaru. *Crop Science, 51*(2), 818-828.

Murakami, Y., & Toriyama, K. (2008). Enhanced high temperature tolerance in transgenic rice seedlings with elevated levels of alternative oxidase, OsAOX1a. *Plant Biotechnology, 25*(4), 361-364.

Nagai, T., & Makino, A. (2009). Differences Between Rice and Wheat in Temperature Responses of Photosynthesis and Plant Growth. *Plant & Cell Physiology, 50*(4), 744-755.

Neilson, K. A., Mariani, M., & Haynes, P. A. (2011). Quantitative proteomic analysis of cold-responsive proteins in rice. *Proteomics, 11*(9), 1696-1706.

Noguchi, K. O., Taylor, N. L., Millar, A. H., Lambers, H., & Day, D. A. (2005). Response of mitochondria to light intensity in the leaves of sun and shade species. *Plant, Cell & Environment, 28*(6), 760-771.

O'Leary, B. M., Asao, S., Millar, A. H., & Atkin, Owen K. (2018). Core principles which explain variation in respiration across biological scales. *New Phytologist, 0*(0).

O'sullivan, O. S., Weerasinghe, K. W. L. K., Evans, J. R., Egerton, J. J. G., Tjoelker, M. G., & Atkin, O. K. (2013). High-resolution temperature responses of leaf respiration in snow gum (Eucalyptus pauciflora) reveal high-temperature limits to respiratory function. *Plant, Cell & Environment, 36*(7), 1268-1284.

Ohama, N., Sato, H., Shinozaki, K., & Yamaguchi-Shinozaki, K. (2017). Transcriptional Regulatory Network of Plant Heat Stress Response. *Trends in Plant Science, 22*(1), 53-65.

Ow, L. F., Griffin, K. L., Whitehead, D., Walcroft, A. S., & Turnbull, M. H. (2008). Thermal acclimation of leaf respiration but not photosynthesis in Populus deltoides×nigra. *New Phytologist, 178*(1), 123-134.

Peak, D., & Mott, K. A. (2010). A new, vapour-phase mechanism for stomatal responses to humidity and temperature. *Plant, Cell & Environment, 34*(1), 162-178.

Peng, S., Huang, J., Sheehy, J. E., Laza, R. C., Visperas, R. M., Zhong, X., . . . Cassman, K. G. (2004). Rice yields decline with higher night temperature from global warming. *Proceedings of the National Academy of Sciences of the United States of America, 101*(27), 9971-9975.

Posch, B. C., Kariyawasam, B. C., Bramley, H., Coast, O., Richards, R. A., Reynolds, M. P., . . . Atkin, O. K. (2019). Exploring high temperature responses of photosynthesis and respiration to improve heat tolerance in wheat. *Journal of Experimental Botany, 70*(19), 5051-5069.

Quinlan, A. R., & Hall, I. M. (2010). BEDTools: a flexible suite of utilities for comparing genomic features. *Bioinformatics, 26*(6), 841-842.

Ramakers, C., Ruijter, J. M., Deprez, R. H. L., & Moorman, A. F. M. (2003). Assumption-free analysis of quantitative real-time polymerase chain reaction (PCR) data. *Neuroscience Letters, 339*(1), 62-66.

Reich, P. B., Sendall, K. M., Stefanski, A., Wei, X., Rich, R. L., & Montgomery, R. A. (2016). Boreal and temperate trees show strong acclimation of respiration to warming. *Nature, 531*(7596), 633-636.

Robinson, J. T., Thorvaldsdóttir, H., Winckler, W., Guttman, M., Lander, E. S., Getz, G., & Mesirov, J. P. (2011). Integrative genomics viewer. *Nature Biotechnology, 29*(1), 24-26.

Robinson, M. D., & Oshlack, A. (2010). A scaling normalization method for differential expression analysis of RNA-seq data. *Genome Biology, 11*(3), R25.

Robinson, M. D., & Smyth, G. K. (2007a). Moderated statistical tests for assessing differences in tag abundance. *Bioinformatics, 23*(21), 2881-2887.

Robinson, M. D., & Smyth, G. K. (2007b). Small-sample estimation of negative binomial dispersion, with applications to SAGE data. *Biostatistics, 9*(2), 321-332.

Rolland, F., Moore, B., & Sheen, J. (2002). Sugar Sensing and Signaling in Plants. *The Plant Cell, 14*, S185-S205.

Ruijter, J. M., Ramakers, C., Hoogaars, W. M. H., Karlen, Y., Bakker, O., van den Hoff, M. J. B., & Moorman, A. F. M. (2009). Amplification efficiency: linking baseline and bias in the analysis of quantitative PCR data. *Nucleic Acids Research, 37*(6), e45-e45.

Scafaro, A. P., & Atkin, O. K. (2016). The Impact of Heat Stress on the Proteome of Crop Species. In G. H. Salekdeh (Ed.), *Agricultural Proteomics Volume 2: Environmental Stresses* (pp. 155-175). Cham: Springer International Publishing.

Scafaro, A. P., Atwell, B. J., Muylaert, S., Reusel, B. V., Ruiz, G. A., Van Rie, J., & Gallé, A. (2018). A thermotolerant variant of rubisco activase from a wild relative improves growth and seed yield in rice under heat stress. *Frontiers in Plant Science, 9*, 1663.

Scafaro, A. P., Xiang, S., Long, B. M., Bahar, N. H. A., Weerasinghe, L. K., Creek, D., . . . Atkin, O. K. (2017). Strong thermal acclimation of photosynthesis in tropical and temperate wet-forest tree species: the importance of altered Rubisco content. *Global Change Biology, 23*(7), 2783-2800.

Seck, P. A., Diagne, A., Mohanty, S., & Wopereis, M. C. S. (2012). Crops that feed the world 7: Rice. *Food Security, 4*(1), 7-24.

Shane, M. W., Cramer, M. D., Funayama-Noguchi, S., Cawthray, G. R., Millar, A. H., Day, D. A., & Lambers, H. (2004). Developmental physiology of cluster-root carboxylate synthesis and exudation in *harsh hakea*. Expression of phosphoenolpyruvate carboxylase and the alternative oxidase. *Plant Physiology, 135*(1), 549.

Shapiguzov, A., Vainonen, J. P., Hunter, K., Tossavainen, H., Tiwari, A., Järvi, S., . . . Kangasjärvi, J. (2019). Arabidopsis RCD1 coordinates chloroplast and mitochondrial functions through interaction with ANAC transcription factors. *eLife, 8*, e43284.

Shen, C., Li, D., He, R., Fang, Z., Xia, Y., Gao, J., . . . Cao, M. (2014). Comparative transcriptome analysis of RNA-seq data for cold-tolerant and cold-sensitive rice genotypes under cold stress. *Journal of Plant Biology, 57*(6), 337-348.

Shope, J. C., Peak, D., & Mott, K. A. (2008). Stomatal responses to humidity in isolated epidermes. *Plant, Cell & Environment, 31*(9), 1290-1298.

Sidaway-Lee, K., Costa, M. J., Rand, D. A., Finkenstadt, B., & Penfield, S. (2014). Direct measurement of transcription rates reveals multiple mechanisms for configuration of the Arabidopsisambient temperature response. *Genome Biology, 15*(3), R45.

Siedow, J. N., & Umbach, A. L. (2000). The mitochondrial cyanide-resistant oxidase: structural conservation amid regulatory diversity. *Biochimica et Biophysica Acta (BBA) - Bioenergetics, 1459*(2), 432-439.

Smith, N. G., & Dukes, J. S. (2017). Short-term acclimation to warmer temperatures accelerates leaf carbon exchange processes across plant types. *Global Change Biology, 23*(11), 4840-4853.

Smyth, G. K., Michaud, J., & Scott, H. S. (2005). Use of within-array replicate spots for assessing differential expression in microarray experiments. *Bioinformatics, 21*(9), 2067-2075.

Stitt, M., & Zeeman, S. C. (2012). Starch turnover: pathways, regulation and role in growth. *Current Opinion in Plant Biology, 15*(3), 282-292.

Strand, A., Hurry, V., Henkes, S., Huner, N., Gustafsson, P., Gardestrom, P., & Stitt, M. (1999). Acclimation of Arabidopsis leaves developing at low temperatures. Increasing cytoplasmic volume accompanies increased activities of enzymes in the calvin cycle and in the sucrose-biosynthesis pathway. *Plant Physiology, 119*(4), 1387-1398.

Thimm, O., Bläsing, O., Gibon, Y., Nagel, A., Meyer, S., Krüger, P., . . . Stitt, M. (2004). mapman: a user-driven tool to display genomics data sets onto diagrams of metabolic pathways and other biological processes. *The Plant Journal, 37*(6), 914-939.

Tjoelker, M. G., Oleksyn, J., & Reich, P. B. (2001). Modelling respiration of vegetation: evidence for a general temperature-dependent Q_{10}. *Global Change Biology, 7*(2), 223-230.

Tjoelker, M. G., Reich, P. B., & Oleksyn, J. (1999). Changes in leaf nitrogen and carbohydrates underlie temperature and CO_2 acclimation of dark respiration in five boreal tree species. *Plant, Cell & Environment, 22*(7), 767-778.

Vanlerberghe, C. G. (2013). Alternative oxidase: A mitochondrial respiratory pathway to maintain metabolic and signaling homeostasis during abiotic and biotic stress in plants. *International Journal of Molecular Sciences, 14*(4).

Wagner, A. M., & Wagner, M. J. (1995). Measurements of *in vivo* ubiquinone reduction levels in plant cells. *Plant Physiology, 108*(1), 277.

Wang, E., Wang, J., Zhu, X., Hao, W., Wang, L., Li, Q., . . . He, Z. (2008). Control of rice grain-filling and yield by a gene with a potential signature of domestication. *Nature Genetics, 40*, 1370.

Way, D. A., & Oren, R. (2010). Differential responses to changes in growth temperature between trees from different functional groups and biomes: a review and synthesis of data. *Tree Physiology, 30*(6), 669-688.

Way, D. A., & Sage, R. F. (2008). Thermal acclimation of photosynthesis in black spruce [*Picea mariana* (Mill.) B.S.P.]. *Plant, Cell & Environment, 31*(9), 1250-1262.

Wei, S.-S., Niu, W.-T., Zhai, X.-T., Liang, W.-Q., Xu, M., Fan, X., . . . Li, B. (2019). Arabidopsis mtHSC70-1 plays important roles in the establishment of COX-dependent respiration and redox homeostasis. *Journal of Experimental Botany, 70*(20), 5575-5590.

Welch, J. R., Vincent, J. R., Auffhammer, M., Moya, P. F., Dobermann, A., & Dawe, D. (2010). Rice yields in tropical/subtropical Asia exhibit large but opposing sensitivities to minimum and maximum temperatures. *Proceedings of the National Academy of Sciences, 107*(33), 14562-14567.

Yamori, W., Noguchi, K., Hikosaka, K., & Terashima, I. (2010). Phenotypic plasticity in photosynthetic temperature acclimation among crop species with different cold tolerances. *Plant Physiology, 152*(1), 388-399.

Yamori, W., Noguchi, K., & Terashima, I. (2005). Temperature acclimation of photosynthesis in spinach leaves: analyses of photosynthetic components and temperature dependencies of photosynthetic partial reactions. *Plant, Cell & Environment, 28*(4), 536-547.

Yang, J., & Zhang, J. (2005). Grain filling of cereals under soil drying. *New Phytologist, 169*(2), 223-236.

Yoshida, S. (1972). Physiological aspects of grain yield. *Annual review of Plant Physiology, 23*, 437-464.

Zhu, J., Dong, C.-H., & Zhu, J.-K. (2007). Interplay between cold-responsive gene regulation, metabolism and RNA processing during plant cold acclimation. *Current Opinion in Plant Biology, 10*(3), 290-295.

Table 1. Differential expression of respiration genes in leaves after exposure to *T* of 40°C relative to 30°C. Differential expression defined as FDR < 0.05, marked as '*'. Electron transport chain (ETC), Pentose Phosphate Pathway (PPP). No TCA cycle genes were differentially expressed.

			Log2 fold-change	
Pathway	Gene_name	locus	2 hours	6 hours
ETC	Complex II (Succinate dehydrogenase)	LOC_Os08g02640	-0.55*	-0.58*
ETC	External NAD(P)H dehydrogenase	LOC_Os06g47000	0.72*	0.44
ETC	Uncoupling protein	LOC_Os11g48040	0.81*	0.46
ETC	Alternative oxidase	LOC_Os02g47200	-0.99*	-1.91*
glycolysis	ATP-dependent phosphofructokinase	LOC_Os01g53680	-0.11	-1.13*
glycolysis	Phosphoglycerate kinase	LOC_Os02g07260	0.78*	0.39
glycolysis	Enolase	LOC_Os10g08550	0.61*	0.34
PPP	Ribulose 5-phosphate 3-epimerase	LOC_Os09g32810	0.53*	0.87*

Table 2. Leaf mass per unit area (LMA), starch and soluble sugars of pre-existing (PE) leaves transferred from 30/25°C to 25/20°C or 40/35°C for one and seven days, and leaves newly-developed (ND) at the prevailing *T*. Data represents mean of three or four separate leaves from separate previously unsampled plants ± SE. The *F*-values and *P*-values of a two-way ANOVA comparing *T*, developmental stage (*D*) and any interaction ($T \times D$) are reported with asterisks indicating significance at $P<0.05$.

		LMA (g m^{-2})	Starch (mg g^{-1} DM)	Soluble sugar (mg g^{-1} DM)
25/20°C	Day 1	20 ± 3	11.3 ± 1.9	13.5 ± 0.2
	Day 7	19 ± 2	5.5 ± 0.3	11.2 ± 0.1
	ND	30 ± 2	14.4 ± 3.0	11.1 ± 0.2
30/25°C	Day 1	19 ± 2	14.9 ± 2.1	13.0 ± 0.5
	Day 7	21 ± 2	4.9 ± 1.0	10.5 ± 0.2
	ND	28 ± 0.4	9.6 ± 1.6	11.0 ± 0.6
40/35°C	Day 1	18 ± 2	8.5 ± 0.4	11.9 ± 0.2
	Day 7	23 ± 2	3.5 ± 0.3	10.9 ± 0.3
	ND	29 ± 1	6.7 ± 0.5	11.6 ± 0.3
$T \times D$		F=0.7, P=0.6	F=1.7, P=0.14	F=0.01, P=0.99
D		F=28, $P<0.001$*	F=13, $P<0.001$*	F=0.14, P=0.94
T		F=0.1, P=0.9	F=4.2, P=0.03*	*F=0.01*, P=0.99

Table 3. Summary of key photosynthetic and respiratory parameters generated from temperature-response curves. Parameters are: leaf mass per area; the temperature at which R_{dark} and A_n exhibited maximum rates (T_{max} and T_{opt}, respectively); the maximum rates of R_{dark} and A_n reached (R_{max} and A_{opt}, respectively); rates of R_{dark} and A_n at the prevailing growth temperature; and, the temperature at which PSII lost functionality as determined by an increase in basal fluorescence (T_{crit}). Data represents means of three or four separate leaves from separate plants ± SE and statistical data (F-value and P-value) based on one-way ANOVA of temperature treatment effect. Superscript letters show significant differences between the T treatments according to a Tukey test.

	25/20°C	30/25°C	40/30°C	F-value	P-value
LMA (g m^{-2})	33±2	30±2	35±3	1.4	0.31
T_{max} (°C)	51± 1^{a}	54 ± $1^{a,b}$	55± 1^{b}	4.7	0.04*
T_{opt} (°C)	29± 1^{a}	31± $1^{a,b}$	33 ± 0.3^{b}	6.1	0.04*
R_{max} (µmol g^{-1} DM s^{-1} ×10^{-3})	120 ± 5	117 ± 6	121 ± 2	0.16	0.86
A_{opt} (µmol g^{-1} DM s^{-1})	0.65 ± 0.05	0.67± 0.02	0.69 ± 0.04	0.28	0.76
R_{dark} (µmol g^{-1} DM s^{-1} ×10^{-3})	24±3 ^{a}	27±3 ^{a}	57±2 ^{b}	35	<0.001*
A_n (µmol m^{-2} s^{-1})	0.62 ± 0.04	0.67 ± 0.02	0.65 ± 0.04	0.52	0.62
T_{crit} (°C)	46.0 ± 0.6	46.9 ± 0.9	49.8 ± 1.5	3.726	0.089

Figure Legends

Figure 1. Quantitative PCR analysis of gene expression over the first 168 hours (7 days) after transfer of leaves from 30/25°C to 25/20°C or 40/35°C. Genes analysed were: the respiratory cytochrome *c* complex (*cox*) subunit II, alternative oxidase complex (*aox*) and uncoupling protein (*ucp*); the photosynthetic genes ferredoxin NADH reductase (*fnr*) and phosphoribulose kinase (*prk*); and the sugar metabolism gene sucrose phosphatase synthase (*sps*). Gene expression was revitalised at each time-point to the non-transferred 30/25°C control.

Figure 2. Principal component analysis of normalised RNA-seq expression values for each sample following temperature treatment for (a) 2 hours and (b) 6 hours. Samples are coloured by treatment, day/night temperatures of 30/25°C (control), 40/35°C (hot), and 25/20°C (cold). The y-axis is principle component 1 (PC1) and the x axis is principle component 2 (PC2); the percent of variation explained by each axis is indicated. RNA-seq libraries were normalised using *edgeR* ("TMM" method) and *voom* transformation, scaled by unit variance and clustered using singular value decomposition.

Figure 3. Identification of genes differentially expressed during temperature treatments. (a, b) Common and time point specific differentially expressed genes under heat treatment (40/35°C). The overlap between genes differentially expressed at 2 and 6 h under heat treatment for (a) upregulated genes and (b) downregulated genes. '*' indicates significant overlap $p << 0.001$, fisher's one-tailed exact test (hypergeometric). (c) Hierarchal clustering of differentially expressed genes. For each time point (2, 6 and 24 h) differentially expressed genes were determined for both the hot (40/35°C) and cold (25/20°C) temperature treatments relative to the 30/25°C control conditions (FDR < 0.05). For each differentially expressed gene, the relative fold-change under each condition over the time series is then displayed on a log2 scale: red = upregulated, blue = downregulated.

Figure 4. Gene ontology (GO) term enrichment among genes differentially Upregulated (a) or downregulated (b) genes after 2 h at 40°C. Ontological annotations downloaded from MSU and ontology enrichment tests performed with topGO in R using the Fisher standard test (on tailed fisher's exact test/ hypergeometric test) with post hoc p value correction for multiple testing using the Benjamini & Hochberg method.

Figure 5. Abundance of mitochondrial electron transport chain proteins and Rubisco determined by Western blot analysis for rice leaves sampled at different developmental stages of; PE leaves six and 24 h after *T* transfer to 25/20°C or 40/35°C, and leaves newly developed (ND) post *T*-transfer. (a) Abundance of CYTOCHROME C OXIDASE (COX) subunit II, (b) ALTERNATIVE OXIDASE (AOX), (c) UNCOUPLING PROTEIN (UCP) and (d) Rubisco large subunit on a leaf area basis with data normalised by adjusting the largest value in each dataset to 100. Data represent mean ± SE of four independent western blots, with each blot representing leaf tissue from a separate plant. The *P*-values of a two-way ANOVA comparing temperature (*T*), developmental stage (*D*) and the interaction between the two (*T*×*D*) are reported on each graph. Representative blots are presented in Figure S5.

Figure 6. Rates of dry mass (DM) based dark respiration (R_{dark}; a), net assimilation (A_n; b), Relative humidity (RH; c), vapour pressure deficit between the leaf and surrounding air (VPD_{Leaf}; d), stomatal conductance (g_s; e), and ratio of intercellular to ambient CO_2 concentrations (Ci/Ca; f) measured at the respective day-time growth temperature of each treatment just prior to (day 0), and 1, 2, 3, 5 and 7-days after transfer of control 30/25°C day/night grown leaves to either 25/20°C, 40/35°C or maintained at 30/25°C. Values are means of four biological replicates ± SE.

Figure 7. Temperature-response curves (a, b) of dark respiration (R_{dark}) and (c, d) net assimilation (A_n), on a dry mass (DM) basis. Values are absolute (a, c) or normalised to values at 30°C (b, d). Measurements were made on whole newly-developed (ND) leaves growing for 21 d at day/night temperatures of 25/20°C, 30/25°C or 40/35°C. Curves fitted to R_{dark} and A_n are quadratic functions. Calculated acclimation parameters from the curves are presented in Table 3. Rates were recorded every 30 sec as leaves were heated at 1°C per minute. Filled area represent standard error of three to four biological replicates.

Figure 8. The percentage of dark respiration (R_{dark}) relative to light-saturated net assimilation (A_n) (a), and leaf elongation rates (LER) over a 24 h day/night cycle (b), for ND leaves growing for 21 d at day/night temperatures of 25/20°C, 30/25°C or 40/35°C. For the R_{dark}/A_n ratio values are calculated from the absolute means presented in Figure 7. For LER the dark (night) period of the 24 h cycle is shaded in grey and values are the means ± SE of four plant replicates.

Summary statement

Leaf respiration and photosynthesis in rice (*Oryza sativa* L.) shows asynchronous acclimation capacity in favour of photosynthesis. Heat acclimation reduced the protein abundance of the respiratory protein cytochrome *c* oxidase (COX), despite respiration and growth being stimulated.

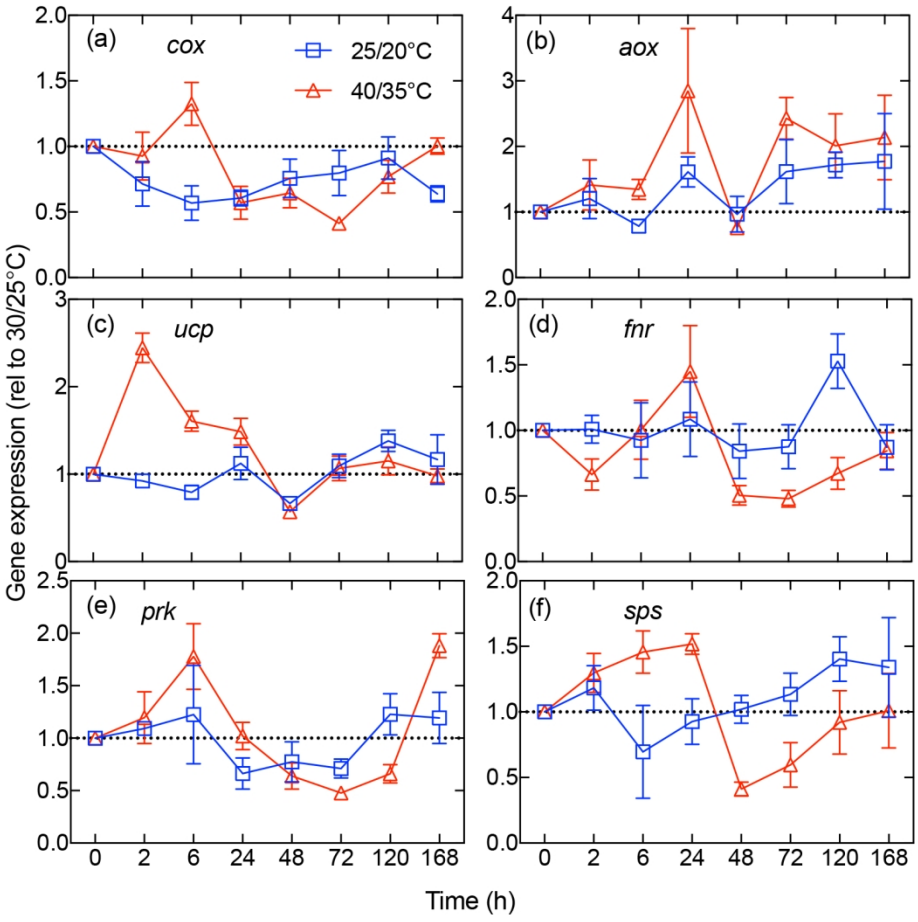

Figure 1. Quantitative PCR analysis of gene expression over the first 168 hours (7 days) after transfer of leaves from 30/25°C to 25/20°C or 40/35°C. Genes analysed were: the respiratory cytochrome c complex (*cox*) subunit II, alternative oxidase complex (*aox*) and uncoupling protein (*ucp*); the photosynthetic genes ferredoxin NADH reductase (*fnr*) and phosphoribulose kinase (*prk*); and the sugar metabolism gene sucrose phosphatase synthase (sps). Gene expression was revitalised at each time-point to the non-transferred 30/25°C control.

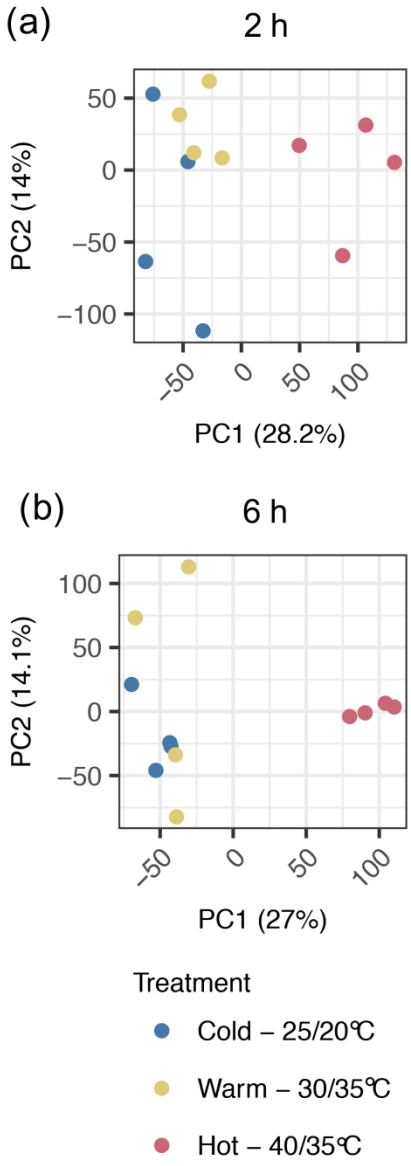

Figure 2. Principal component analysis of normalised RNA-seq expression values for each sample following temperature treatment for (a) 2 hours and (b) 6 hours. Samples are coloured by treatment, day/night temperatures of 30/25°C (control), 40/35°C (hot), and 25/20°C (cold). The y-axis is principle component 1 (PC1) and the x axis is principle component 2 (PC2); the percent of variation explained by each axis is indicated. RNA-seq libraries were normalised using edgeR ("TMM" method) and voom transformation, scaled by unit variance and clustered using singular value decomposition.

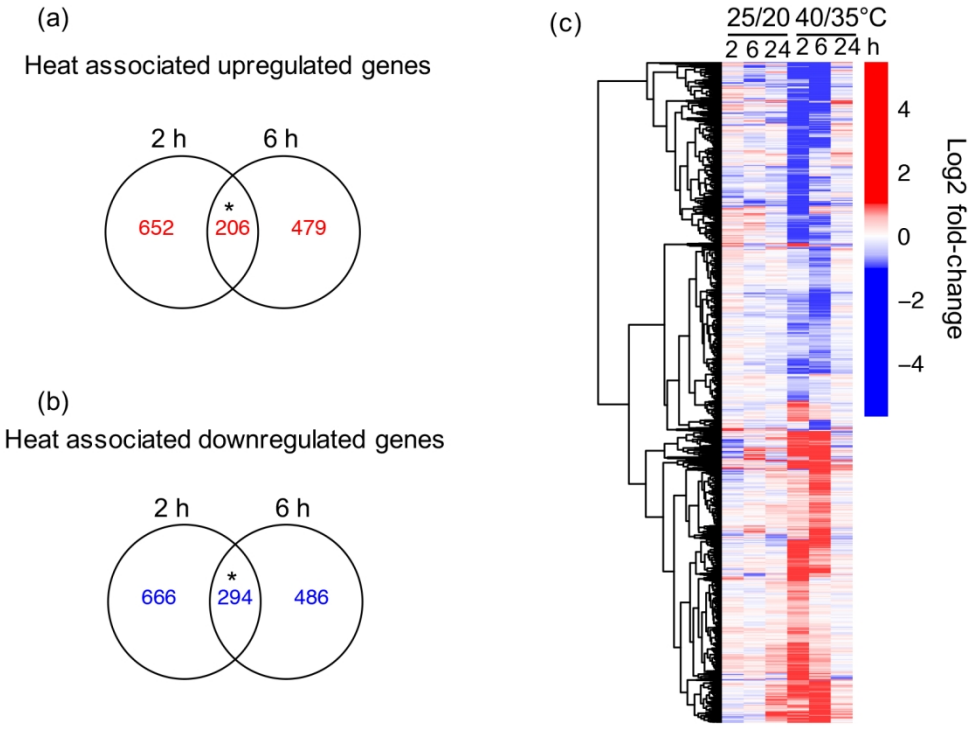

Figure 3. Identification of genes differentially expressed during temperature treatments. (a, b) Common and time point specific differentially expressed genes under heat treatment (40/35°C). The overlap between genes differentially expressed at 2 and 6 h under heat treatment for (a) upregulated genes and (b) downregulated genes. '*' indicates significant overlap $p << 0.001$, fisher's one-tailed exact test (hypergeometric). (c) Hierarchal clustering of differentially expressed genes. For each time point (2, 6 and 24 h) differentially expressed genes were determined for both the hot (40/35°C) and cold (25/20°C) temperature treatments relative to the 30/25°C control conditions (FDR < 0.05). For each differentially expressed gene, the relative fold-change under each condition over the time series is then displayed on a log2 scale: red = upregulated, blue = downregulated.

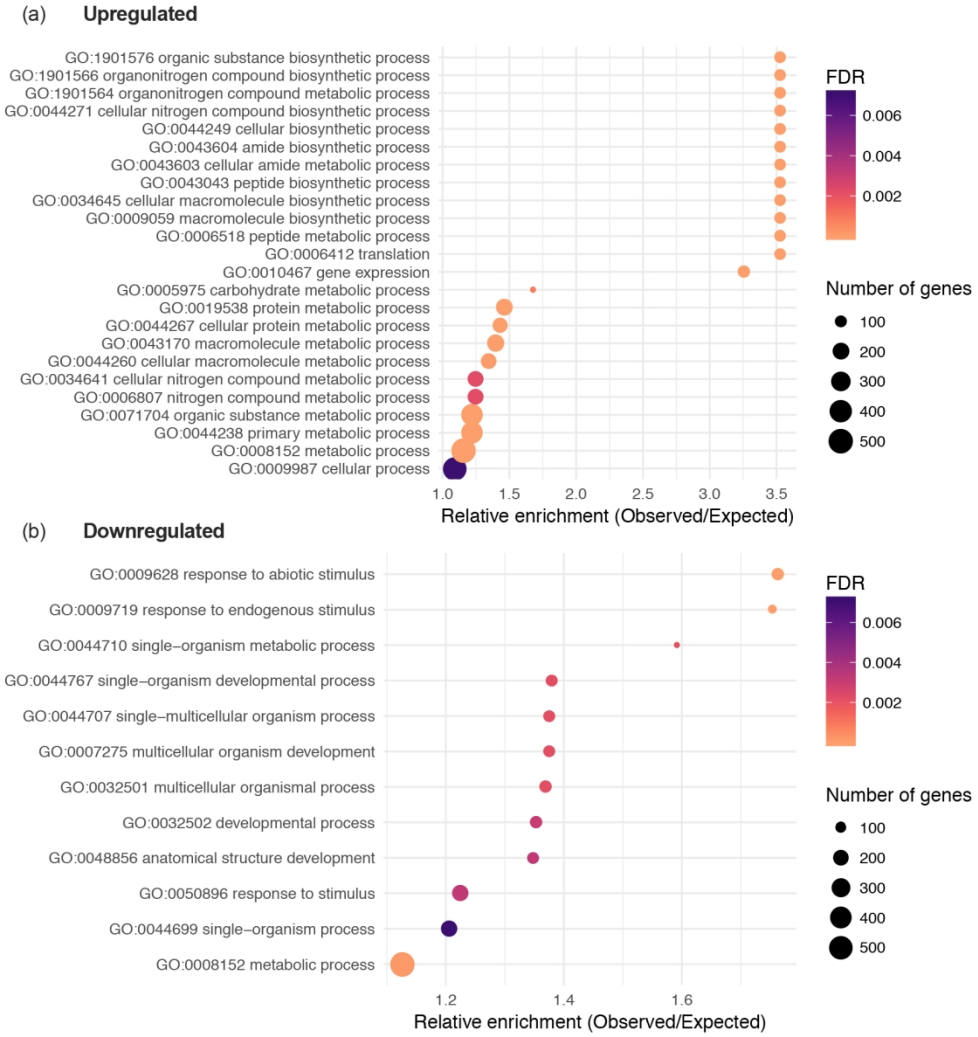

Figure 4. Gene ontology (GO) term enrichment among genes differentially Upregulated (a) or downregulated (b) genes after 2 h at 40°C. Ontological annotations downloaded from MSU and ontology enrichment tests performed with topGO in R using the Fisher standard test (on tailed fisher's exact test/ hypergeometric test) with post hoc *p*-value correction for multiple testing using the Benjamini & Hochberg method.

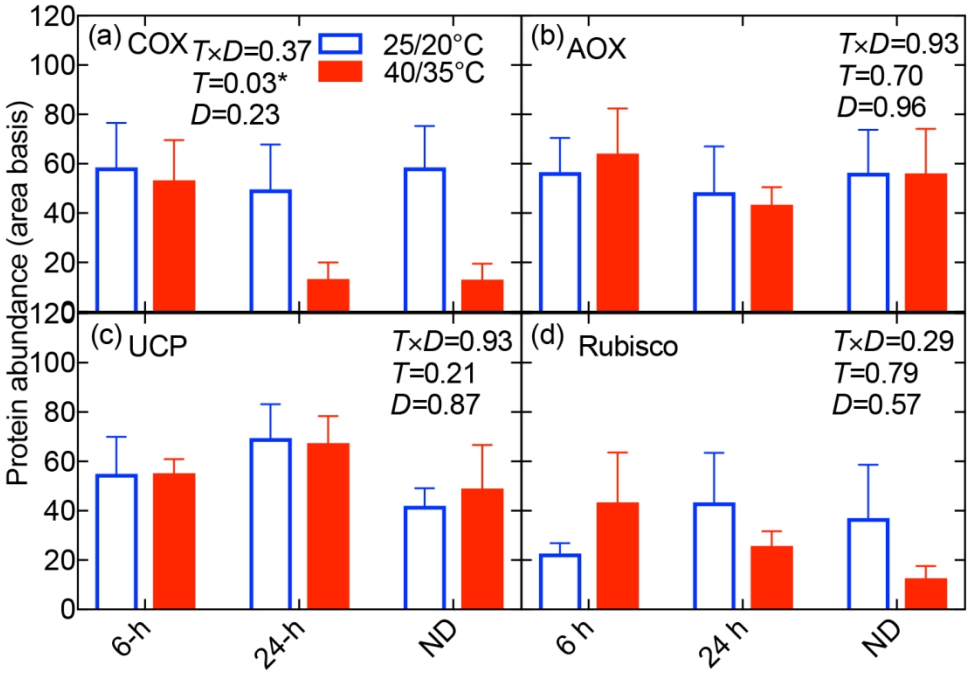

Figure 5. Abundance of mitochondrial electron transport chain proteins and Rubisco determined by Western blot analysis for rice leaves sampled at different developmental stages of; PE leaves six and 24 h after *T* transfer to 25/20°C or 40/35°C, and leaves newly developed (ND) post *T*-transfer. (a) Abundance of CYTOCHROME C OXIDASE (COX) subunit II, (b) ALTERNATIVE OXIDASE (AOX), (c) UNCOUPLING PROTEIN (UCP) and (d) Rubisco large subunit on a leaf area basis with data normalised by adjusting the largest value in each dataset to 100. Data represent mean ± SE of four independent western blots, with each blot representing leaf tissue from a separate plant. The *P*-values of a two-way ANOVA comparing temperature (*T*), developmental stage (*D*) and the interaction between the two (*T*×*D*) are reported on each graph. Representative blots are presented in Figure S5.

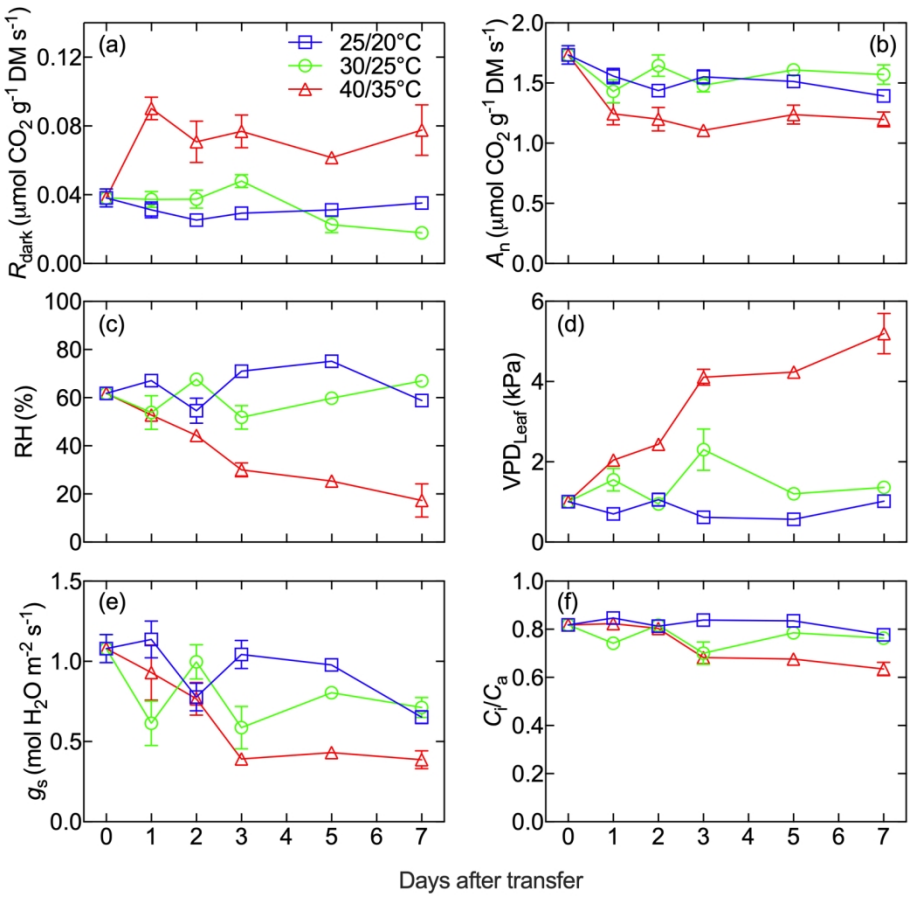

Figure 6. Rates of dry mass (DM) based dark respiration (R_{dark}; a), net assimilation (A_n; b), Relative humidity (RH; c), vapour pressure deficit between the leaf and surrounding air (VPD_{Leaf}; d), stomatal conductance (g_s; e), and ratio of intercellular to ambient CO2 concentrations (C_i/C_a; f) measured at the respective day-time growth temperature of each treatment just prior to (day 0), and 1, 2, 3, 5 and 7-days after transfer of control 30/25°C day/night grown leaves to either 25/20°C, 40/35°C or maintained at 30/25°C. Values are means of four biological replicates ± SE.

152x141mm (300 x 300 DPI)

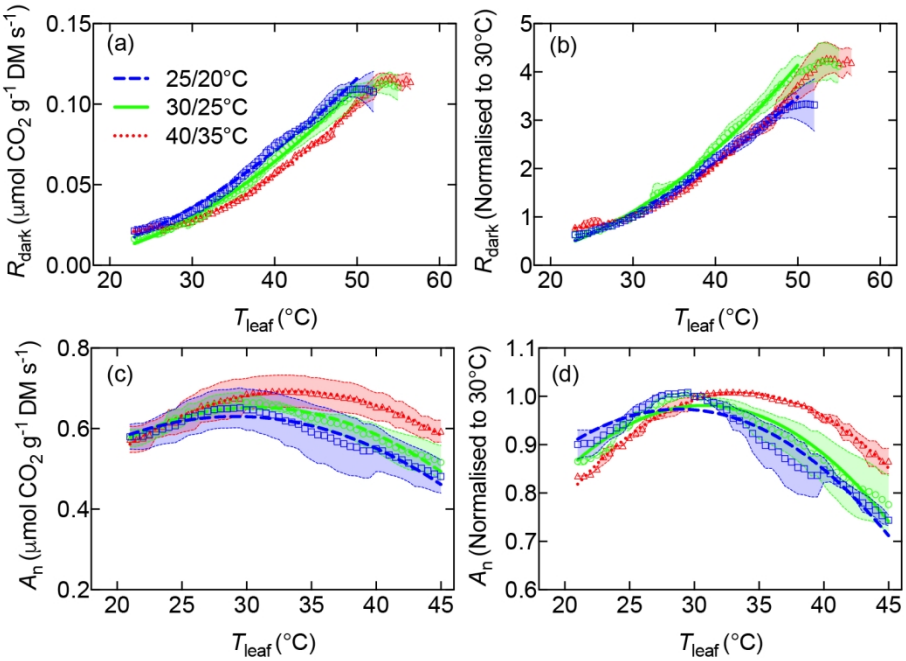

Figure 7. Temperature-response curves (a, b) of dark respiration (R_{dark}) and (c, d) net photosynthesis (A_n), on a dry mass (DM) basis. Values are absolute (a, c) or normalised to values at 30°C (b, d). Measurements were made on whole newly-developed (ND) leaves growing for 21 d at day/night temperatures of 25/20°C, 30/25°C or 40/35°C. Curves fitted to R_{dark} and A_n are quadratic functions. Calculated acclimation parameters from the curves are presented in Table 3. Rates were recorded every 30 sec as leaves were heated at 1°C per minute. Filled area represent standard error of three to four biological replicates.

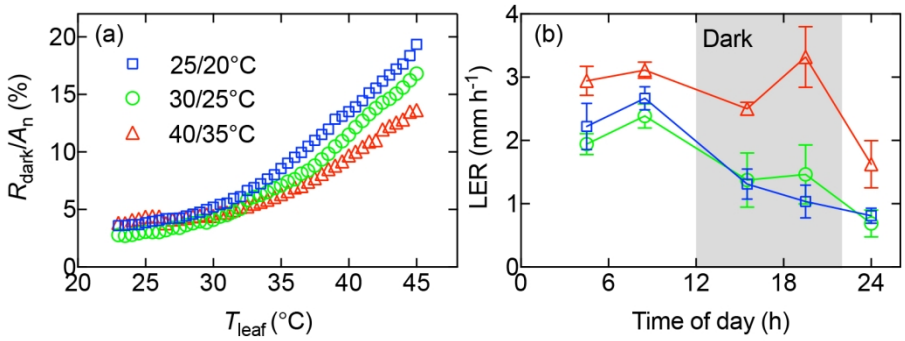

Figure 8. The percentage of dark respiration (R_{dark}) relative to light-saturated net assimilation (A_n) (a), and leaf elongation rates (LER) over a 24 h day/night cycle (b), for ND leaves growing for 21 d at day/night temperatures of 25/20°C, 30/25°C or 40/35°C. For the R_{dark}/A_n ratio values are calculated from the absolute means presented in Figure 7. For LER the dark (night) period of the 24 h cycle is shaded in grey and values are the means ± SE of four plant replicates.

Supporting Information

Molecular and physiological responses during thermal acclimation of leaf photosynthesis and respiration in rice

Fatimah Azzahra Ahmad Rashid[1, 2], Peter A. Crisp[3], You Zhang[4], Oliver Berkowitz[5], Barry J. Pogson[1], David A. Day[6,7], Josette Masle[8], James Whelan[5], Owen K. Atkin[1], Andrew P. Scafaro[1]

[1] Australian Research Council Centre of Excellence in Plant Energy Biology, Research School of Biology, The Australian National University, Canberra, ACT, 2601, Australia

[2] Current address: Department of Biology, Faculty of Science and Mathematics, Sultan Idris education University, 35900 Tanjung Malim, Perak, Malaysia

[3] Department of Plant and Microbial Biology, University of Minnesota, Saint Paul, MN, 55108 USA

[4] CSIRO Plant Industry, GPO Box 1700, Canberra, ACT, 2601, Australia

[5] Australian Research Council Centre of Excellence in Plant Energy Biology, School of Life Science, AgriBio Building, La Trobe University, Bundoora, Victoria, 3083, Australia

[6] College of Science and Engineering, Flinders University, South Australia, 5001, Australia

[7] Department of Animal, Plant and Soil Sciences, AgriBio Building, La Trobe University, 5 Ring Road, Bundoora, VIC, 3086, Australia

[8] Research School of Biology, The Australian National University, Canberra, ACT, 2601, Australia

Table S1. Concentrations of essential macro- and micro-nutrients in hydroponic solution for rice plants.

Element	Chemical formula	Concentration (mM)
Macronutrients		
Nitrogen (N)	NH_4NO_3	1.4
Phosphorus (P)	$NaH_2PO_4.2H_2O$	0.6
Potassium (P), Sulfur (S)	K_2SO_4	0.5
Calcium (Ca)	$CaCl_2.2H_2O$	0.2
Magnesium (Mg)	$MgSO_4.7H_2O$	0.8
Micronutrients		
Iron (Fe)	Fe-EDTA	0.07
Boron (B)	H_3BO_3	0.037
Manganese (Mn)	$MnCl_2.4H_2O$	0.009
Zinc (Zn)	$ZnSO_4.7H_2O$	0.00075
Copper (Cu)	$CuSO_4.5H_2O$	0.0003
Molybdenum (Mo)	$(NH_4)_6Mo_7O_{24}.4H_2O$	0.0001
Vanadium (V)	NH_4VO_3	0.000138
Silicon (Si)	Na_2SiO_3	0.0012963

Table S2. Primers used for qPCR gene expression analysis

Protein	Sequence (5'->3')	Length	Start	Stop	Tm	GC%	Size	location	mRNA
Ferredoxin NADP reductase	TCAGGCTCTACTCCATCGCC	20	487	506	58.9	60	152	exon 2	NM_001063105.1
	ACCAGGCTTCAAGTCACAGAGG	22	638	617	60	54.6		exon 3 or 4	
Phosphoribulokinase	TTTGATGCCTTCATTGATCCCC	22	865	886	56.8	45.5	80	exon 3 or 4	NM_001054360.1
	TCATCAGGAATAAGCTGGGTTGG	23	944	922	58.1	47.8		exon 4	
Uncoupling protein	CCTCTACGAGCCCGTGAAATCC	22	348	369	60.6	59.1	134	exon 2 or 3	NM_001075091.1
	TGACAAGGTCAGTGGGGTTGG	21	481	461	60	57.1		exon 4	
Cytochrome oxidase (COX)	GCCATTGCAGGAGTGATGGG	20	73	92	59.2	60	85		LOC_Os12g33946.1
	TCCCACCAAGAATTTGATCGCC	22	157	136	59	50			
Alternative oxidase (AOX)	TGCTTTAGGCCATGGGAGACC	21	416	436	59.9	57.1	84	exon 1 or 2	NM_001060293.1
	CTTGTCGAGCAGCGTCTTGG	20	499	480	59.5	60		exon 1	
Sucrose-phosphate synthase (SPS)	ATGCGAAGCCTGAAACCCCC	20	1317	1336	60.9	60	124	exon 8 or 9	NM_001052401.1
	CACACGGAGGTGCAGAAAAGG	21	1440	1420	59.6	57.1		exon 9	
eIF4-gamma/eIF5/eIF2-epsilon domain containing protein (Eukaryotic initiation facctor 5C)	CTGATGGAGGCTGTTCAGTGG	21	1035	1055	58.5	57.1	81	exon 6 or 7	NM_001074292.1
	AGCCCATGCTTTCACCTGCC	20	1115	1096	61.2	60		exon 7	

Table S3 Differentially expressed genes. At each time point, differential expressed genes were assessed for the hot and cold treated plants relative to the warm grown control plants sampled at the same time ($n = 4$). Genes were considered differentially expressed an FDR adjusted p (padj) < 0.05.

Treatment	Time point	Upregulated	Downregulated
Cold	2 hr	4	0
Hot	2 hr	858	960
Cold	6 hr	2	0
Hot	6 hr	685	780
Cold	24 hr	0	0
Hot	24 hr	0	0

Table S4. Protein concentrations of 25/20°C and 40/35°C day/night grown leaves. Data represents mean of three to four biological replicates ± SE.

	Protein concentration (mg ml^{-1})	
	25/20°C	40/35°C
6 hr [Pre-existing (PE) leaves]	7.7 ± 0.8	7.0 ± 1.0
Day 1 [Pre-existing (PE) leaves]	8.8 ± 1.9	6.9 ± 1.3
Newly-developed (ND) leaves	8.5 ± 0.7	7.8 ± 0.8

Table S5. Pearson's correlation coefficients between rates of dark respiration and concentration of soluble sugars for plants grown at different growth temperature regimes.

	Dark respiration x soluble sugars		
	25/20°C	30/25°C	40/35°C
Day 1			
Correlation coefficient	-0.999	-0.999	0.049
P-value	0.024*	0.032*	0.969
Day 7			
Correlation coefficient	-0.805	-0.990	-0.461
P-value	0.405	0.090	0.695
Newly developed (ND)			
Correlation coefficient	-0.420	-0.560	0.879
P-value	0.724	0.621	0.317

Table S6. Quadratic equations for the short-term temperature (*T*)-response curves of dark respiration (R_{dark}) and net assimilation (A_n) as presented in Figure 7. The equations were fitted to the mean values of each temperature treatment and their Absolute Sum of Squares (ASS) and goodness-of-fit (R^2) are provided. Equations for R_{dark} were only fitted in the range of 22 to 50°C. R_{dark} and A_n units are in µmol CO_2 g^{-1} DM s^{-1} $\times 10^{-3}$ and T is in °C.

Day/night temperatures	Equation	ASS	R^2
25/20°C	$R_{dark} = -7.2 - 0.094 \times T + 0.051 \times T^2$	2.5×10^{-5}	0.99
	$A_n = 60 + 39 \times T - 0.67 \times T^2$	9.0×10^{-5}	0.92
30/25°C	$R_{dark} = 2.4 - 0.096 \times T + 0.063 \times T^2$	1.7×10^{-5}	0.99
	$A_n = 89 + 48 \times T - 0.72 \times T^2$	6.0×10^{-5}	0.94
40/35°C	$R_{dark} = 5.8 - 3.7 \times T + 0.092 \times T^2$	1.1×10^{-5}	0.99
	$A_n = -240 + 56 \times T - 0.83 \times T^2$	7.3×10^{-5}	0.99

Figure S1 A photo of a LI-6400XT portable gas exchange system (top) and Walz 3010-GWK1 chamber (bottom) used in quantification of short-term temperature-response curves of R_{dark} and A_n in new-developed (ND) leaves. Airline tubes were used to connect the Walz 3010-GWK1 chamber to the LICOR Infrared gas analyser head with a water trap in between to remove excess humidity. Photos are courtesy of www.licor.com and www.walz.com.

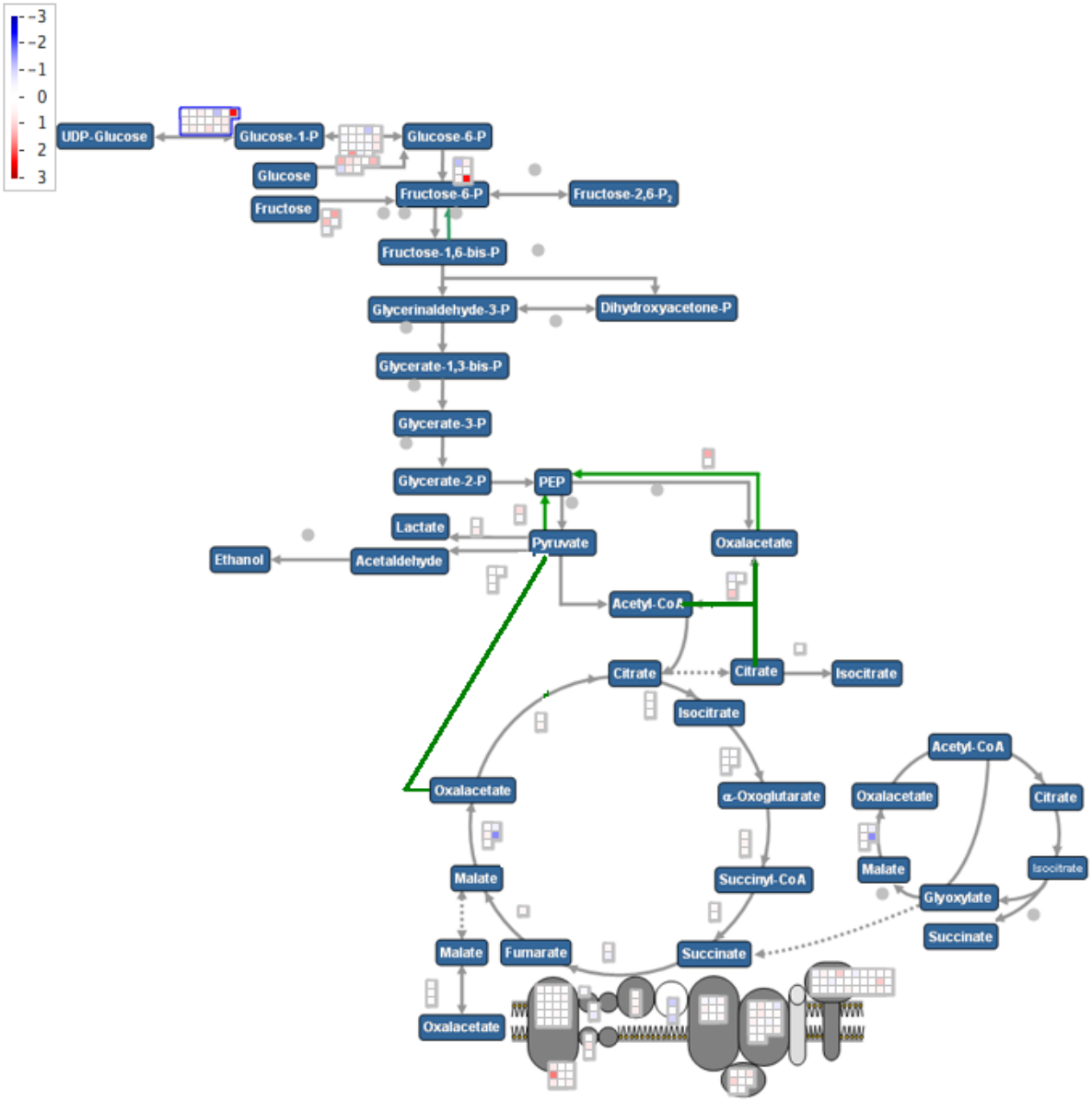

Figure S2 Differential gene expression in the Glycolysis and TCA under hot treatment Gene expression is visualised in a MapMap pathway view of Glycolysis and the tricarboxylic acid (TCA) cycle. Each box represents a rice gene with homology to an Arabidpsis gene annotated in the MapMan pathway. Data show for the comparison of 2 hours hot treatment compared to 2 hours control treatment (warm); red shading represents up-regulation and blue shading down-regulation on a log2 fold-change scale.

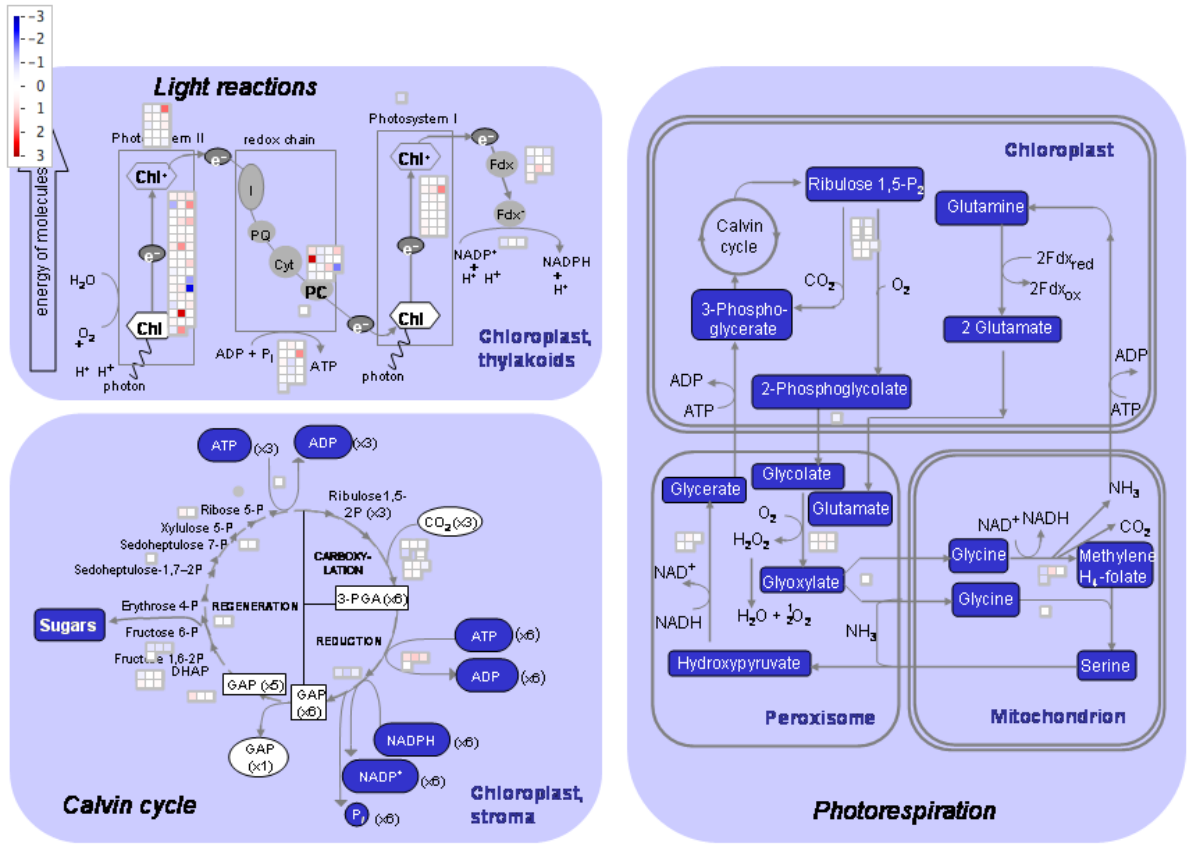

Figure S3. Differential gene expression of photosynthetic genes under hot (40/35°C) treatment. Gene expression is visualised in a MapMap pathway view of photosynthesis. Each box represents a rice gene with homology to an Arabidpsis gene annotated in the MapMan pathway. Data show for the comparison of two hours hot treatment compared to two hours control (30/25°C) treatment; red shading represents up-regulation and blue shading down-regulation on a log2 fold-change scale.

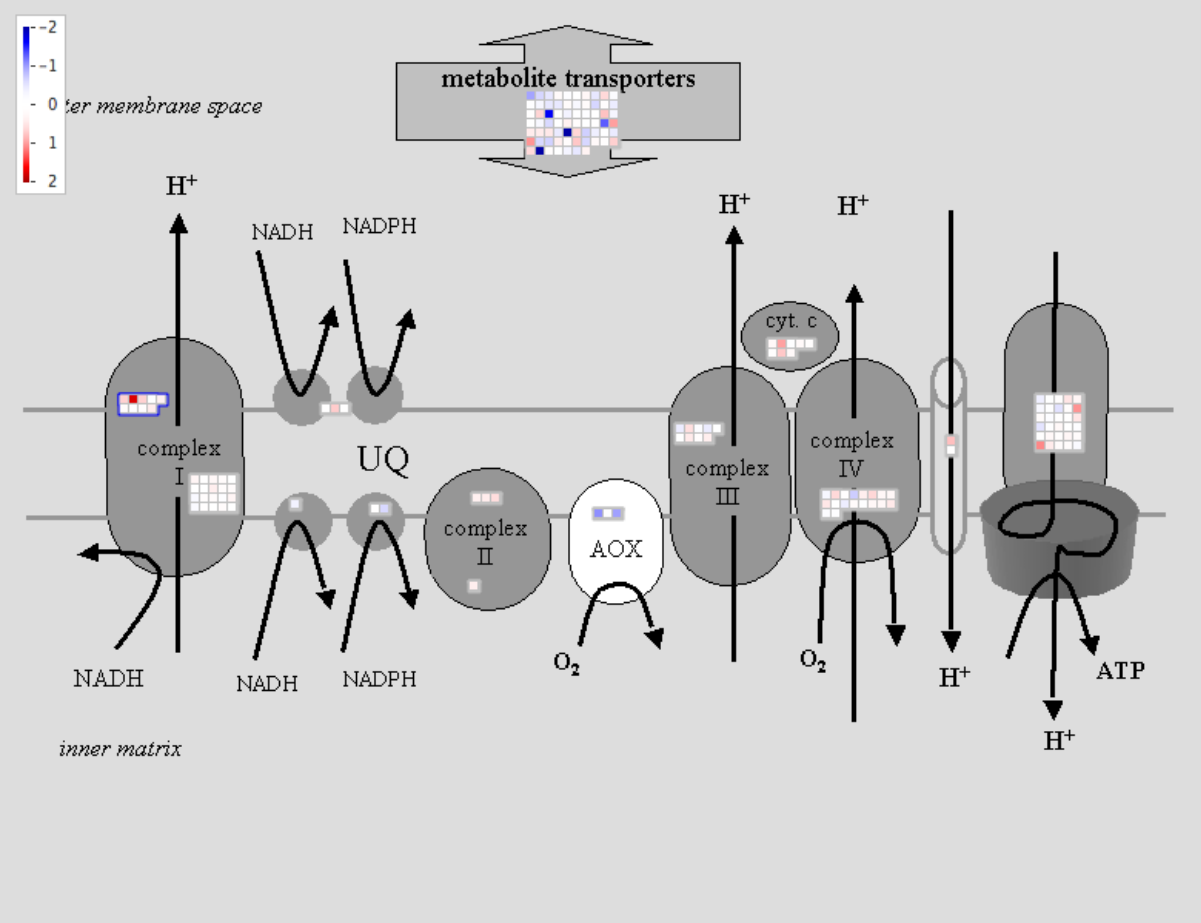

Figure S4. Differential gene expression in the mitochondrial electron transport chain under hot treatment. Gene expression is visualised in a MapMap pathway view of the mitochondrial electron transport. Each box represents a rice gene with homology to an Arabidopsis gene annotated in the MapMan pathway. Data show for the comparison of two hours hot (40/35°C) treatment compared to two hours control treatment (30/25°C); red shading represents up-regulation and blue shading down-regulation on a log2 fold-change scale.

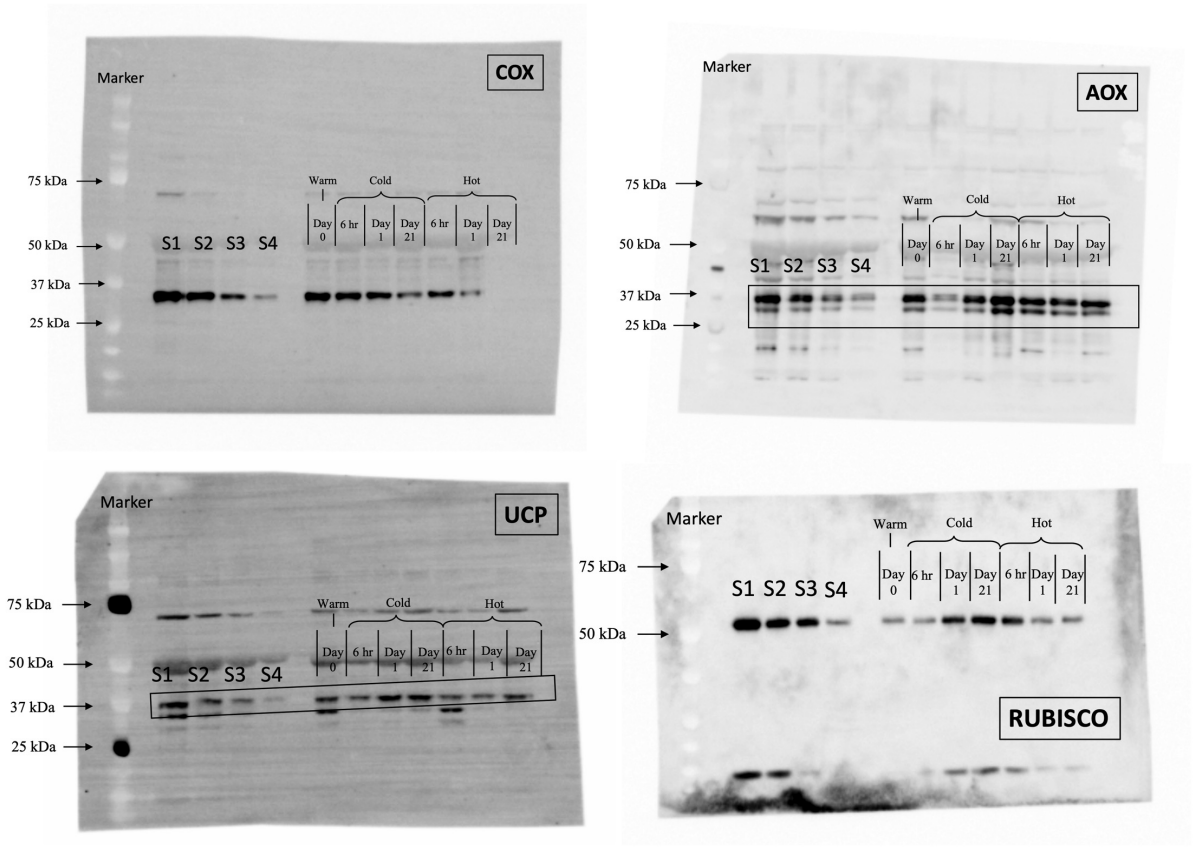

Figure S5. Representative western blots of cytochrome c oxidase (COX) subunit II, alternative oxidase (AOX), uncoupling protein (UCP), and Rubisco, used for determination of protein content of leaves. S1 to S4 is a dilution series of the warm/control (30/25°C) samples. This is followed by the initial day 0 warm leaves prior to temperature transfer, the 6-h and 1-day times after transfer of PE leaves, and ND leaves after 21 days of temperature transfer, for the cold (25/20°C) and hot (40/35°C) treatments as indicated on the images. For AOX and UCP, the bands within the box are what was classified and analysed as the proteins of interest based on the molecular weight marker markers.

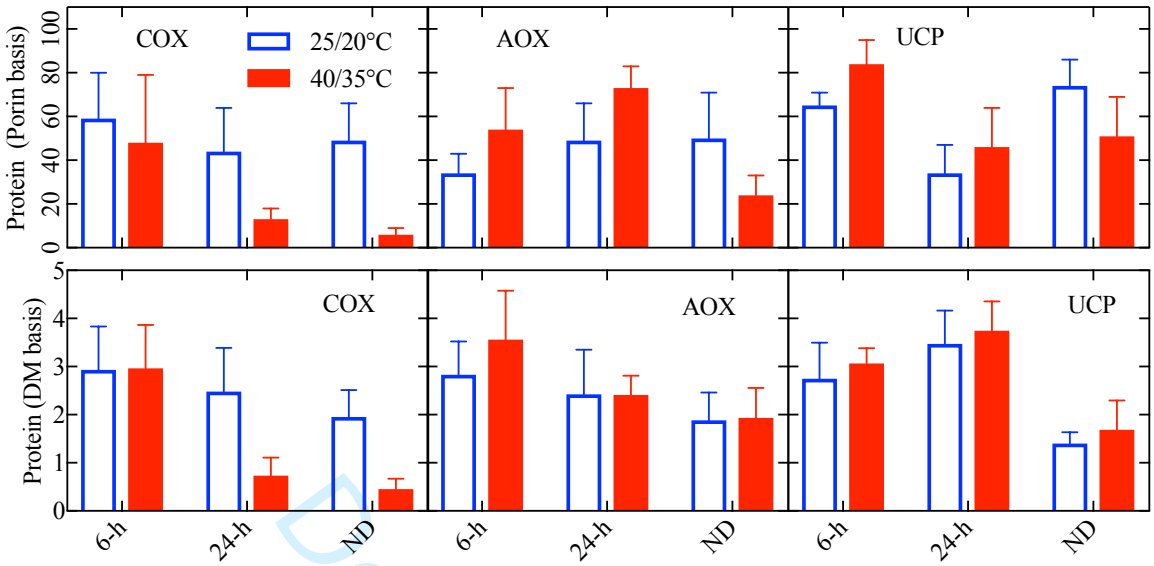

Figure S6. Abundance of mitochondrial electron transport chain proteins determined by Western blot analysis for pre-existing rice leaves sampled at; six and 24 h after *T* transfer to 25/20°C or 40/35°C, and leaves newly developed (ND) post *T*-transfer. The top three panels are protein abundance of cytochrome *c* oxidase (COX), alternative oxidase (AOX), and uncoupling protein (UCP) normalised to porin abundance and adjusting the largest value in each dataset to 100. The bottom three panels are leaf area values normalised to a dry mass (DM) basis by factoring in the leaf mass per area of pre-existing and newly developed leaves as presented in Table 2 of the text. Data represent mean ± SE of four independent western blots, with each blot representing leaf tissue from a separate plant.

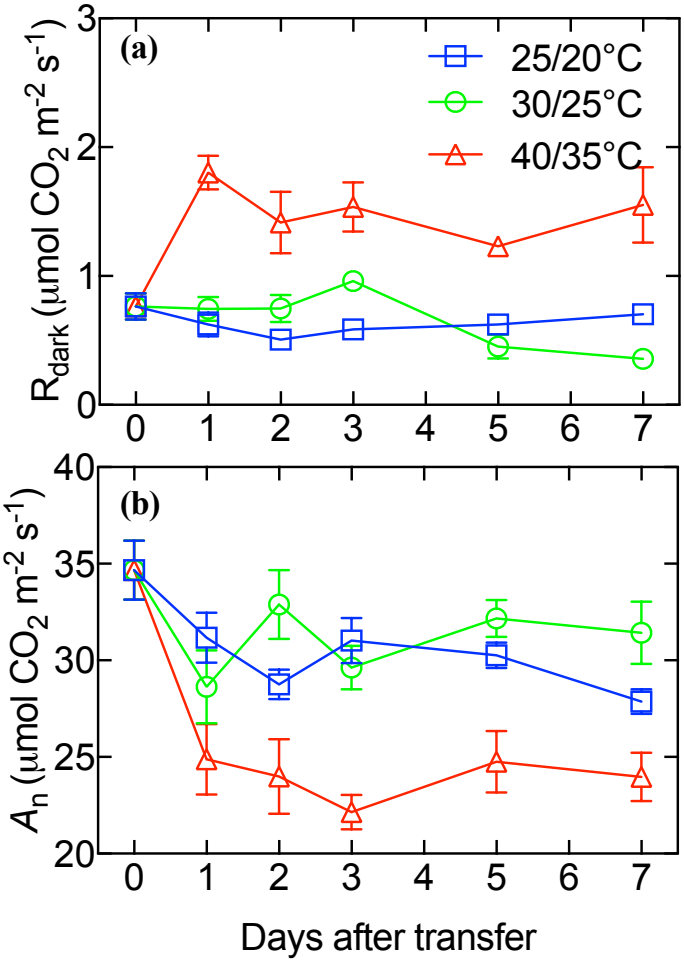

Figure S7. Rates of leaf area based dark respiration (R_{dark}) and net photosynthesis (A_n). Rates were measured at the respective day-time growth temperature of each treatment just prior to (day 0), and 1, 2, 3, 5 and 7-days after transfer of control 30/25°C day/night grown leaves to either 25/20°C, 40/35°C or maintained at 30/25°C. Values are means of four biological replicates ± SE.

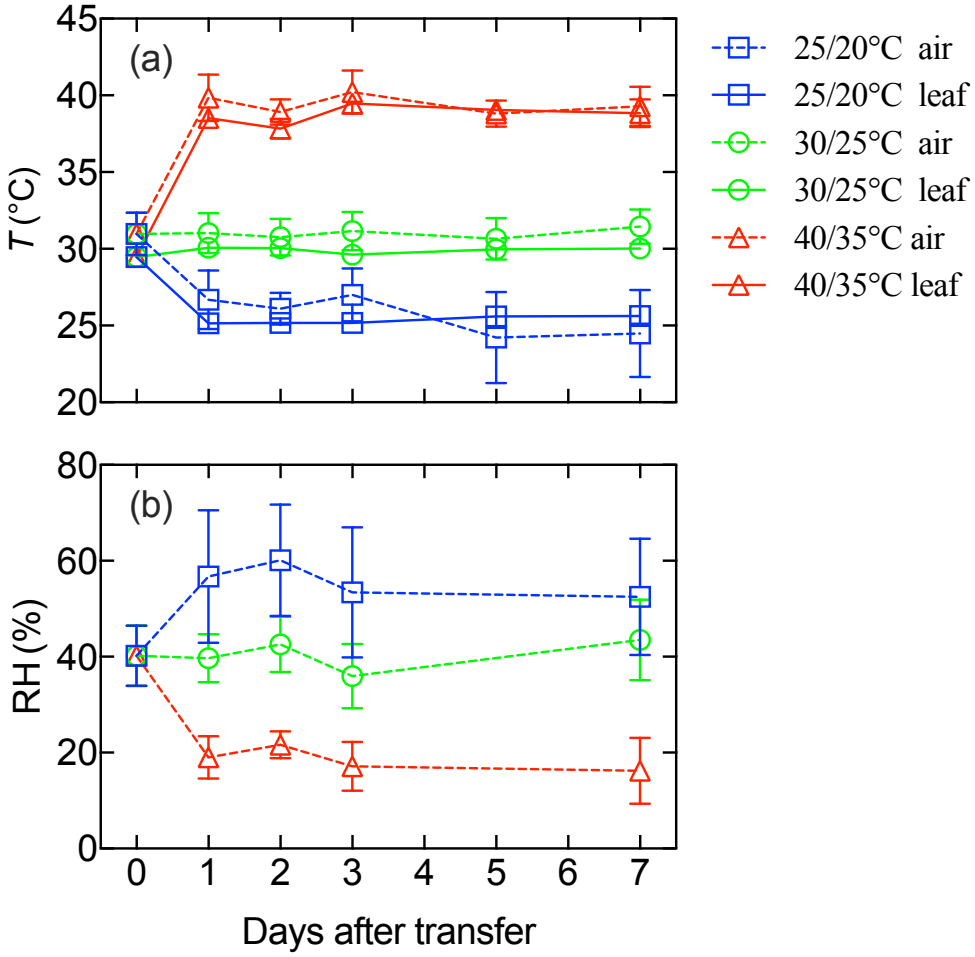

Figure S8. Room (dashed lines) and leaf (solid lines) temperatures and relative humidity (RH) over the steady-state gas exchange experimental period. Temperatures (*T*) were measured in the room by a thermometer and at the leaf surface by a thermocouple and relative humidity (RH) was measured in the room by a hygrometer. Values are means ± SD.

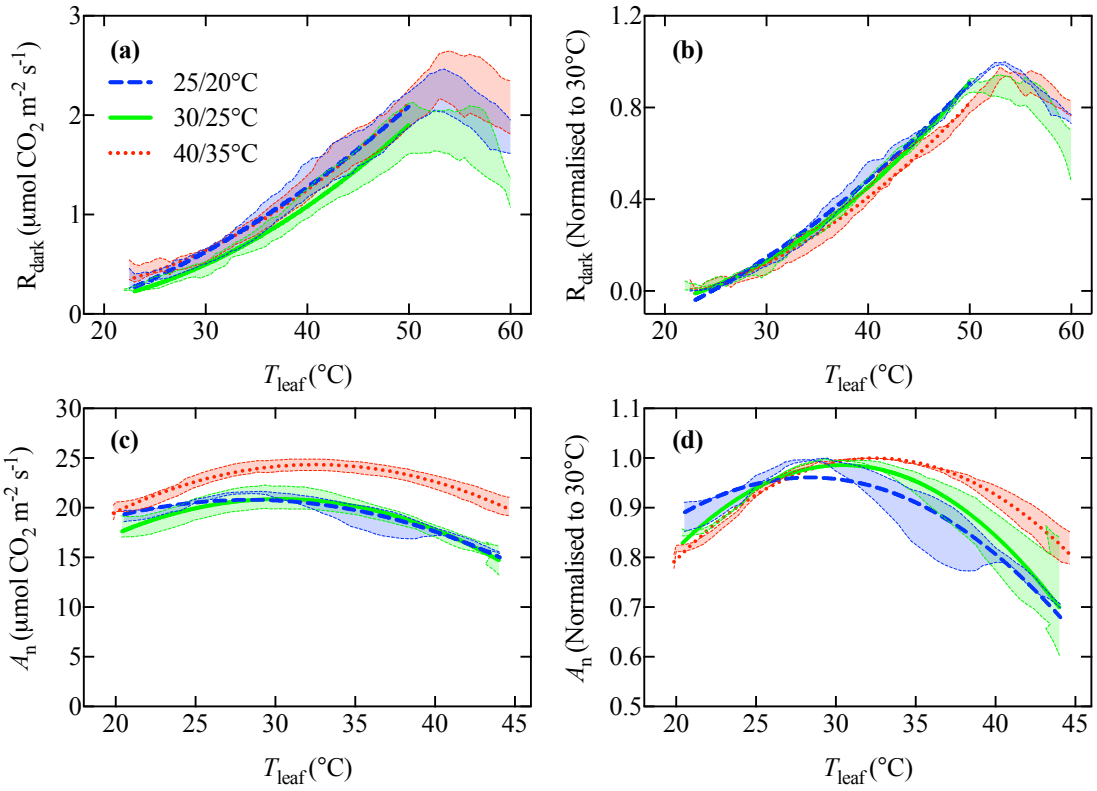

Figure S9. Temperature-response curves (a, b) of dark respiration (R_{dark}) and (c, d) net photosynthesis (A_n), on an area basis. Values are absolute (a, c) or normalised to values at 30°C (b, d). Measurements were made on whole newly-developed (ND) leaves growing for 21 d at day/night temperatures of 25/20°C, 30/25°C or 40/35°C. Curves fitted to R_{dark} and A_n are quadratic functions. Rates were recorded every 30 sec as leaves were heated at 1°C per minute. Filled area represent standard error of three to four biological replicates.

Molecular and physiological responses during thermal acclimation of leaf photosynthesis and respiration in rice

Fatimah Azzahra Ahmad Rashid[1, 2], Peter A. Crisp[3], You Zhang[4], Oliver Berkowitz[5], Barry J. Pogson[1#], David A. Day[6,7], Josette Masle[8], Roderick C. Dewar[8], James Whelan[5#], Owen K. Atkin[1#], Andrew P. Scafaro[1]

[1] Australian Research Council Centre of Excellence in Plant Energy Biology, Research School of Biology, The Australian National University, Canberra, ACT, 2601, Australia

[2] Current address: Department of Biology, Faculty of Science and Mathematics, Sultan Idris education University, 35900 Tanjung Malim, Perak, Malaysia

[3] Department of Plant and Microbial Biology, University of Minnesota, Saint Paul, MN, 55108 USA

[4] CSIRO Plant Industry, GPO Box 1700, Canberra, ACT, 2601, Australia

[5] Australian Research Council Centre of Excellence in Plant Energy Biology, School of Life Science, AgriBio Building, La Trobe University, Bundoora, Victoria, 3083, Australia

[6] College of Science and Engineering, Flinders University, South Australia, 5001, Australia

[7] Department of Animal, Plant and Soil Sciences, AgriBio Building, La Trobe University, 5 Ring Road, Bundoora, VIC, 3086, Australia

[8] Research School of Biology, The Australian National University, Canberra, ACT, 2601, Australia

[#] The support of the Australian Research Council (ARC) Centre of Excellence in Plant Energy Biology (CE140100008) is acknowledged

Abstract

To further our understanding of how sustained changes in temperature affect the carbon economy of rice (*Oryza sativa*), hydroponically-grown plants of the IR64 cultivar were developed at 30/25°C (day/night) before being shifted to 25/20°C or 40/35°C. Leaf mRNA and protein abundance, sugar and starch ~~content~~concentrations, gas-exchange and elongation rates were measured on pre-existing leaves (PE) already developed at 30/25°C, or leaves newly-developed (ND) subsequent to temperature transfer. Following a shift in growth temperature, there was a transient adjustment in metabolic gene transcript abundance of PE leaves before homeostasis was reached within 24 h, aligning with R_{dark}

(leaf dark respiratory CO_2 release) and A_n (net CO_2 assimilation) changes. With longer exposure, the central respiratory protein CYTOCHROME C OXIDASE (COX) declined in abundance at 40/35°C. In contrast to R_{dark}, A_n was maintained across the three growth temperatures in ND leaves. Soluble sugars did not differ significantly with growth temperature, and growth was fastest with extended exposure at 40/35°C. The results highlight that acclimation of photosynthesis and respiration is asynchronous in rice, with heat-acclimated plants exhibiting a striking ability to maintain net carbon gain and growth when exposed to heat-wave temperatures, even while reducing investment in energy-conserving respiratory pathways.

Keywords: rice, thermal stress, acclimation, respiration, photosynthesis, heat, cold, CYTOCHROME C OXIDASE (COX)

Introduction

The response of net CO_2 assimilation (A_n) and leaf respiration in the dark (R_{dark}) to changes in temperature (T) is often dynamic. Acclimation – i.e. physiological changes that enable adjustments in the rate of A_n and R_{dark} at a given measuring T in response to sustained changes in growth T – occurs in many species, in natural and controlled environments (Atkin, Bruhn, Hurry, & Tjoelker, 2005; Berry & Bjorkman, 1980; Campbell et al., 2007; Reich et al., 2016; Smith & Dukes, 2017; Tjoelker, Oleksyn, & Reich, 2001). Acclimation can also lead to metabolic homeostasis, where similar rates of A_n and R_{dark} are exhibited by hot- and cold-acclimated plants, when compared at their respective growth Ts. Determining the extent to which R_{dark} and A_n acclimate to sustained changes in T is of growing interest, as global warming is resulting in plants of natural and managed ecosystems experiencing higher average growth Ts, often in conjunction with more frequent and severe heat waves (CSIRO & BOM, 2018; Hartmann et al., 2013). The impact of heat on A_n and R_{dark} of cereal crops, including rice (*Oryza sativa*), is of particular interest given the need to increase food production to meet the requirements of a growing and more affluent world population (Godfray et al., 2010). Rice contributes substantially to global food demand, particularly in Asia where it makes up more than 30% of all dietary energy intake (Seck, Diagne, Mohanty, & Wopereis, 2012). However, in recent years rice yields have declined in regions such as South-East Asia, with the declines being more strongly correlated with nightly minimum than daytime maximum *Ts* (Peng et al., 2004; Welch et al., 2010). Reduced yields and grain quality were also observed for rice in North America when exposed to warmer night T (Lanning, Siebenmorgen, Counce, Ambardekar, & Mauromoustakos, 2011). Given this, and the likely importance of A_n and R_{dark} for biomass and grain production (Posch et al., 2019; Yoshida, 1972), it is

crucial that we develop a better understanding of how changes in T affect these key metabolic processes in rice.

In rice and a range of other crops, RNA sequencing analysis has shown large scale perturbations to the transcript profile of plants exposed to colder or warmer T, with the changes occurring over a period of hours to days and across multiple functional categories, but especially in genes involved in primary metabolism (Bhardwaj et al., 2015; Hu, Sun, Zhang, Nevo, & Fu, 2014; Shen et al., 2014). The vast gene expression response to T-perturbations is likely mediated through heat shock transcription factors, which regulate changes in transcriptional networks. These are induced by heat stress and other abiotic stimuli, changing the protein complement of a cell (Morimoto, 1998; Ohama, Sato, Shinozaki, & Yamaguchi-Shinozaki, 2017). However, changes in protein abundance may not necessarily match changes in transcript abundance due to transcription and RNA turnover rates being influenced by T (Sidaway-Lee, Costa, Rand, Finkenstadt, & Penfield, 2014), and post-transcriptional regulation. In cases where heat stress results in changes in protein abundance, the greatest changes are seen in proteins associated with primary metabolism, with about 50% of all leaf protein abundance changes seeming to be in A_n and R_{dark} metabolic pathways (Scafaro & Atkin, 2016). In rice, cold-stress similarly perturbs a large proportion of energy metabolism pathways (Neilson, Mariani, & Haynes, 2011), emphasising the importance of changes in protein abundance in chloroplasts and mitochondria as part of the thermal acclimation process. There is growing evidence that plants can acclimate to T variations by stimulating energy metabolism at colder T and suppressing energy metabolism at warmer T, either through regulation of enzymatic velocities or changes in enzyme abundance (Armstrong et al., 2008; Badger, Björkman, & Armond, 1982; Campbell et al., 2007; Hikosaka, Ishikawa, Borjigidai, Muller, & Onoda, 2006; Scafaro et al., 2017; Strand et al., 1999; Yamori, Noguchi, & Terashima, 2005). Whether the same is true for rice remains unclear, both for pre-existing (PE) leaves that experience a sustained change in growth T, and in newly-developed (ND) leaves that form under a new thermal regime. In species other than rice, the extent of changes underpinning thermal acclimation (including changes in leaf structure, nitrogen partitioning and organelle abundance), is typically greater in ND than PE leaves (Armstrong et al., 2008; Gorsuch, Pandey, & Atkin, 2010; O'Leary, Asao, Millar, & Atkin, 2018; Tjoelker, Reich, & Oleksyn, 1999; Yamori et al., 2005).

Past studies on rice conducted during the vegetative (Glaubitz et al., 2014; Kurimoto, Day, Lambers, & Noguchi, 2004) and reproductive (Bahuguna, Solis, Shi, & Jagadish, 2017; Mohammed, Cothren, & Tarpley, 2013) phases of development have reported limited and variable levels of acclimation of R_{dark}. By contrast, A_n of rice shows strong thermal acclimation, with rates of net CO_2 uptake measured at the prevailing growth T being homeostatic or increasing as growth T is increased

from 15 to 37°C (Nagai & Makino, 2009; Yamori, Noguchi, Hikosaka, & Terashima, 2010). Such studies point to a possible asynchrony in rice acclimation, with a more dynamic A_n than R_{dark} response, although further work simultaneously comparing A_n and R_{dark} in rice is needed. Interestingly, a range of other crops and non-crop species show the opposite – greater R_{dark} than A_n acclimation capacity (Campbell et al., 2007; Drake et al., 2016; Way & Oren, 2010). Although such studies detail the physiological acclimation of energy metabolism in plants, including rice, less is known about the molecular and biochemical responses that underpin this phenotypic *T* acclimation.

It is with the above issues in mind that we conducted a study using the IR64 cultivar of *Oryza sativa* to address the following aims: (1) characterise the extent of thermal acclimation of R_{dark} and A_n; and, (2) link physiological acclimation to the underlying processes through analysis of leaf transcript, protein, sugar, and starch abundance, following changes in growth *T*. We hypothesized that: (1) initial exposure to very high growth *T* increases and decreases the rates of respiratory CO_2 release and net photosynthetic CO_2 uptake, respectively; (2) subsequent acclimation is associated with recovery of A_n, and reduced rates of R_{dark}; and (3) thermal acclimation of R_{dark} and A_n is associated with dynamic changes in gene expression and protein abundance in key pathways associated with energy capture and use.

Materials and methods

Plant material and temperature treatments

Rice (*Oryza sativa*) cultivar IR64 plants were grown hydroponically in a glasshouse facility at the Research School of Biology, Australian National University in Canberra between October and December 2015. Seeds were initially incubated at 40-42°C for two days before soaking in water for eight hours, placed on wet Whatman filter papers in petri dishes and kept in the dark at 30°C for five days. The germinated seedlings were then transferred to trays of vermiculite and placed in temperature-controlled glasshouses (30°C day and 25°C night) under natural sunlight and photoperiod, with photosynthetically active radiation (PAR) between 400 and 1200 µmol m^{-2} s^{-1}. When the third leaf had emerged, seedlings were transplanted from vermiculite to a hydroponic system. Individual plants were placed within PVC tubes with a 3.7 cm diameter and 13 cm height. Tubes were then suspended at the top of 20 L capacity hydroponic tanks (12 tanks in total), with each tank holding a maximum of 20 plants. Each tank was filled with hydroponic solution (Table S1) (Hubbart, Peng, Horton, Chen, & Murchie, 2007). The nutrient solution was replaced weekly. Sulphuric acid or sodium hydroxide were used to adjust the pH to 5-6, with pH monitored using a portable pH meter (Rowe Scientific Pty. Ltd.,

NSW, Australia). The hydroponic solution was aerated continuously using Infinity AP-950 air pumps (Kong's Pty. Ltd., Ingleburn, Australia).

After two weeks of hydroponic growth at 30/25°C ('warm' treatment), the most recently fully-expanded leaves were labelled as pre-existing (PE) leaves. Following labelling, four tanks were randomly chosen and shifted to an adjacent glasshouse room set to 25˚C day and 20˚C night (25/20˚C – 'cold' treatment), and four other tanks were moved to a room set at 40˚C day and 35˚C night (40/35˚C – 'hot' treatment); four tanks were retained at 30/25°C as controls. Relative humidity was not controlled. Newly-developed (ND) leaves that emerged under each thermal regime were labelled, with all measurements reported on ND leaves made 21 days after *T*-transfer.

Determination of transcript abundance

Plants were transferred to new thermal regimes three hours after sunrise. To quantify transcript abundance, the labelled pre-existing (PE) leaves were harvested during the photoperiod: two, six and 24 h after *T*-transfer. For each time-point and temperature treatment, approximately 8 cm long segments (less than 100 mg of fresh mass) were sampled half-way along the leaf blade, and immediately frozen in liquid N_2 and stored at -80°C until RNA extraction. Total RNA was extracted using the RNeasy plant mini protocol (Qiagen, Doncaster, VIC, AU) and treated with DNase I (Qiagen, Doncaster, VIC, AU) to remove any contaminating DNA.

For qPCR analysis, 1 µg of total RNA in a 10 µL volume was reverse- transcribed into cDNA using SuperScript III First-Strand cDNA Synthesis Kit (Invitrogen, Carlsbad, CA, USA), according to the manufacturer's instructions. The reverse-transcribed cDNA samples were diluted 10-fold. Transcript levels of six selected genes and one reference gene (refer to Table S2 for gene accession numbers and primer sequences) were analysed using a Light-Cycler® 480 System (Roche Holding AG, Basel, Switzerland) with SYBR Green I Dye (QIAGEN, Doncaster, Victoria, AU). cDNA samples from each biological replicate were assayed in two technical duplicates. The reaction-mix in each qPCR contained 0.4 µM of each pair of primers, 5 µL of SYBR Master Mix, and 4.6 µL of the diluted cDNA sample in a 10 µL total reaction volume. The raw fluorescence data were analysed using LinRegPCR (Ramakers, Ruijter, Deprez, & Moorman, 2003; Ruijter et al., 2009). Data were normalized to the reference gene, eukaryotic initiation factor 5c (*EIF5C*; LOC_Os11g21990.1), and were expressed as fold-changes against control conditions.

RNAseq libraries were prepared using the Illumina Stranded Total RNAseq kit with RiboZero rRNA depletion as per the manufacturer's guidelines (Illumina). Libraries were pooled and sequenced on a HiSeq1500 for 61 cycles in single end mode at the Centre for AgriBioscience, University of LaTrobe. Analysis pipelines for pre-processing and mapping of sequence data are available online on

GitHub (https://github.com/pedrocrisp/NGS-pipelines). Quality control was performed with *FastQC* v.0.11.2. Adapters were removed using *scythe* v.0.991 with flags -p 0. and reads were quality trimmed with *sickle* v.1.33 with flags -q 20 (quality threshold), and -l 20 (minimum read length after trimming). The trimmed and quality-filtered reads were aligned to the rice reference genome Os-Nipponbare-Reference-IRGSP-1.0 from the MSU Rice Genome Annotation Project Database v7 (http://rice.plantbiology.msu.edu/) using the *subjunc* aligner v1.5.0-p1 with -u and -H flags to report only reads with a single unambiguous best mapping location, -P 3 for phred+33 encoding (Liao, Smyth, & Shi, 2013b). Reads were then sorted, indexed and compressed using *samtools* v1.1-26-g29b0367 (Li et al., 2009) and strand-specific bigwig files were generated using *bedtools genomecov* v2.16.1 (Quinlan & Hall, 2010) and the UCSC utility *bedGraphToBigWig* for viewing in IGV (Robinson et al., 2011). Summary statistics for each sample are provided in Supplementary Dataset S1: Summary of transcriptomic datasets.

For standard differential gene expression testing, the number of reads mapping per IRGSP-1.0 gene loci was summarised using *featureCounts* v1.5.0-p1(Liao, Smyth, & Shi, 2013a) with flags -P and -c to discard read pairs mapping to different chromosomes and the -s flag set to 2 for strand specificity for a strand specific library, multimapping reads and multioverlapping reads were not counted. Reads were summarised to parent IRGSP-1.0 gene loci rather than individual splice variants by summarising to the genomic coordinates defined by the feature "gene" in the IRGSP-1.0.gff reference (last modified 7/2/2012 ftp://ftp.plantbiology.msu.edu/pub/data/Eukaryotic_Projects/o_sativa/annotation_dbs/pseudomolecules/version_7.0/all.dir/all.gff3). Only loci with an abundance of at least 1 CPM (approximately 5 reads) in at least 4 samples were retained. Statistical testing for relative gene expression was performed in R following the "*edgeR-limma-voom*" approach (https://www.bioconductor.org/help/workflows/RNAseq123/); using, *edgeR* v.3.4.2 (McCarthy, Chen, & Smyth, 2012; Robinson & Oshlack, 2010; Robinson & Smyth, 2007a, 2007b), and *voom* in the *limma* package 3.20.1 (Law, Chen, Shi, & Smyth, 2014; Smyth, Michaud, & Scott, 2005).

Determination of protein abundance

Samples of frozen PE leaf material six and 24 h after *T* transfer, as well as frozen ND leaf material, were ground to a fine powder using a chilled mortar and pestle, and protein was extracted in extraction buffer containing 100 mM tricine pH 8.0, 1 mM EDTA, 1 mM PMSF, 1x protease inhibitor cocktail, 2% (w/v) PVPP, 10 mM (w/v) ascorbate, 5 mM DTT, and distilled water. The sample was then solubilized in a NuPAGE LDS Sample Buffer (Invitrogen, Carlsbad, CA, USA) with 10% (v/v) DTT, then heated for 10 minutes at 95˚C, and centrifuged for 30 sec at 12,000 RPM. Thereafter, supernatant

was collected and 8 uL were loaded and separated on 4-12% NuPAGE Bis-Tris gel (Invitrogen, Carlsbad, CA, USA) using the MOPS-based buffer system. To blot, proteins from the gel were transferred to Immobilon-P Polyvinylidene fluoride (PVDF) membranes (Merck Millipore, Kilsyth, VIC, AU) using an XCell II Blot module (Invitrogen, Carlsbad, CA, USA). Membranes were then blocked for 2 h with 5% (w/v) skim-milk powder in Tris-buffered saline containing 0.1% (v/v) Tween-20 (TBST). To probe for cytochrome *c* oxidase (*COX*) subunit II, alternative oxidase (*AOX*), uncoupling protein (*UCP*) and voltage-dependent anion-selective channel protein (*VDAC1*-porin), the membranes were incubated for 2 h in primary antibody solution (5% w/v skim milk powder in TBST) containing commercially available polyclonal antibodies (Agrisera, Vännäs, Västerbotten, Sweden). All antibodies were diluted 1:5000. An antibody for ribulose-1,5-bisphosphate carboxylase/oxygenase (Rubisco) was received from Assoc. Prof. Spencer Whitney (Research School of Biology, Australian National University, Canberra, ACT, AU) and used at a dilution of 1:10 000. After washing with TBST, the membranes were incubated for 1 h in goat anti-rabbit antibody solution (5% w/v skim milk powder in TBST) at a dilution of 1:8000. Proteins were then visualized using the AttoPhos AP fluorescent substrate system (Promega, Madison, WI, USA), imaged using a Versa-Doc (Bio-Rad, Hercules, CA, USA) imaging system and quantified using Image Lab software (Bio-Rad, Hercules, CA, USA). Protein concentrations were determined by the Bradford method using Bovine Serum Albumin (BSA) as a standard.

Determination of soluble sugar and starch ~~content~~concentrations

Starch and soluble sugars of PE leaves transferred from 30/25°C to 25/20°C or 40/35°C for one and seven days, and ND leaves at the prevailing *T* were collected from separate, previously unsampled plants. Samples were collected at 9:30 to 10:00 am, corresponding to 3 h into the light period, frozen and stored at -80°C before freeze-drying at -105°C for two days (Virtis Benchtop™ "K", SP, Scientific, Gardiner, NY, USA), then ground to a fine powder from which a 5-10 mg aliquot was taken. Five-hundred µL of 80% (v/v) ethanol was added and vortexed for 20 sec. Thereafter, leaf tissues were incubated at 80°C while being centrifuged at 500 RPM for 20 min. Following further centrifugation at 12,000 RPM for 5 min, the resulting pellet and supernatant were separated. This procedure was repeated a two more times, and the three pellets and three supernatants were pooled. The pooled supernatants and pellets were used for determination of soluble sugars and starch ~~contents~~concentrations, using a Fructose Assay Kit (Sigma-Aldrich, St Louis, MO, USA) and a Total Starch Assay Kit (Megazyme, Chicago, IL, USA), respectively. Following manufacturer's instructions, measurements were made in triplicate, at a wavelength of 340 nm, using a microtitre plate reader

(Infinite® M1000 Pro; Tecan US, Morrisville, NC) and standard curves were generated for soluble sugars using sucrose, glucose and fructose (Sigma-Aldrich, St Louis, MO, USA) at known concentrations.

Gas exchange measurements using Licor 6400XT 6 cm^2 cuvettes

Gas-exchange was measured on fully-expanded pre-existing (PE) leaves just prior to- and one, two, three, five and seven days after *T* transfer, as well as on fully-expanded newly-developed (ND) leaves 21 days after transfer, using two matched LI-6400 instruments equipped with 6 cm^2 cuvettes and a 6400-02B red-blue light source (Li-Cor, Lincoln, NE, USA). At each time point, light-saturated net CO_2 assimilation rates (A_n) and then dark respiration rates (R_{dark}) were measured during the light period (between 10 am and 2 pm) in the glasshouses, at the prevailing day-time *T* of each treatment as well as at a common temperature of 30°C for ND leaves. In call cases, A_n was measured first, with the following settings: 1000 µmol m^{-2} s^{-1} photosynthetic photon flux density (PPFD), relative humidity of 60–70%, 400 ppm reference CO_2, and a flow rate of 500 µmol s^{-1}. Photosynthesis was measured when CO_2 concentrations in the sample IRGA had stabilized, typically within 10 minutes of exposure to 1000 µmol m^{-2} s^{-1} PPFD. Thereafter, R_{dark} was measured as above but with the flow rate slowed to 300 µmol s^{-1} and turning off the light source for at least 30 minutes of darkness before taking measurements.

Gas exchange measurements using using Walz chambers

High resolution temperature response curves of R_{dark} and light-saturated A_n were made on intact ND leaves using two matched LI-6400XT portable gas exchange systems (Li-Cor, Lincoln, NE, USA) each connected to a 14 x 10 cm well-mixed, temperature-controlled Walz Gas-Exchange Chamber 3010-GWK1 (Heinz Walz GmbH, Effeltrich, Germany). For each temperature-response curve, leaf *T* was measured with a small-gauge wire copper constantan thermocouple pressed against the lower surface of the leaf and attached to a LI-6400 external thermocouple adaptor (LI6400-13, Li-Cor Inc., Lincoln, NE, USA) that enabled leaf temperature to be recorded by the LI-6400XT. As leaves were heated, net CO_2 exchange was recorded at 30 s intervals using the LI-6400XT portable gas exchange systems fitted with an empty and closed 6 cm^2 chamber that was plumbed into the airstream exiting the Walz leaf chamber (Fig. S1). A_n was measured as described for the 6 cm^2 cuvette but using a Walz LED-Panel RGBW-L084 light source (Heinz Walz GmbH, Effeltrich, Germany). A_n was monitored as leaves were heated at 1°C min^{-1} from 20 to 45°C. A water trap was used to remove water vapour, as transpiration from whole intact leaves was incompatible with Licor instrumentation. Therefore, stomatal conductance (g_s) and associated water parameters were not recorded. For R_{dark}, on separate

leaves to those used for measuring A_n, the flow rate was reduced to 300 µmol s^{-1}, the light source was turned off, and the chamber was covered with a black cloth, before increasing the leaf temperature in steps of 1°C min^{-1}, from 20 to 60°C. In parallel to quantifying the temperature-response of R_{dark}, we measured minimal chlorophyll *a* fluorescence (F_o) in the presence of a low-intensity far-red light pulse (necessary to maintain PSII in the oxidized state) every 30 sec using a Mini-PAM portable chlorophyll fluorometer (Heinz Walz, Effeltrich, Germany) fitted above the glass surface of the leaf chamber. The temperature at which F_o increased was used as an indication of heat-induced damage to photosystem II, which we hereafter refer to as T_{crit}, calculated using the template of O'Sullivan *et al.* (2013). At the cessation of measurements, leaves were photographed and analysed for leaf area using ImageJ software (Abramoff, Magelhaes, & Ram, 2004). Leaves were stored in paper bags, oven-dried at 70°C for two days and weighed to obtain the dry mass. Quadratic equations were fit to A_n temperature curves and the x- and y-axis values corresponding to the vertex taken as the *T*-optimum (T_{opt}) and A_n-optimum (A_{opt}) of net assimilation, respectively. For the R_{dark} temperature curves, the x- and y-axis values corresponding to the maximum recorded R_{dark} were taken as the *T* at which R_{dark} reached a maximum (T_{max}) and the maximum R_{dark} value recorded (R_{max}), respectively.

Leaf elongation rates

The leaf elongation rates (LER) of four leaves from separate plants from each temperature regime were measured at five separate time-points over a 24 h period. Measurements were made using a ruler, starting from the ligule of the second youngest leaf to its tip.

Statistical analysis

For all *T*-treatments and collection times, four separate leaves from four separate previously unsampled plants, one plant from each of the four hydroponic tanks (pot replicates) were sampled. One-way Analysis of Variance (ANOVA) was performed on R_{dark} and A_n gas-exchange experiments comparing temperature treatments. Two-way ANOVA was performed on LMA and protein, starch, and sugar ~~contents~~ concentrations comparing time of sampling and temperature treatments. Gas-exchange and leaf biochemical statistical analysis was performed using GraphPad Prism (v 7) software. Statistical analysis of transcript abundance was performed using *R* statistical software (v 3.6.1) and packages as mentioned above.

Data availability

RNA-seq data is available under the GEO identifier GSE136045.

Results

Molecular and biochemical responses of leaves to T

Quantitative PCR was performed on specific genes of interest to elucidate the genetic response of pre-existing (PE) leaves exposed to a change in *T* (Fig. 1). Apart from a sharp rise 6 h into the 40/35°C *T*-transfer, there was a general reduction in transcript abundance of *cytochrome c* ~~*complex*~~ *oxidase* (*cox*), a gene encoding the central respiratory electron transport chain. This reduction occurred in leaves transferred to 25/20°C and 40/35°C, over the seven days post-transfer period, . Two genes encoding respiratory proteins that potentially reduce the production of ATP – *alternative oxidase* (*aox*) and *uncoupling protein* (*ucp*) – both showed an initial increase in expression within the first 24 h of transfer to the hotter 40/35°C, followed by a decline to 30/25°C levels by 48 h. The photosynthetic electron transport gene *ferredoxin NADP reductase* (*fnr*), and the Calvin/Benson cycle gene *phosphoribulokinase* (*prk*) generally showed an increase in expression in the first 48 h at 40/35°C before being supressed for up to 5 days post-transfer. *Sucrose phosphate synthase* (*sps*), involved in the synthesis of sucrose from its precursors, also initially spiked in the first 24 h following transfer to 40/35°C, before being transiently suppressed. Both *sps* and the respiratory and photosynthetic genes – apart from *aox* – followed a similar expression profile when heat-treated, suggesting that assimilate production/consumption and sucrose synthesis were coordinated in response to heat perturbations. In general, the greatest perturbation to gene expression occurred within the first 24 h after transfer.

Based on the qPCR results, we conducted RNA-seq at two, six and 24 h after transfer of PE leaves to new *T*. Following data quality control and filtering, transcript abundance of 19,308 rice genes were retained for differential expression testing. Around 20 M reads were obtained per sample, which were aligned to the Os-Nipponbare-Reference-IRGSP-1.0 rice reference genome (Data Set S1). Principal component analysis showed a substantial treatment effect on gene expression for the heat-exposed leaves (40/35°C) during the first six hours after *T*-transfer compared to the other two 30/25°C and 25/20°C growth regimes (Fig. 2). Globally, there was little gene expression variation between the cold (25/20°C) and the warm (30/25°C) control conditions. After 24 h of growth at new *T*-regimes, limited variation in gene expression was observed between all of the three *Ts* (Table S3).

To assess changes in the expression of individual genes to the hot or cold treatments, differentially expressed genes were identified at each time point by comparison to the warm control expression levels (Data Set S2). There were very few genes differentially expressed under the cold conditions, only six genes in total (Table S3). By contrast, under hot conditions, there were 1,818 and 1,465 genes differentially expressed after two and six hours, respectively. After 24 hours, there were

no differentially expressed genes under the hot conditions compared to the control plants. There was a significant overlap between the genes differentially expressed after two and six hours of heat treatment, (Fig. 3a, b). In total, 30% of the genes upregulated after six hours were already upregulated by two hours, and 38% of genes downregulated after six hours were already downregulated by two hours. Many of the remaining genes that were significantly different in transcript abundance only after six hours were already trending in the same direction at the two-hour time point, but the difference compared to the controls did not pass the significance threshold (Fig. 3 c). Overall, these results show that there are significant short-term changes in transcript abundance in rice plants exposed to heat stress. The expression profiles of samples exposed for two and six hours show consistent changes; however, some of the changes peak at two hours and others peak at six hours and most changes dissipate within 24 hours.

In total, the heat treatment led to the up- and down-regulation of 1,337 and 1,446 genes, respectively. To investigate the extent to which these genes have a photosynthetic or respiratory function, we first examined expression of genes involved in photosynthesis, glycolysis, TCA and mitochondrial electron transport using MapMan pathway annotations (Fig. S2-4) (Thimm et al., 2004). This qualitative analysis revealed that the expression of only a small number of photosynthetic/respiratory genes were affected. To extract a list of high-confidence differentially expressed respiration-related genes, we manually curated a list of rice loci with homology to Arabidopsis respiration genes (Data Set S3). Using this list, we found that eight genes were differentially expressed at high temperature, with two genes downregulated more than 2-fold: *aox* and ATP-dependent *phosphofructokinase* (Table 1). The seemingly conflicting result of an initial increase in *aox* from the qPCR results, but a decline in *aox* during the same period from the RNA-seq results, can be explained by our qPCR primers targeting the *aox1a* isoform while the RNA-seq identified a decline in the *aox1c* isoform (Data Set S3).

It is interesting that in addition to the increase in *aox* and *ucp* gene expression, the expression of an external NAD(P)H dehydrogenase also increased, while that of Complex II decreased significantly (Table 1). Together these changes suggest that an increase in non-phosphorylating electron transport occurred in response to exposure to higher *T*, at the expense of electron transport coupled to ATP synthesis, at least in the short term. The increase in external NAD(P)H dehydrogenase gene expression may also indicate an increased need for mitochondrial oxidation of excess reductant produced in the chloroplast at higher *T*.

Given the relatively small effect of the heat treatment on the expression of respiration- or photosynthesis-related genes, we next performed Gene Ontology enrichment analysis. This revealed a

notable enrichment for genes involved in primary metabolism (eg GO:0044238) and response to abiotic stimuli (eg GO:0050896), as well as in many biosynthetic pathways (Fig 4).

Protein abundance (expressed on a leaf area basis) of key mitochondrial electron transport components – CYTOCHROME C OXIDASE (COX) subunit II, ALTERNATIVE OXIDASE (AOX) and UNCOUPLING PROTEIN (UCP) – were determined by Western blots in PE leaves 6 h and one-day after *T*-transfer, and in newly developed (ND) leaves that formed under each prevailing growth *T* (Fig. 5, Fig. S4). The cold (20/25°C) and heat (40/35°C) treatments did not affect the total protein concentration of leaves, at any time after *T*-transfer (Table S4). As was the case for gene expression, there was a significant decline in COX subunit II protein abundance after 24 h. COX subunit II also declined in abundance in ND leaves when grown at 40/35°C compared to 25/20°C (Fig. 5a). We assume the changes observed in COX subunit II reflect changes in abundance of the entire complex. The abundance of AOX and UCP protein did not vary in response to growth *T* or duration of exposure to heat for either PE or ND leaves, despite the initial spike in *aox* and *ucp* gene expression after transfer to 40/35°C (Fig. 1). Interestingly two bands of AOX that varied relative to one another with temperature treatment were evident in the Western blot (Fig. S5). This is consistent with the fluctuations in expression of different *aox* genes noted above. Patterns of protein abundance were similar when the analysis was standardised to dry mass or porin abundance (Fig. S6). Porin is a voltage-dependent channel protein located at the outer membrane of mitochondria and is widely used as a proxy for mitochondrial surface area due to its stability under a wide range of environmental conditions (Noguchi, Taylor, Millar, Lambers, & Day, 2005; Shane et al., 2004). Thus, the matching results using leaf area, dry mass or porin abundance indicate that the decline in COX abundance with increased *T* was not a result of changes in Leaf Mass to Area ratio (LMA) or reduced mitochondria per unit area of leaf. There was a trend for the abundance of Rubisco to decline with the amount of time a leaf developed under 40/35°C (Fig. 5d), although there were no statistically significant *T* or developmental stage effect.

LMA and starch, glucose, fructose and sucrose ~~contents~~ concentrations were measured in PE leaves one and seven days after *T*-transfer, and in ND leaves at the prevailing temperature (Table 2). LMA did not change significantly in response to *T*, for either transferred PE leaves or ND leaves, similar to previous observations in rice over a similar *T* range (Nagai & Makino, 2009). However, ND leaves did exhibit significantly greater LMA than PE transferred leaves, suggesting an effect of leaf rank on LMA. Transferred PE and subsequently formed ND leaves exhibited consistently lower starch ~~content~~ concentrations with increasing *T* and significantly lower starch with extended duration of development at the prevailing *T*. Unlike the dynamic responses of leaf starch ~~content~~ concentrations

to T change, ~~contents~~ concentrations of soluble sugars were remarkably stable across both PE and ND leaves, in terms of both T-regime and exposure time. Negative correlations between R_{dark} and soluble sugars were observed among leaves within each individual T treatment but not among the three T treatments (Table S5).

CO_2 flux in responses to T

How molecular changes altered the physiological performance of rice carbon metabolism at differing growth T was investigated through gas-exchange measurements. Rates of A_n and R_{dark} are here presented on a dry mass (DM) basis, noting that the patterns are similar when expressed on a leaf area basis (Fig S7), reflecting the fact that growth T had no significant effect on LMA (Table 2). A significant change in both A_n and R_{dark} (using mid-sections of leaves placed in Licor 6400 3 x 2 cm chambers) occurred within the first 24 h of transfer to a 40/35°C T-regime for PE leaves, with A_n falling and R_{dark} increasing when measured at the prevailing growth T (Fig. 6). This was followed by stabilisation at the new rate over the subsequent six days. By contrast, A_n and R_{dark} remained relatively constant at both 30/25°C and 25/20°C over a seven-day period monitoring period. Interestingly, rates of R_{dark} for the 30/25°C treated plants decreased from day 3 to 7, compared to the first three days, resulting in slightly lower rates of R_{dark} than for the 25/20°C treated plants by day 7. This possibly reflects temperature-dependent differences in leaf senescence rates. ~~Interestingly~~As it could not be controlled, relative humidity in the 40/35°C glasshouse room (Fig. S8) was substantially lower than the other two rooms, leading to reduced humidity during gas-exchange measurements (Fig. 6c). As a consequence,~~,~~ the vapour pressure deficit between the leaf and surrounding air (VPD_{Leaf}) increased ~~consistently~~ over the first seven days in PE leaves transferred to 40/35°C, resulting in a dramatic difference by day seven (Fig. 6d~~e~~). Th~~is, and the associated reduction in~~ e higher VPD_{Leaf} coincided with lower ~~*stomatal conductance*~~g_s ~~of the~~in 40/35°C treated leaves at days three, five and seven, and lower intercellular to ambient CO_2 concentration ratios (C_i/C_a) at days five and seven (Fig. 6e, f~~d~~). ~~,~~ However, for the first two days post transfer~~,~~ both~~the~~ VPD_{Leaf}~~vapour pressure deficit~~ and g_s~~stomatal conductance~~ ~~was~~were similar between the three growth Ts, ~~and~~ Ttherefore, the ~~did not explain the initial 48 h~~ decline in A_n and changes in transcript abundance ~~at~~ within one day of transfer to 40/35°C were not attributable to water relations~~likely contributing to the longer-term limitation in photosynthesis at this warmer temperature in PE leaves~~. Over the longer-term, water relations may have contributed to a slight reduction in C_i/C_a, but not enough to influence A_n, with A_n being stable from one to seven days after transfer irrespective of changes in g_s and C_i/C_a (Fig. 6b). The changes in g_s were not substantive enough to change leaf T, which was stable over the seven days, with both air

T and leaf *T* deviating by less than 2°C from the set room *T* (Fig. S8).~~However, for the first two days post transfer, the vapour pressure deficit and stomatal conductance was similar between the three growth *T*s, and therefore did not explain the initial 48 h decline in A_n at 40/35°C.~~

Short-term temperature response curves of entire ND leaves that formed at each prevailing growth *T* regime were quantified over a 20 to 60°C range using the Walz large leaf chamber (Fig. 7; refer to Figure S9~~8~~ for area-based rates and Table S6 for quadratic equations fit to curves). Over most of the range of measuring *T*s, leaves developed at 25/20°C exhibited higher rates of R_{dark} than those developed under the other two *T*-regimes. Rates were lowest in leaves developed at 40/35°C (Fig. 7a). When normalised to rates at 30°C, differences in R_{dark} were less pronounced (Fig. 7b), indicating that while R_{dark} at a given measuring *T* was affected by growth *T*, the general shape of the R_{dark}-*T* curves remained largely similar across the three treatments. These observations are consistent with a Type II (changes in baseline) rather than Type I (changes in Q_{10}, the increase in R_{dark} with a 10°C increase in *T*) respiratory acclimation response (Atkin & Tjoelker, 2003). Importantly, while respiratory thermal acclimation occurred, it was not sufficient to result in R_{dark} being homeostatic across the three growth *T* treatments. As a result, R_{dark} measured at the growth *T* was significantly ~~faster~~ greater in the leaves developed under hot conditions than under the other two treatments (Table 3). Growth *T* also had a significant effect on the measuring *T* at which R_{dark} and A_n reached their maximum rates, with leaves developed under high *T* exhibiting higher *T*-maxima than control 30/25°C leaves (Table 3). When measured at the prevailing growth *T* of each treatment, mass-based rates of light-saturated A_n were stable (i.e. homeostatic), further supporting the occurrence of strong thermal acclimation of A_n in ND leaves (Fig. 7), contrary to PE leaves (Fig. 6). The temperature at which PSII lost functionality (T_{crit}) ~~also increased~~tended to increase with growth *T* (being 3.8°C higher in the hot-grown plants compared to those grown at 25/20°C), although the differences were not statistically significant at $p<0.05$ (Table 3). The high degree of thermal acclimation exhibited by photosynthesis resulted in the ratio of R_{dark} to A_n being lowest in the hot-grown plants, particularly at high measuring *T* (Fig. 8a); at a measuring *T* of 40°C, hot-acclimated plants exhibited R_{dark}/A_n ratios that were 50% lower than those measured for their cold-grown counterparts. Further evidence that rice acclimated to heat is seen in the fact that leaf elongation rates – taken over the day and night period – were faster for the 40/35°C grown plants at all times (Fig. 8b). Interestingly, A_n of PE leaves ranged from 1.2 to 1.8 μmol g^{-1} DM s^{-1} (Fig. 6), substantially faster than the 0.6 μmol g^{-1} DM s^{-1} in ND leaves (Fig. 7). The former were obtained from measurements on mid-leaf sections placed in a 6 cm^2 chamber, while the latter were obtained from whole leaves placed in a 14 x 10 cm Walz chamber. The lower A_n rates in the latter might reflect a

lower proportion of mesophyll cells per unit of area or DM across whole blades compared to the mid-blade section.

Discussion

Our study investigated the response of photosynthetic and respiratory metabolism to short- and long-term changes in growth T – the highest of which is indicative of heat-wave Ts – to explore: (1) the extent of thermal acclimation of photosynthesis and respiration; and, (2) what underlying changes in gene expression and protein abundance occur during the acclimation process. The results demonstrate that the process of acclimation begins with abrupt changes in gene expression in PE leaves within the first 24 h of heat exposure, followed by a return to homeostatic gene expression (Fig. 1). Importantly, the abundance of the key energy-conserving respiratory protein, COX, declines in abundance when pre-existing leaves are heat-treated for 24 hours, with this phenotype being maintained in newly-developed leaves formed at 40/35°C (Fig. 5). This decline in COX was linked to a slight decline in overall rates of R_{dark} (Fig. 7). The results support the hypothesis that acclimation of photosynthesis and dark respiration are asynchronous in rice, but contrary to observations in non-crop species (Campbell et al., 2007), light-saturated A_n acclimated to a greater extent than R_{dark} (Fig. 7; Table 3). This ability to maintain photosynthetic carbon gain at 40°C is likely to be of crucial importance in helping rice maintain growth during heat-wave conditions.

Acclimation to changes in T are rapid and involve a multitude of genes

There was a substantial change in the gene expression profile of rice leaves shifted from 30°C to 40°C within the first 24 h of transfer (Figs. 1, 2, 3, and 4). As might be expected, the largest number of gene expression perturbations were in primary and cellular metabolic processes (Fig. 4). This extensive metabolic response aligns with the instability in R_{dark} and A_n fluxes over the initial 24 h post T-transfer (Fig. 6), which would have contributed to a metabolic imbalance through changes in assimilate supply and demand. Interestingly, the most responsive genes to the initial exposure to heat among upregulated genes were genes involved in biosynthetic processes (Fig. 4) suggesting a stimulation of growth. This is supported by the longer-term increase in leaf elongation rates observed in the 40/35°C grown plants.

When analysed in more detail, we observed that heat ~~to~~ induced genes linked to energy dissipation (*aox* and *ucp*) over the first 24 h of 40°C heat exposure (Fig. 1, Table 1). AOX and UCP are involved in the diversion of electrons for formation of proton gradients and subsequent ATP synthesis (Krauss, Zhang, & Lowell, 2005; Vanlerberghe, 2013). Past work has shown that

overexpressing *aox* in young rice seedlings imparts a benefit on growth under a *T* of 37°C for eight days, which was attributed to a reduction of excessive proton motive force and reactive oxygen species (Murakami & Toriyama, 2008). Given that AOX and UCP both divert electrons away from ATP synthesis under conditions of high reductant supply, the rapid upregulation of these genes following the initial changes in growth *T* – with rapid stimulation of R_{dark} and presumably greater reduction of ubiquinone pools (UQ) – indicates that there may have been a temporary imbalance between NAD(P)H supply and demand for ATP. The initial increases in *aox* and *ucp* gene expression (Fig. 1) did not translate into increased total AOX and UCP protein abundance (Fig. 5). However, qPCR results indicate upregulation of the *aox1a* isoform, responsive to abiotic stress in Arabidopsis mitochondria (Clifton, Millar, & Whelan, 2006; Shapiguzov et al., 2019), while over the same period RNA-seq analysis indicated a significant decline in a separate *aox1c* isoform. It is possible that the AOX1C isoform is less tolerant of high temperatures and therefore is partially replaced by the AOX1a isoform. In this context it is interesting that in Arabidopsis AOX1a is the major stress-inducible isoform. Since AOX operates as a non-covalently linked dimer (Siedow & Umbach, 2000), the change in the relative expressions of *aox1a* and *1c* isoforms may also indicate a change in the conformation of the AOX dimer, with a different mix of homo- and hetero-dimers in response to heat. This suggests that AOX may have shifted to a more heat-tolerant conformation at 40/35°C, at least when the initial shock was imposed. This is an illustration that enzyme isoforms can be an important part of abiotic stress responses that can be easily overlooked when only considering total protein abundance.

The limited gene induction when leaves were transferred from 30 to 25°C (Fig. 3c) suggests that a shift to this colder growth *T* did not significantly perturb metabolic processes in rice leaves, consistent with the limited PE leaf response of R_{dark} or A_n when exposed to the cold (Fig. 6). However, cold-responsive transcriptional regulators and associated changes in metabolism expected from cold exposure (Zhu, Dong, & Zhu, 2007) must have been triggered by the colder *T*s. Regulatory adjustments did indeed occur in ND rather than PE leaves, with R_{dark} at a given *T* being higher in the cold-grown ND leaves (Fig. 7), and homeostasis of A_n being reached in ND leaves when measured at the prevailing growth *T* (Table 3, Fig. 7).

The most evident longer-term acclimation response is reduced COX abundance

The clearest biochemical response to increasing growth *T*, both in PE and ND leaves, was a decline in the abundance of COX (Fig. 5). A decline in COX has been reported for rice roots when grown at 25°C relative to 15°C (Kurimoto, Millar, Lambers, Day, & Noguchi, 2004). Conversely, COX content increased in *Arabidopsis thaliana* leaves grown at 5°C relative to 21°C (Armstrong et al., 2008). In

all these cases, COX protein content and rates of respiration at a common measuring *T* (including in our study; Fig. 5 and Fig. 7) decreased when plants grew at hotter *T*, suggesting that thermal acclimation results in changes not only in overall rates of respiration but also in the capacity to produce ATP. The acclimation response was rapid as COX declined in abundance by 24 h after 40°C *T* transfer in PE leaves (Fig. 5).

The decline in COX abundance with hotter growth *T* is intriguing. If COX activity became rate-limiting, it is likely that more ROS would be produced as the UQ pool would quickly become over-reduced. However, other reports suggest that the UQ redox state is relatively stable, including during changes in *T*, despite ~~faster~~ higher R_{dark} (Covey-Crump et al., 2007; Wagner & Wagner, 1995). If we assume that UQ redox poise was also stable during the ~~faster~~ greater R_{dark} at the hottest growth *T* in our experiments, there are two possible explanations. (1) The absolute flux of electrons through COX actually increased despite the decrease in protein abundance. This could be due to COX capacity being far greater than the capacity of the overall mETC. But since increasing *T*s stimulates the relative activity of enzymes (Copeland, 2000), it is possible that the smaller amount of COX protein had higher activity. In other words, the plants could make do with less COX at hotter *T*. (2) Alternatively, activation of AOX at the higher *T* may have occurred to supplement COX activity thereby preventing overload of the UQ pool. Measuring *T*-dependent *in vivo* ^{18}O fluxes through COX and AOX, as well as leaf ATP content is required to determine terminal oxidase activity and ATP synthesis. Understanding what, if any, biological benefit arises from synthesising less COX at warmer growth *T* is another important consideration. Alternatively, a reduction in COX might be a consequence of heat directly interfering with its synthesis. In support of this, a recent report shows that COX abundance and capacity in Arabidopsis is significantly reduced by knocking out a HSP70 isoform, suggesting that heat in some way interacts with COX formation (Wei et al., 2019).

Acclimation of R_{dark} and A_n is asynchronous in rice

The R_{dark}/A_n ratio increased with short-term increases in measuring *T* (Fig. 8), reflecting the fact that R_{dark} is more temperature dependent than is A_n. R_{dark}/A_n ratios were similar in 25 and 30°C grown leaves, when measured at the prevailing growth *T* of each treatment (i.e. R_{dark}/A_n was homeostatic). Thus, the acclimation process led to the balance between carbon gain and release being maintained across this moderate range of growth *T*s (Fig. 8). Acclimation was not, however, sufficient to maintain homeostasis of R_{dark}/A_n in 40°C grown plants (Fig. 8). Similar results of R_{dark}/A_n ratios in leaves and whole plants remaining relatively stable over moderate but not extremely high *T* have been reported (Atkin, Scheurwater, & Pons, 2006, 2007; Campbell et al., 2007; Drake et al., 2016; Loveys et al.,

2003). Different to past studies, our findings in rice show that homeostasis of R_{dark}/A_n is largely the result of maintenance of A_n more than through a marked reduction in rates of R_{dark}. Our results categorically show A_n acclimates to a greater extent than R_{dark} in rice, supporting previous studies of rice that collectively point to greater A_n than R_{dark} acclimation capacity (Bahuguna et al., 2017; Glaubitz et al., 2014; Kurimoto, Millar, et al., 2004; Mohammed et al., 2013; Nagai & Makino, 2009; Yamori et al., 2010), and field studies that infer limited rice R_{dark} acclimation capacity (Peng et al., 2004; Welch et al., 2010). However, for many plant functional types, including temperate grasses, the opposite occurs; R_{dark} acclimates to a greater extent than A_n (Campbell et al., 2007; Ow, Griffin, Whitehead, Walcroft, & Turnbull, 2008; Way & Oren, 2010; Way & Sage, 2008; Yamori et al., 2005). In this context, it should be noted that the previous studies are of species from temperate rather than tropical habitats, raising the question of whether, beyond rice, tropical grasses generally have asynchronous acclimation favouring A_n. The homeostasis of A_n and superior LER of hot-grown ND rice leaves was more remarkable when viewed alongside evidence that prolonged exposure to drier air was closing stomata and presenting slight reductions in CO_2 availability, at least in PE leaves (Fig. 6). There is evidence that stomata close following a T-dependent increase in VPD_{Leaf}, with the mechanism yet uncharacterised but likely involving guard cell sensing of water potential below the epidermis (Peak & Mott, 2010; Shope, Peak, & Mott, 2008). It seems that declining VPD_{Leaf} triggers stomatal closure in rice, even with unlimited root water supply.

As noted earlier, in recent years, rice yields have declined in response to increased daily mean Ts, with the decline being more strongly correlated with increasing night rather than day Ts (Peng et al., 2004; Welch et al., 2010). Our finding that A_n is homeostatic across growth T, whereas R_n is not (Table 3) – underpinned by greater acclimation of photosynthesis than respiration – suggests that one reason why yields are declining with increasing night temperatures is because high temperatures stimulate respiratory CO_2 release. This would have a negative effect on daily net carbon gain, and thus the ability to accumulate biomass in the lead up to anthesis.

Potential implications of rice leaf acclimation and starch ~~content~~ concentration on crop yield

We found that soluble sugar ~~contents~~ concentrations of rice leaves were remarkably stable, irrespective of growth T or developmental time at each growth T (Table 2). Maintaining soluble sugar homeostasis is an important physiological requirement for many plant species, achieved through balancing CO_2 uptake and release in source leaves with sugar export to sink tissues (Rolland, Moore, & Sheen, 2002). Homeostasis of sucrose concentrations in rice leaves has been observed even when carbon demand by sink tissues is limited [e.g. reduced partitioning of sugars to grain (Wang et al., 2008)]. In our study, homeostasis of soluble sugar concentrations occurred even at 40°C, where rates of R_{dark} where

significantly higher than in plants at the cooler growth *Ts*. Associated with the maintenance of sugar concentrations was a *T*-dependent decline in starch ~~content~~concentration, both in PE and ND leaves (Table 2). For PE leaves exposed to 40°C, assimilate supply declined, particularly for 40°C transferred leaves, due to a marked increase in R_{dark} and a decline in A_n (Fig. 6). Starch content also significantly declined with developmental duration under high *T*, contrary to soluble sugar concentrations (Table 2). It seems likely, therefore, that the reason soluble sugars did not significantly decline at warmer *T* for PE leaves – even though assimilate supply fell – was a greater draw-down in the starch pool to maintain soluble sugar ~~contents~~ concentrations (i.e. a reliance on stored assimilate). Other studies [e.g. on the temperate tree *Populus tremula* (Hüve et al., 2012)] have highlighted the importance of starch degradation in maintaining soluble sugar concentrations, particularly under conditions that stimulate CO_2 release by respiration. Interestingly, in our study, ND leaves exhibited reduced starch ~~content~~ concentrations while also maintaining assimilate supply; one explanation for this might be that the decline in starch and maintenance of sugars of ND leaves was linked to the increased leaf elongation rates we observed for 40°C ND leaves (Fig. 8b), with increased growth (i.e. sink demand) necessitating a greater supply of sugars mediated by the starch pool (Stitt & Zeeman, 2012).

The decline in starch ~~content~~ concentrations for PE and ND leaves at 40°C (Table 2) has interesting implications for rice development and yield. Starch is stored in the stems in the late vegetative stage of rice, and accounts for a large proportion of the carbon accumulated in seeds, a process that is detrimentally affected by heat stress (Blum, Sinmena, Mayer, Golan, & Shpiler, 1994; Impa et al., 2018; Morita & Nakano, 2011; Yang & Zhang, 2005). Other studies using the IR64 cultivar exposed to hot night temperatures have shown an increase in R_{dark} and associated cost to vegetative growth and starch content of panicles, ultimately reducing yield (Bahuguna et al., 2017; Glaubitz et al., 2014). The reduced storage of starch in leaves with increasing *T* that we observed at the vegetative stage – assuming it did not reflect diversion of starch to stems – would suggest reduced potential for the storage of starch in stems and a penalty to yield of rice growing in warmer environments. This would be particularly true for rice plants exposed to transient extreme *T* – such as during heat waves – as we postulate the reduction in starch for PE leaves was due to a reduction in assimilate acquisition due to stimulated R_{dark} and supressed A_n. However, ND leaves did show reduced starch ~~content~~concentration, not as a result of reduced assimilate acquisition, but most likely associated with an increase in growth rates (Table 2; Fig. 8). Thus, it is likely that rice will experience different limitations on yield depending on the duration of thermal changes, with shorter-term exposure to rising *T* – over a period in which tissue cannot develop anew – likely leading to a greater suppression of yield than leaves developed under the prevailing growth *T*. Rice may even experience increased yield with

sustained mild warming of both night and particularly day *T*. However, yield potential is dependent on whether heat-dependent changes in growth at the vegetative stage of rice positively contributes to yield, which may be true (Glaubitz et al., 2014; Scafaro et al., 2018), and not simply accelerate development and shorten the time to flowering.

Conclusions

Overall, the results we present here demonstrate that both leaf respiration and photosynthesis can acclimate in rice but the extent of acclimation is asynchronous and dependent on the timeframe of *T* exposure. Warmer growth *T* of 40°C relative to 25°C will have a greater impact on rice CO_2 flux, metabolic pathways, starch concentration~~content~~ and ultimately growth. Consequently, rice growing in a warmer climate with more extreme heating events will likely experience *T*-dependent alterations in growth and yield. The duration and intensity of *T* changes, together with complex interactions between assimilate acquisition, storage and utilisation will determine if this warmer environment will be beneficial or detrimental to rice productivity over the coming decades. We suggest that enhancing the acclimation capacity of R_{dark} for rice at warmer growth *T* – potentially through COX, AOX and UCP regulation – could be a key target for improving rice productivity in a warmer world.

Acknowledgements

We thank Assoc. Prof Spencer Whitney for providing Rubisco antibody. The support of the Australian Research Council (ARC) Centre of Excellence in Plant Energy Biology (CE140100008) to OA, BP and JM is acknowledged. The authors have no conflict of interest to declare.

References

Abramoff, M. D., Magelhaes, P. J., & Ram, S. J. (2004). Image Processing with ImageJ. *Biophotonics International, 11*(7), 36-42.

Armstrong, A. F., Badger, M. R., Day, D. A., Barthet, M. M., Smith, P. M. C., Millar, A. H., . . . Atkin, O. K. (2008). Dynamic changes in the mitochondrial electron transport chain underpinning cold acclimation of leaf respiration. *Plant, Cell & Environment, 31*(8), 1156-1169.

Atkin, O. K., Bruhn, D., Hurry, V. M., & Tjoelker, M. G. (2005). Evans Review No. 2: The hot and the cold: unravelling the variable response of plant respiration to temperature. *Functional Plant Biology, 32*(2), 87-105.

669 Atkin, O. K., Scheurwater, I., & Pons, T. L. (2006). High thermal acclimation potential of both
670 photosynthesis and respiration in two lowland *Plantago* species in contrast to an alpine
671 congeneric. *Global Change Biology, 12*(3), 500-515.
672 Atkin, O. K., Scheurwater, I., & Pons, T. L. (2007). Respiration as a percentage of daily
673 photosynthesis in whole plants is homeostatic at moderate, but not high, growth temperatures.
674 *New Phytologist, 174*(2), 367-380.
675 Atkin, O. K., & Tjoelker, M. G. (2003). Thermal acclimation and the dynamic response of plant
676 respiration to temperature. *Trends in Plant Science, 8*(7), 343-351.
677 Badger, M. R., Björkman, O., & Armond, P. A. (1982). An analysis of photosynthetic response and
678 adaptation to temperature in higher plants: temperature acclimation in the desert evergreen
679 *Nerium oleander* L*. *Plant, Cell & Environment, 5*(1), 85-99.
680 Bahuguna, R. N., Solis, C. A., Shi, W., & Jagadish, K. S. V. (2017). Post-flowering night respiration
681 and altered sink activity account for high night temperature-induced grain yield and quality
682 loss in rice (Oryza sativa L.). *Physiologia Plantarum, 159*(1), 59-73.
683 Berry, J., & Bjorkman, O. (1980). Photosynthetic response and adaptation to temperature in higher
684 plants. *Annual Review of Plant Physiology, 31*(1), 491-543.
685 Bhardwaj, A. R., Joshi, G., Kukreja, B., Malik, V., Arora, P., Pandey, R., . . . Agarwal, M. (2015).
686 Global insights into high temperature and drought stress regulated genes by RNA-Seq in
687 economically important oilseed crop Brassica juncea. *BMC Plant Biology, 15*(1), 9.
688 Blum, A., Sinmena, B., Mayer, J., Golan, G., & Shpiler, L. (1994). Stem reserve mobilisation
689 supports wheat-grain filling under heat stress. *Functional Plant Biology, 21*(6), 771-781.
690 Campbell, C., Atkinson, L., Zaragoza-Castells, J., Lundmark, M., Atkin, O., & Hurry, V. (2007).
691 Acclimation of photosynthesis and respiration is asynchronous in response to changes in
692 temperature regardless of plant functional group. *New Phytologist, 176*(2), 375-389.
693 Clifton, R., Millar, A. H., & Whelan, J. (2006). Alternative oxidases in Arabidopsis: A comparative
694 analysis of differential expression in the gene family provides new insights into function of
695 non-phosphorylating bypasses. *Biochimica et Biophysica Acta (BBA) - Bioenergetics,*
696 *1757*(7), 730-741.
697 Copeland, R. A. (2000). *Enzymes: A Practical Introduction to Structure, Mechanism, and Data*
698 *Analysis* (Second Edition ed.). New York, NY: JOHN WILEY & SONS.
699 Covey-Crump, E. M., Bykova, N. V., Affourtit, C., Hoefnagel, M. H. N., Gardeström, P., & Atkin,
700 O. K. (2007). Temperature-dependent changes in respiration rates and redox poise of the
701 ubiquinone pool in protoplasts and isolated mitochondria of potato leaves. *Physiologia*
702 *Plantarum, 129*(1), 175-184.
703 CSIRO, & BOM. (2018). *State of the Climate 2018*. Retrieved from Canberra, Australia:
704 https://www.csiro.au/en/Research/OandA/Areas/Assessing-our-climate/State-of-the-Climate-
705 2018
706 Drake, J. E., Tjoelker, M. G., Aspinwall, M. J., Reich, P. B., Barton, C. V. M., Medlyn, B. E., &
707 Duursma, R. A. (2016). Does physiological acclimation to climate warming stabilize the ratio
708 of canopy respiration to photosynthesis? *New Phytologist, 211*(3), 850-863.
709 Glaubitz, U., Li, X., Köhl, K. I., van Dongen, J. T., Hincha, D. K., & Zuther, E. (2014). Differential
710 physiological responses of different rice (*Oryza sativa*) cultivars to elevated night
711 temperature during vegetative growth. *Functional Plant Biology, 41*(4), 437-448.
712 Godfray, H. C. J., Beddington, J. R., Crute, I. R., Haddad, L., Lawrence, D., Muir, J. F., . . . Toulmin,
713 C. (2010). Food security: the challenge of feeding 9 billion people. *Science, 327*(5967), 812-
714 818.
715 Gorsuch, P. A., Pandey, S., & Atkin, O. K. (2010). Temporal heterogeneity of cold acclimation
716 phenotypes in Arabidopsis leaves. *Plant, Cell & Environment, 33*(2), 244-258.
717 Hartmann, D. L., A.M.G. Klein Tank, M. Rusticucci, L.V. Alexander, S. Brönnimann, Y.
718 Charabi, . . . Zhai, P. M. (2013). *Observations: Atmosphere and Surface. In: Climate Change*

2013: The Physical Science Basis. Contribution of Working Group I to the Fifth Assessment Report of the Intergovernmental Panel on Climate Change. Retrieved from Cambridge, United Kingdom and New York, NY, USA:

Hikosaka, K., Ishikawa, K., Borjigidai, A., Muller, O., & Onoda, Y. (2006). Temperature acclimation of photosynthesis: mechanisms involved in the changes in temperature dependence of photosynthetic rate. *Journal of Experimental Botany, 57*(2), 291-302.

Hu, T., Sun, X., Zhang, X., Nevo, E., & Fu, J. (2014). An RNA sequencing transcriptome analysis of the high-temperature stressed tall fescue reveals novel insights into plant thermotolerance. *BMC Genomics, 15*(1), 1147.

Hubbart, S., Peng, S., Horton, P., Chen, Y., & Murchie, E. H. (2007). Trends in leaf photosynthesis in historical rice varieties developed in the Philippines since 1966. *Journal of Experimental Botany, 58*(12), 3429-3438.

Hüve, K., Bichele, I., Ivanova, H., Keerberg, O., Pärnik, T., Rasulov, B., . . . Niinemets, Ü. (2012). Temperature responses of dark respiration in relation to leaf sugar concentration. *Physiologia Plantarum, 144*(4), 320-334.

Impa, S. M., Sunoj, V. S. J., Krassovskaya, I., Bheemanahalli, R., Obata, T., & Jagadish, S. V. K. (2018). Carbon balance and source-sink metabolic changes in winter wheat exposed to high night-time temperature. *Plant, Cell & Environment, 0*(ja).

Krauss, S., Zhang, C.-Y., & Lowell, B. B. (2005). The mitochondrial uncoupling-protein homologues. *Nature Reviews Molecular Cell Biology, 6*, 248.

Kurimoto, K., Day, D. A., Lambers, H., & Noguchi, K. (2004). Effect of respiratory homeostasis on plant growth in cultivars of wheat and rice. *Plant, Cell & Environment, 27*(7), 853-862.

Kurimoto, K., Millar, A. H., Lambers, H., Day, D. A., & Noguchi, K. (2004). Maintenance of growth rate at low temperature in rice and wheat cultivars with a high degree of respiratory homeostasis is associated with a high efficiency of respiratory ATP production. *Plant and Cell Physiology, 45*(8), 1015-1022.

Lanning, S. B., Siebenmorgen, T. J., Counce, P. A., Ambardekar, A. A., & Mauromoustakos, A. (2011). Extreme nighttime air temperatures in 2010 impact rice chalkiness and milling quality. *Field Crops Research, 124*(1), 132-136.

Law, C. W., Chen, Y., Shi, W., & Smyth, G. K. (2014). voom: precision weights unlock linear model analysis tools for RNA-seq read counts. *Genome Biology, 15*(2), R29.

Li, H., Handsaker, B., Wysoker, A., Fennell, T., Ruan, J., Homer, N., . . . Genome Project Data Processing, S. (2009). The Sequence Alignment/Map format and SAMtools. *Bioinformatics, 25*(16), 2078-2079.

Liao, Y., Smyth, G. K., & Shi, W. (2013a). featureCounts: an efficient general purpose program for assigning sequence reads to genomic features. *Bioinformatics, 30*(7), 923-930.

Liao, Y., Smyth, G. K., & Shi, W. (2013b). The Subread aligner: fast, accurate and scalable read mapping by seed-and-vote. *Nucleic Acids Research, 41*(10), e108-e108.

Loveys, B. R., Atkinson, L. J., Sherlock, D. J., Roberts, R. L., Fitter, A. H., & Atkin, O. K. (2003). Thermal acclimation of leaf and root respiration: an investigation comparing inherently fast- and slow-growing plant species. *Global Change Biology, 9*(6), 895-910.

McCarthy, D. J., Chen, Y., & Smyth, G. K. (2012). Differential expression analysis of multifactor RNA-Seq experiments with respect to biological variation. *Nucleic Acids Research, 40*(10), 4288-4297.

Mohammed, R., Cothren, J. T., & Tarpley, L. (2013). High night temperature and abscisic acid affect rice productivity through altered photosynthesis, respiration and spikelet fertility. *Crop Science, 53*(6), 2603-2612.

Morimoto, R. I. (1998). Regulation of the heat shock transcriptional response: cross talk between a family of heat shock factors, molecular chaperones, and negative regulators. *Genes & Development, 12*(24), 3788-3796.

769 Morita, S., & Nakano, H. (2011). Nonstructural carbohydrate content in the stem at full heading
770 contributes to high performance of ripening in heat-tolerant rice cultivar Nikomaru. *Crop*
771 *Science, 51*(2), 818-828.
772 Murakami, Y., & Toriyama, K. (2008). Enhanced high temperature tolerance in transgenic rice
773 seedlings with elevated levels of alternative oxidase, OsAOX1a. *Plant Biotechnology, 25*(4),
774 361-364.
775 Nagai, T., & Makino, A. (2009). Differences Between Rice and Wheat in Temperature Responses of
776 Photosynthesis and Plant Growth. *Plant & Cell Physiology, 50*(4), 744-755.
777 Neilson, K. A., Mariani, M., & Haynes, P. A. (2011). Quantitative proteomic analysis of cold-
778 responsive proteins in rice. *Proteomics, 11*(9), 1696-1706.
779 Noguchi, K. O., Taylor, N. L., Millar, A. H., Lambers, H., & Day, D. A. (2005). Response of
780 mitochondria to light intensity in the leaves of sun and shade species. *Plant, Cell &*
781 *Environment, 28*(6), 760-771.
782 O'Leary, B. M., Asao, S., Millar, A. H., & Atkin, Owen K. (2018). Core principles which explain
783 variation in respiration across biological scales. *New Phytologist, 0*(0).
784 O'sullivan, O. S., Weerasinghe, K. W. L. K., Evans, J. R., Egerton, J. J. G., Tjoelker, M. G., & Atkin,
785 O. K. (2013). High-resolution temperature responses of leaf respiration in snow gum
786 (Eucalyptus pauciflora) reveal high-temperature limits to respiratory function. *Plant, Cell &*
787 *Environment, 36*(7), 1268-1284.
788 Ohama, N., Sato, H., Shinozaki, K., & Yamaguchi-Shinozaki, K. (2017). Transcriptional Regulatory
789 Network of Plant Heat Stress Response. *Trends in Plant Science, 22*(1), 53-65.
790 Ow, L. F., Griffin, K. L., Whitehead, D., Walcroft, A. S., & Turnbull, M. H. (2008). Thermal
791 acclimation of leaf respiration but not photosynthesis in Populus deltoides×nigra. *New*
792 *Phytologist, 178*(1), 123-134.
793 Peak, D., & Mott, K. A. (2010). A new, vapour-phase mechanism for stomatal responses to humidity
794 and temperature. *Plant, Cell & Environment, 34*(1), 162-178.
795 Peng, S., Huang, J., Sheehy, J. E., Laza, R. C., Visperas, R. M., Zhong, X., . . . Cassman, K. G.
796 (2004). Rice yields decline with higher night temperature from global warming. *Proceedings*
797 *of the National Academy of Sciences of the United States of America, 101*(27), 9971-9975.
798 Posch, B. C., Kariyawasam, B. C., Bramley, H., Coast, O., Richards, R. A., Reynolds, M. P., . . .
799 Atkin, O. K. (2019). Exploring high temperature responses of photosynthesis and respiration
800 to improve heat tolerance in wheat. *Journal of Experimental Botany, 70*(19), 5051-5069.
801 Quinlan, A. R., & Hall, I. M. (2010). BEDTools: a flexible suite of utilities for comparing genomic
802 features. *Bioinformatics, 26*(6), 841-842.
803 Ramakers, C., Ruijter, J. M., Deprez, R. H. L., & Moorman, A. F. M. (2003). Assumption-free
804 analysis of quantitative real-time polymerase chain reaction (PCR) data. *Neuroscience*
805 *Letters, 339*(1), 62-66.
806 Reich, P. B., Sendall, K. M., Stefanski, A., Wei, X., Rich, R. L., & Montgomery, R. A. (2016).
807 Boreal and temperate trees show strong acclimation of respiration to warming. *Nature,*
808 *531*(7596), 633-636.
809 Robinson, J. T., Thorvaldsdóttir, H., Winckler, W., Guttman, M., Lander, E. S., Getz, G., & Mesirov,
810 J. P. (2011). Integrative genomics viewer. *Nature Biotechnology, 29*(1), 24-26.
811 Robinson, M. D., & Oshlack, A. (2010). A scaling normalization method for differential expression
812 analysis of RNA-seq data. *Genome Biology, 11*(3), R25.
813 Robinson, M. D., & Smyth, G. K. (2007a). Moderated statistical tests for assessing differences in tag
814 abundance. *Bioinformatics, 23*(21), 2881-2887.
815 Robinson, M. D., & Smyth, G. K. (2007b). Small-sample estimation of negative binomial dispersion,
816 with applications to SAGE data. *Biostatistics, 9*(2), 321-332.
817 Rolland, F., Moore, B., & Sheen, J. (2002). Sugar Sensing and Signaling in Plants. *The Plant Cell,*
818 *14*, S185-S205.

Ruijter, J. M., Ramakers, C., Hoogaars, W. M. H., Karlen, Y., Bakker, O., van den Hoff, M. J. B., & Moorman, A. F. M. (2009). Amplification efficiency: linking baseline and bias in the analysis of quantitative PCR data. *Nucleic Acids Research, 37*(6), e45-e45.

Scafaro, A. P., & Atkin, O. K. (2016). The Impact of Heat Stress on the Proteome of Crop Species. In G. H. Salekdeh (Ed.), *Agricultural Proteomics Volume 2: Environmental Stresses* (pp. 155-175). Cham: Springer International Publishing.

Scafaro, A. P., Atwell, B. J., Muylaert, S., Reusel, B. V., Ruiz, G. A., Van Rie, J., & Gallé, A. (2018). A thermotolerant variant of rubisco activase from a wild relative improves growth and seed yield in rice under heat stress. *Frontiers in Plant Science, 9*, 1663.

Scafaro, A. P., Xiang, S., Long, B. M., Bahar, N. H. A., Weerasinghe, L. K., Creek, D., . . . Atkin, O. K. (2017). Strong thermal acclimation of photosynthesis in tropical and temperate wet-forest tree species: the importance of altered Rubisco content. *Global Change Biology, 23*(7), 2783-2800.

Seck, P. A., Diagne, A., Mohanty, S., & Wopereis, M. C. S. (2012). Crops that feed the world 7: Rice. *Food Security, 4*(1), 7-24.

Shane, M. W., Cramer, M. D., Funayama-Noguchi, S., Cawthray, G. R., Millar, A. H., Day, D. A., & Lambers, H. (2004). Developmental physiology of cluster-root carboxylate synthesis and exudation in *harsh hakea*. Expression of phosphoenolpyruvate carboxylase and the alternative oxidase. *Plant Physiology, 135*(1), 549.

Shapiguzov, A., Vainonen, J. P., Hunter, K., Tossavainen, H., Tiwari, A., Järvi, S., . . . Kangasjärvi, J. (2019). Arabidopsis RCD1 coordinates chloroplast and mitochondrial functions through interaction with ANAC transcription factors. *eLife, 8*, e43284.

Shen, C., Li, D., He, R., Fang, Z., Xia, Y., Gao, J., . . . Cao, M. (2014). Comparative transcriptome analysis of RNA-seq data for cold-tolerant and cold-sensitive rice genotypes under cold stress. *Journal of Plant Biology, 57*(6), 337-348.

Shope, J. C., Peak, D., & Mott, K. A. (2008). Stomatal responses to humidity in isolated epidermes. *Plant, Cell & Environment, 31*(9), 1290-1298.

Sidaway-Lee, K., Costa, M. J., Rand, D. A., Finkenstadt, B., & Penfield, S. (2014). Direct measurement of transcription rates reveals multiple mechanisms for configuration of the Arabidopsisambient temperature response. *Genome Biology, 15*(3), R45.

Siedow, J. N., & Umbach, A. L. (2000). The mitochondrial cyanide-resistant oxidase: structural conservation amid regulatory diversity. *Biochimica et Biophysica Acta (BBA) - Bioenergetics, 1459*(2), 432-439.

Smith, N. G., & Dukes, J. S. (2017). Short-term acclimation to warmer temperatures accelerates leaf carbon exchange processes across plant types. *Global Change Biology, 23*(11), 4840-4853.

Smyth, G. K., Michaud, J., & Scott, H. S. (2005). Use of within-array replicate spots for assessing differential expression in microarray experiments. *Bioinformatics, 21*(9), 2067-2075.

Stitt, M., & Zeeman, S. C. (2012). Starch turnover: pathways, regulation and role in growth. *Current Opinion in Plant Biology, 15*(3), 282-292.

Strand, A., Hurry, V., Henkes, S., Huner, N., Gustafsson, P., Gardestrom, P., & Stitt, M. (1999). Acclimation of Arabidopsis leaves developing at low temperatures. Increasing cytoplasmic volume accompanies increased activities of enzymes in the calvin cycle and in the sucrose-biosynthesis pathway. *Plant Physiology, 119*(4), 1387-1398.

Thimm, O., Bläsing, O., Gibon, Y., Nagel, A., Meyer, S., Krüger, P., . . . Stitt, M. (2004). mapman: a user-driven tool to display genomics data sets onto diagrams of metabolic pathways and other biological processes. *The Plant Journal, 37*(6), 914-939.

Tjoelker, M. G., Oleksyn, J., & Reich, P. B. (2001). Modelling respiration of vegetation: evidence for a general temperature-dependent Q_{10}. *Global Change Biology, 7*(2), 223-230.

Tjoelker, M. G., Reich, P. B., & Oleksyn, J. (1999). Changes in leaf nitrogen and carbohydrates underlie temperature and CO_2 acclimation of dark respiration in five boreal tree species. *Plant, Cell & Environment, 22*(7), 767-778.

Vanlerberghe, C. G. (2013). Alternative oxidase: A mitochondrial respiratory pathway to maintain metabolic and signaling homeostasis during abiotic and biotic stress in plants. *International Journal of Molecular Sciences, 14*(4).

Wagner, A. M., & Wagner, M. J. (1995). Measurements of *in vivo* ubiquinone reduction levels in plant cells. *Plant Physiology, 108*(1), 277.

Wang, E., Wang, J., Zhu, X., Hao, W., Wang, L., Li, Q., . . . He, Z. (2008). Control of rice grain-filling and yield by a gene with a potential signature of domestication. *Nature Genetics, 40*, 1370.

Way, D. A., & Oren, R. (2010). Differential responses to changes in growth temperature between trees from different functional groups and biomes: a review and synthesis of data. *Tree Physiology, 30*(6), 669-688.

Way, D. A., & Sage, R. F. (2008). Thermal acclimation of photosynthesis in black spruce [*Picea mariana* (Mill.) B.S.P.]. *Plant, Cell & Environment, 31*(9), 1250-1262.

Wei, S.-S., Niu, W.-T., Zhai, X.-T., Liang, W.-Q., Xu, M., Fan, X., . . . Li, B. (2019). Arabidopsis mtHSC70-1 plays important roles in the establishment of COX-dependent respiration and redox homeostasis. *Journal of Experimental Botany, 70*(20), 5575-5590.

Welch, J. R., Vincent, J. R., Auffhammer, M., Moya, P. F., Dobermann, A., & Dawe, D. (2010). Rice yields in tropical/subtropical Asia exhibit large but opposing sensitivities to minimum and maximum temperatures. *Proceedings of the National Academy of Sciences, 107*(33), 14562-14567.

Yamori, W., Noguchi, K., Hikosaka, K., & Terashima, I. (2010). Phenotypic plasticity in photosynthetic temperature acclimation among crop species with different cold tolerances. *Plant Physiology, 152*(1), 388-399.

Yamori, W., Noguchi, K., & Terashima, I. (2005). Temperature acclimation of photosynthesis in spinach leaves: analyses of photosynthetic components and temperature dependencies of photosynthetic partial reactions. *Plant, Cell & Environment, 28*(4), 536-547.

Yang, J., & Zhang, J. (2005). Grain filling of cereals under soil drying. *New Phytologist, 169*(2), 223-236.

Yoshida, S. (1972). Physiological aspects of grain yield. *Annual review of Plant Physiology, 23*, 437-464.

Zhu, J., Dong, C.-H., & Zhu, J.-K. (2007). Interplay between cold-responsive gene regulation, metabolism and RNA processing during plant cold acclimation. *Current Opinion in Plant Biology, 10*(3), 290-295.

Table 1. Differential expression of respiration genes in leaves after exposure to *T* of 40°C relative to 30°C. Differential expression defined as FDR < 0.05, marked as '*'. Electron transport chain (ETC), Pentose Phosphate Pathway (PPP). No TCA cycle genes were differentially expressed.

			Log2 fold-change	
Pathway	Gene_name	locus	2 hours	6 hours
ETC	Complex II (Succinate dehydrogenase)	LOC_Os08g02640	-0.55*	-0.58*
ETC	External NAD(P)H dehydrogenase	LOC_Os06g47000	0.72*	0.44
ETC	Uncoupling protein	LOC_Os11g48040	0.81*	0.46
ETC	Alternative oxidase	LOC_Os02g47200	-0.99*	-1.91*
glycolysis	ATP-dependent phosphofructokinase	LOC_Os01g53680	-0.11	-1.13*
glycolysis	Phosphoglycerate kinase	LOC_Os02g07260	0.78*	0.39
glycolysis	Enolase	LOC_Os10g08550	0.61*	0.34
PPP	Ribulose 5-phosphate 3-epimerase	LOC_Os09g32810	0.53*	0.87*

Table 2. Leaf mass per unit area (LMA), starch and soluble sugars of pre-existing (PE) leaves transferred from 30/25°C to 25/20°C or 40/35°C for one and seven days, and leaves newly-developed (ND) at the prevailing *T*. Data represents mean of three or four separate leaves from separate previously unsampled plants ± SE. The *F*-values and *P*-values of a two-way ANOVA comparing *T*, developmental stage (*D*) and any interaction ($T \times D$) are reported with asterisks indicating significance at $P<0.05$.

		LMA (g m^{-2})	Starch (mg g^{-1} DM)	Soluble sugar (mg g^{-1} DM)
25/20°C	Day 1	20 ± 3	11.3 ± 1.9	13.5 ± 0.2
	Day 7	19 ± 2	5.5 ± 0.3	11.2 ± 0.1
	ND	30 ± 2	14.4 ± 3.0	11.1 ± 0.2
30/25°C	Day 1	19 ± 2	14.9 ± 2.1	13.0 ± 0.5
	Day 7	21 ± 2	4.9 ± 1.0	10.5 ± 0.2
	ND	28 ± 0.4	9.6 ± 1.6	11.0 ± 0.6
40/35°C	Day 1	18 ± 2	8.5 ± 0.4	11.9 ± 0.2
	Day 7	23 ± 2	3.5 ± 0.3	10.9 ± 0.3
	ND	29 ± 1	6.7 ± 0.5	11.6 ± 0.3
$T \times D$		F=0.7, P=0.6	F=1.7, P=0.14	F=0.01, P=0.99
D		F=28, $P<0.001$*	F=13, $P<0.001$*	F=0.14, P=0.94
T		F=0.1, P=0.9	F=4.2, P=0.03*	*F=0.01*, P=0.99

952
953
954
955
956
957
958
959
960
961
962
963
964
965
966
967
968
969
970
971
972

Table 3. Summary of key photosynthetic and respiratory parameters generated from temperature-response curves. Parameters are: leaf mass per area; the temperature at which R_{dark} and A_n exhibited maximum rates (T_{max} and T_{opt}, respectively); the maximum rates of R_{dark} and A_n reached (R_{max} and A_{opt}, respectively); rates of R_{dark} and A_n at the prevailing growth temperature; and, the temperature at which PSII lost functionality as determined by an increase in basal fluorescence (T_{crit}). Data represents means of three or four separate leaves from separate plants ± SE and statistical data (*F*-value and *P*-value) based on one-way ANOVA of temperature treatment effect. Superscript letters show significant differences between the *T* treatments according to a Tukey test.

	25/20°C	30/25°C	40/30°C	*F*-value	*P*-value
LMA (g m^{-2})	33±2	30±2	35±3	1.4	0.31
T_{max} (°C)	51± 1^{a}	54 ± $1^{a,b}$	55± 1^{b}	4.7	0.04*
T_{opt} (°C)	29± 1^{a}	31± $1^{a,b}$	33 ± 0.3^{b}	6.1	0.04*
R_{max} (μmol g^{-1} DM s^{-1} ×10^{-3})	120 ± 5	117 ± 6	121 ± 2	0.16	0.86
A_{opt} (μmol g^{-1} DM s^{-1})	0.65 ± 0.05	0.67± 0.02	0.69 ± 0.04	0.28	0.76

R_{dark} (μmol g^{-1} DM s^{-1} $\times 10^{-3}$)	24±3 [a]	27±3 [a]	57±2 [b]	35	<0.001*
A_n (μmol m^{-2} s^{-1})	0.62 ± 0.04	0.67 ± 0.02	0.65 ± 0.04	0.52	0.62
T_{crit} (°C)	46.0 ± 0.6	46.9 ± 0.9	49.8 ± 1.5	3.726	0.089

Figure Legends

Figure 1. Quantitative PCR analysis of gene expression over the first 168 hours (7 days) after transfer of leaves from 30/25°C to 25/20°C or 40/35°C. Genes analysed were: the respiratory cytochrome *c* complex (*cox*) subunit II, alternative oxidase complex (*aox*) and uncoupling protein (*ucp*); the photosynthetic genes ferredoxin NADH reductase (*fnr*) and phosphoribulose kinase (*prk*); and the sugar metabolism gene sucrose phosphatase synthase (*sps*). Gene expression was revitalised at each time-point to the non-transferred 30/25°C control.

Figure 2. Principal component analysis of normalised RNA-seq expression values for each sample following temperature treatment for (a) 2 hours and (b) 6 hours. Samples are coloured by treatment, day/night temperatures of 30/25°C (control), 40/35°C (hot), and 25/20°C (cold). The y-axis is principle

component 1 (PC1) and the x axis is principle component 2 (PC2); the percent of variation explained by each axis is indicated. RNA-seq libraries were normalised using *edgeR* ("TMM" method) and *voom* transformation, scaled by unit variance and clustered using singular value decomposition.

Figure 3. Identification of genes differentially expressed during temperature treatments. (a, b) Common and time point specific differentially expressed genes under heat treatment (40/35°C). The overlap between genes differentially expressed at 2 and 6 h under heat treatment for (a) upregulated genes and (b) downregulated genes. '*' indicates significant overlap $p << 0.001$, fisher's one-tailed exact test (hypergeometric). (c) Hierarchal clustering of differentially expressed genes. For each time point (2, 6 and 24 h) differentially expressed genes were determined for both the hot (40/35°C) and cold (25/20°C) temperature treatments relative to the 30/25°C control conditions (FDR < 0.05). For each differentially expressed gene, the relative fold-change under each condition over the time series is then displayed on a log2 scale: red = upregulated, blue = downregulated.

Figure 4. Gene ontology (GO) term enrichment among genes differentially Upregulated (a) or downregulated (b) genes after 2 h at 40°C. Ontological annotations downloaded from MSU and ontology enrichment tests performed with topGO in R using the Fisher standard test (on tailed fisher's exact test/ hypergeometric test) with post hoc p value correction for multiple testing using the Benjamini & Hochberg method.

Figure 5. Abundance of mitochondrial electron transport chain proteins and Rubisco determined by Western blot analysis for rice leaves sampled at different developmental stages of; PE leaves six and 24 h after *T* transfer to 25/20°C or 40/35°C, and leaves newly developed (ND) post *T*-transfer. (a) Abundance of CYTOCHROME C OXIDASE (COX) subunit II, (b) ALTERNATIVE OXIDASE (AOX), (c) UNCOUPLING PROTEIN (UCP) and (d) Rubisco large subunit on a leaf area basis with data normalised by adjusting the largest value in each dataset to 100. Data represent mean ± SE of four independent western blots, with each blot representing leaf tissue from a separate plant. The *P*-values of a two-way ANOVA comparing temperature (*T*), developmental stage (*D*) and the interaction between the two (*T*×*D*) are reported on each graph. Representative blots are presented in Figure S5.

Figure 6. Rates of dry mass (DM) based dark respiration (R_{dark}; a), net photosynthesis (A_n; b), Relative humidity (RH; c), vapour pressure deficit between the leaf and surrounding air (VPD_{Leaf}; de), ~~and~~ stomatal conductance (g_s; e~~d~~), and ratio of intercellular to ambient CO_2 concentrations (Ci/Ca; f)

measured at the respective day-time growth temperature of each treatment just prior to (day 0), and 1, 2, 3, 5 and 7-days after transfer of control 30/25°C day/night grown leaves to either 25/20°C, 40/35°C or maintained at 30/25°C. Values are means of four biological replicates ± SE.

Figure 7. Temperature-response curves (a, b) of dark respiration (R_{dark}) and (c, d) net photosynthesis (A_n), on a dry mass (DM) basis. Values are absolute (a, c) or normalised to values at 30°C (b, d). Measurements were made on whole newly-developed (ND) leaves growing for 21 d at day/night temperatures of 25/20°C, 30/25°C or 40/35°C. Curves fitted to R_{dark} and A_n are quadratic functions. Calculated acclimation parameters from the curves are presented in Table 3. Rates were recorded every 30 sec as leaves were heated at 1°C per minute. Filled area represent standard error of three to four biological replicates.

Figure 8. The percentage of dark respiration (R_{dark}) relative to light-saturated net assimilation (A_n) (a), and leaf elongation rates (LER) over a 24 h day/night cycle (b), for ND leaves growing for 21 d at day/night temperatures of 25/20°C, 30/25°C or 40/35°C. For the R_{dark}/A_n ratio values are calculated from the absolute means presented in Figure 7. For LER the dark (night) period of the 24 h cycle is shaded in grey and values are the means ± SE of four plant replicates.